The Design and Synthesis of Novel EGFR Inhibitors

by

Robyn Elizabeth Carnie

A dissertation submitted to the Faculty of Science, University of the Witwatersrand, Johannesburg, in fulfillment of the requirements for the degree of Master of Science.

Supervisor: Dr Allan Prior
Supervisor: Dr Amanda Rousseau

March 2019

Declaration

I declare that the work presented in this thesis was carried out exclusively by me under the supervision of Dr A.M Prior and Dr A.L Rousseau. It is being submitted for the degree of Master of Science in the University of the Witwatersrand, Johannesburg, and has not been submitted before for any degree or examination in any other university.

Robyn Elizabeth Carnie

14 March 2019

Abstract

Lung cancer is the second most common form of cancer, accounting for approximately 13% of all new cancer cases.Of these cancers about 85% are non-small cell lung carcinoma (NSCLC). The epidermal growth factor (EGF) receptor is a protein kinase, which is crucial in a cell's life cycle, from cell growth to cell death. The over expression of the EGF receptor is observed in many forms of cancers including NSCLC, breast, ovarian, colorecteral and brain cancers.

Although there are current kinase inhibitors on the market, they suffer from dose limiting toxicity or drug resistance due to mutations in the kinase domain of EGFR. The focus of this body of work is on the development of more efficacious EGFR inhibitors that can overcome drug resistance issues associated with current EGFR inhibitors, as well as being less toxic to the body. This class of inhibitor should be a covalent inhibitor, requiring it to react with the solvent exposed cysteine residue that is positioned on the edge of the ATP binding pocket of EGFR. The carbonyl group of the ketoamide should undergo a 1,2 addition with this cysteine residue to form a covalent, yet reversible bond.

We report herein our progress towards the synthesis and biological evaluation of a novel class of quinazoline ketoamides. The key step in this synthesis route was to form a thiol on the quinazoline core. This was to be achieved by the addition of a thiocabamoyl group to the exposed alcohol **33** to form *O*-4-[(3-bromophenyl)amino]-7-methoxyquinazolin-6-yldimethylcarbamothioate **49**, this compound successfully underwent the Miyazaki-Newman-Kwart rearrangement, in which the oxygen and sulfur are exchanged to form *S*-4-[(3-bromophenyl)amino]-7-methoxyquinazolin-6-yldimethyl-

carbamothioate **48** , allowing the sulfur to be on the quinazoline core. the characterisation for this compound included ^{1}H NMR spectroscopy and ^{13}C NMR spectroscopy to confirm it's structure. The same rearrangement was attempted on the 3-chloro-4-fluoro analogue *O*-4-[(3-chloro-4-fluorophenyl)amino]-7-methoxyquinazolin-6-yldimethylcarbamothioate **66**, however this rearrangement was not successfully isolated and characterised. The next step required the carbamoyl group to be removed to expose the thiol. Although this step was attempted on both analogues, the products 4-[(3-bromo)amino]-7-methoxyquinazolin-6-thiol **47** and 4-[(3-chloro-4-fluoro)amino]-7-methoxyquinazolin-6-thiol **67** were not successfully synthesised and isolated.

Acknowledgements

I would like to express my sincerest gratitude to both my supervisors Dr Allan Prior and Dr Amanda Rousseau. Allan inspired this project and supported me, and celebrated my successes and sympathised in my frustrations. I will always be grateful for the support positivity you brought to my project even from afar. Mandy, you have championed this project over the finish line and I am incredibly grateful for your support especially through the write up process. Your generosity with your patience, support and time have been invaluable to me. From both of you, I could not have asked for more, thank you.

Thank you to the National Research Foundation for the generous financial support.

I would also like to express my gratitude to the Organic group staff members who supported me and encouraged me through the years. Professor Charles De Koning, Dr Moira Bode, Professor Dean Brady, Professor Joseph Michael and Dr Myron Johnson, thank you for the support. To my colleagues, Jean, Gciniwe, Memory, Kamogelo, Tebogo, Hendrik, Songz, Kennedy, Donald, Charles, Xolani and William I will never forget my time in the lab with you. The cake, the laughs and general support for one another was incredible.

To Monika, thank you for letting me vent, making me laugh and supporting my crazy ideas. To Bronwyn, thank you for always having a positive outlook and for reminding me that life is bigger than right now. To Amy, we have been through so much. Thank you for the croissants, late nights, early mornings and weekends. I will forever be grateful for having someone to do this with. I am very grateful to have you all in

my life.

To my family, Dad, Mom and Byron I have no words to describe the love and support you have shown me. Your unwaiving faith in me is always appreciated. No matter where in the world my journey takes me, I know I always have a place to call my home and the love and support of an incredible family.

To Adam, thank you for always pushing me to be my best self and supporting me through the times that I doubt myself. You are an incredible source of strength for me and I will always be grateful for your presence in my life.

Contents

List of Figures

List of Schemes

Chapter 1

Introduction

1.1 Cancer

According to the World Health Organisation (WHO), cancer is a generic term for a large range of diseases that can affect any part of the body.[1] Cancer is defined by WHO as the uncontrolled growth of cells, which can invade and spread to different parts of the body.[1] Cancer is a leading cause of death throughout the world. In 2012 alone there were 8 million deaths associated with cancer.[2] The concerning fact is that this number is expected to rise by 70% over the next 20 years.[1] The majority of cancer-related deaths occur in Central and South America, Asia and Africa.[3]

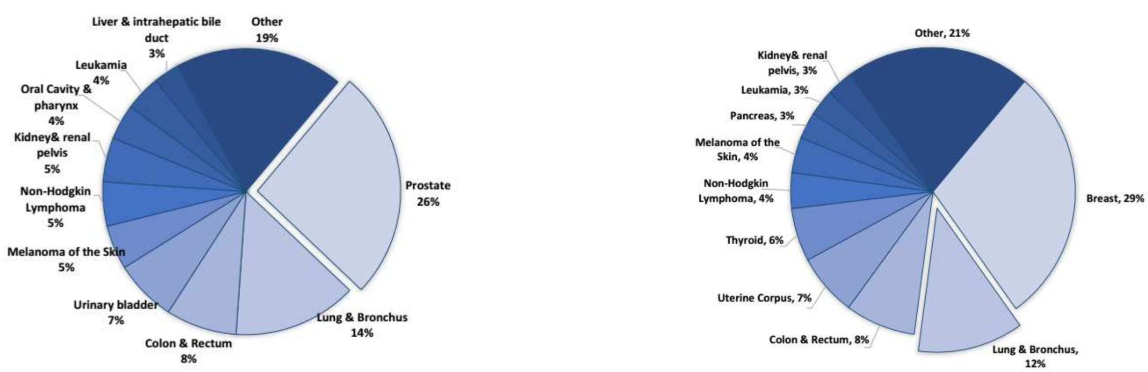

(a) Males **(b)** Females

Figure 1: Estimated world cancer incidence proportions by major sites, in a) Males and b) Females, 2015.[3]

Lung cancer is responsible for 1.8 million new cancer cases every year.[4] It is the second most common cancer in men, after prostate cancer, and the second most common in women after breast and colon cancer, as can be seen in Figure 1.[3,5] Even though lung cancer is not the most common in either men or women it still has the highest mortality rate of all the cancers (Figure 2), with a 5 year survival rate of 20%.[3,4,6,7]

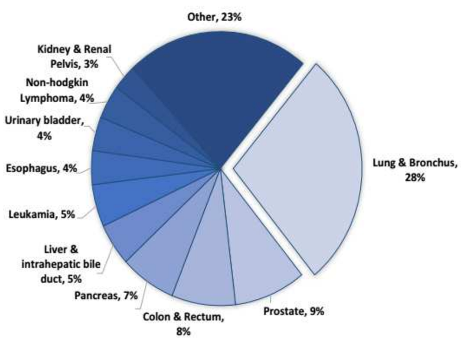

(a) Males

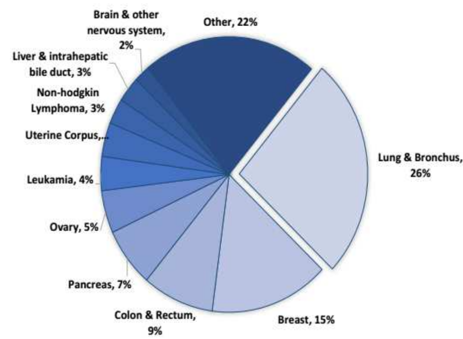

(b) Females

Figure 2: Estimated world cancer mortality proportions by major sites, in a) Males and b) Females, 2015.[3]

Lung cancer is often not diagnosed until it is at an advanced non-curable stage, and is considered life threatening. Lung cancer is also able to spread to other organs in the body by entering the lymph system.[5] There are the obvious risk factors, like smoking, alcohol and second hand smoke; however, it is important to note that there are risk factors that cannot be controlled nor prevented. These include the genetic make-up and origin of a person, from their gender to their genes as well as reproductive history and hormonal response.[3]

Lung cancer can be further identified as non-small cell lung cancer (NSCLC) or small cell lung cancer (SCLC). NSCLC accounts for around 85% of all lung cancer cases; it also only has a 15% survival rate.[4] The identifying feature of NSCLC is that it is common in non-smokers ,whereas SCLC is most common in patients who were or are considered heavy smokers.[3] NSCLC can then be divided into squamous cell carcinoma, adenocarcinoma and large cell carcinoma.[5,8] Adenocarcinoma is the most common form of lung cancer, making up approximately 40% of all lung cancers.[3,9] An adenocarcinoma tumor can be found in smokers, as well as being the most common type of lung cancer in a person who has never smoked.[3,5] In these patients, 38% of the adenocarcinoma tumors form due to common mutations that involve the epidermal growth factor receptor (EGFR).[3]

The tumour growth in NSCLC is often associated with oncogene driven malignancies, in particular EGFR is involved.[10] The majority of activating mutations in the EGFR are contributed to the exon 19 deletion and the exon 21 point mutation.[11] Cytotoxic drugs are inefficient at killing these tumours or even in reducing the size.[12] In addition, the toxicity to "normal" cells makes the therapy unbearable for the majority of patients. The development of target-based drug design is thus necessary, and the potential of this method is in the ability to distinguish between normal cells and cancer cells.[12] The overall aim of cancer treatment is to disrupt the growth of cancer cells, while leaving normal cells untouched.

1.2 Kinases

Protein kinases are identified by their ability to catalyse the transfer of a phosphate from adenosine triphosphate (ATP) to a substrate. As the majority of signaling pathways are initiated by a phosphotransfer, targeting these kinases can have a real physiological response.[13] Although the catalytic site of protein kinases have been identified as potential targets for cancer treatment, the question of selectivity has been raised.[14] There are more than 600 protein kinases in the human genome and these can be subdivided further.[14] More than 50% of protein kinase receptors have been found to be mutated or over expressed in tumors.[14] These kinases can become involved in the growth of malignancies through different mechanisms, mainly genomic rearrangements, mutations, deregulation by over expression and activation of oncogenes and unscheduled expression.[14] Another advantage of targeting kinases is that the "normal cells", that are severely affected by cytotoxic drugs, are tolerable to the inhibitors and so allow for the killing of the cancer cells while leaving the normal cells relatively unaffected.[13] This tolerance is due to the fact that the inhibitors are reversible and so the inhibitor does not remain in the active site. The cancer cells are also seen to be addicted to the oncogene, and so become completely reliant on the mutated kinase.[13] By designing the inhibitor to inhibit the specific mutated kinase, the selectivity of the inhibitor can be enhanced. Optimising the design of the inhibitor can be done using docking and binding studies of the inhibitor in the target site *in silico*.

1.3 Epidermal growth factor receptor

The EGFR was first described by Stanley Cohen in 1962.[15] Cohen would later go on to win the Nobel Prize in Physiology and Medicine, along with Rita Levi-Montalcini for this discovery.[16] The receptor tyrosine kinase (RTK) family of cell-surface receptors, have received attention due to their prevalence in malignant tumours.[17] The receptor is prone to hyperactivity which explains its prevelance in tumours. This hyperactivity is due to the overexpression of the EGFR and the fact that EGFR is an autocrine receptor that produces its own growth factor and stimulates itself.[17] A subset of the RTK family is a family of tyrosine kinase proteins called the ErbB family.[12] The ErbB family is made up of four members;

1. EGFR (Her1/ErbB1)
2. ErbB2 (Her2/Neu)
3. ErbB3 (Her3)
4. ErbB4 (Her4).[12]

The ErbB family is crucially important in a cell's life cycle, with functions that range from angiogenisis, leading to cell growth, to the inhibition of apoptosis.[18] It is the protein kinase which regulates the signalling pathways which determine these important cell functions.[14,16] A direct link has been found between EGFR and the vascular endothelial growth factor (VEGR) and hence a link between EGFR and angiogenisis.[18] They are also found to be fundamentally involved in pathways such as cell proliferation and survival that lead to the tumor growth.[13] For these reasons, EGFR is considered a promising target for the development of tyrosine kinases inhibitors (TKI).

Tyrosine kinases are all enzymes that need to be phosphorylated in order to be activated. All TKI's aim to inhibit this phosphorylation step and hence prevent the signal transduction pathways.[16] Each tyrosine kinase protein is made up of three domains: the extracellular domain that detects the binding ligand, the membrane spanning sequence that allows for interaction between the receptors, and the intracelluar domain that promotes the enzymatic activity of the kinase.[12,15] Specificity among the four receptors is due to the extracellular domain not being similar. Each receptor binds different ligands and the binding of such ligands stabilizes the EGFR, hence allowing for the dimerisation of the receptors This can occur in either a homo or hetero fashion.[19] All the possible combinations of dimerisation have been observed in different systems.[12] However, not all combinations are useful; ErbB2 can only induce a signal if it forms a hetero-dimer and the same is seen for ErbB3, where the homodimers are inactive. The deficiencies of these two receptors are overcome when they form a ErbB2-ErbB3 dimer, which is the most potent signalling complex.[12] Both EGFR and ErbB3 prefer to dimerise with ErbB2 as it is permanently in an active conformation and does not require a ligand to activate it.[15] This means that when EGFR binds with ErbB2, it does not require a ligand in order to perform functions such as endocytosis and intracellular trafficking. The binding of a ligand causes two monomers to bind. This can be seen in Figure 3, where the EGF locks into the monomer of the EGFR, causing two monomers to bind to form the dimer. This dimerisation leads to the phosphorylation of approximately 10 tyrosine residues, and this results in the activation of the signalling pathways of proteins responsible for growth in cells, RAS, MAPK and PKC amongst others.[19]

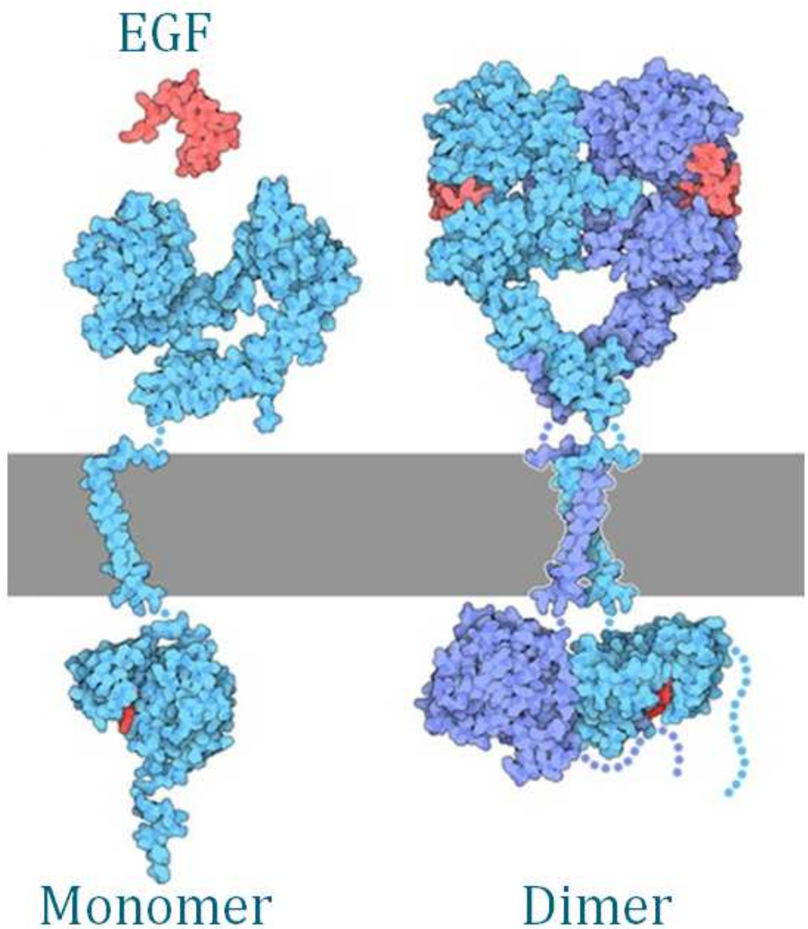

Figure 3: Showing the monomer and dimer of the EGFR..[20]

The 170kDa glycoprotein, EGFR, of the ErbB family was of particular interest.[18,21] This was due to the formidable presence of EGFR in solid tumors,[12] and activating mutations like the deletion at exon 19, LREA deletion, and the L858R mutation, a substitution at exon 21. These mutations in the EGFR have been identified as the primary cause of NSCLC.[10,22,23] The high metastatic rate, poor differentiation and rate at which tumours in NSCLC grow, is attributed to the overexpression of EGFR.[18] The common activating L858R point mutation, in which a leucine is substituted with an arginine, is thought to destabilise the conformation of the EGFR, hence allowing unihibited growth and the formation of a tumor.[18] Interestingly, although the mutation causes the tumor, it also makes the tumor more suseceptible to drug treatment. The mutation causes the EGFR to be more sensitive to designed inhibitors, as well as decreasing the EGFR's affinity for ATP. Since the mode of action of the inhibitor is to compete with the ATP for binding in the EGFR, this can be taken advantage of.[22] For all of these reasons, the EGFR is a promising potential target for cancer chemotherapy and understanding the binding site allows for the design of potential inhibitors. The binding site can be divided into 5 key regions:[14]

1. Adenine region
2. Sugar region of the ATP
3. Hydrophobic pocket
4. Hydrophobic channel
5. Phosphate binding site.

The hydrophobic adenine ring usually forms hydrogen bonds with the kinase region that connects the amino and carboxyl terminal kinase domains.[14] Inhibitors often form at least one of these hydrogen bonds within the protein.[14] Using hydrogen bonds allows the inhibitor to act as the ATP would and is therefore competitive with the ATP.[13] The second region is the sugar region of the ATP, and this region is considered to be hydrophillic in the majority of protein kinases. However, in EGFR, the cysteine residue C733 makes the region hydrophobic, and so this can be used in the design process to promote selectivity to EGFR.[14] Region 3, the hydrophobic pocket and region 4, the hydrophobic channel in the EGFR are not utilised at all by ATP, but is often used by the inhibitors to afford some selectivity through interaction at an additional binding site.[14] The final site is the phosphate binding site. This region is not critical for the binding of the potential inhibitors; however, it can be beneficial for selectivity.[14]

Resistance to treatment is a major biological concern for patients with NSCLC, and resistance occurs via many different mechanisms. The T790M mutation is the most common resistance mechanism, making up approximately 50% of all TKI resistance. It is also the mechanism of interest in this research.[24] Other examples of resistance mechanisms include MET and HER 2 amplification and conversion to SCLC.[24] The chance of a patient exhibiting an activating mutation like L858R is related to the race of the patient; in the case of a caucasian patient the chance is 10-15%, while in the case of an Asian patient it will be much higher.[7] It is also serendipitous that tumours with activating mutations like L858R have a higher affinity for the inhibitors when compared to the wildtype EGFR.[10]

1.4 Current accepted treatments

According to the National Cancer Institute, there are nine standard treatments for non-small cell lung cancer.[25] The first four of these are the most important and will be discussed briefly here, with an emphasis on targeted therapy.

1. Surgery
2. Radiation therapy
3. Chemotherapy
4. Targeted Therapy
5. Laser therapy
6. Photodynamic Therapy
7. Cryosurgery
8. Electrocautery
9. Watchful Waiting

Surgery is usually conducted on patients with stage I, II or IIIA NSCLC- it is only done if the cancer is able to be resected and if the patient can handle the surgery.[9] The size of the section removed can range from a small wedge to the entire lung being removed, (known as a pneumonectomy).[9,25] Radiation therapy is often used as an adjuvant therapy to ensure that all the remaining cancer cells have been removed.[9]

Radiation can also be used as an alternative to surgery or as palliative care for patients who are either not responsive to surgery or cannot handle the surgery.[9] Stereostatic body radiation therapy (SBRT) is particularly well received for early NSCLC, where there is a single nodule in a lung and metastases has not occurred in the lymph nodes.[9] Overall, SBRT has been found to provide a much higher overall survival rate of 2 years and at a lower cost.[9] Approximately 40% patients diagnosed with NSCLC already have stage IV cancer.[9] It has been observed that a tumor exposed to ionizing radiation can in fact grow instead of shrink. This is due to the radiation activating the EGFR in the same way its activating ligands would.[18] The radiation can also promote the increased expression of EGFR and so the tumour cycle could be perpetuated.[18] The first line therapy of cytotoxic combination chemotherapy is primarily to improve the survival rate of the patient.[9] Performance status (PS) is a rating given to a patient in order to understand their chance of responding to treatment, with a PS of 0 being very responsive and the higher rating, less responsive. Patients with a performance status of 3 are primarily given basic supportive care, while a patient with a PS rating of 2 respond best to treatments that do not include platinum-based therapy.[9] Platinum-based therapy is predominantly used in combination with drugs like paclitaxal and gemcitabine for patients with a PS of 0 or 1, this combination therapy has a median survival rate of 8-10 months.[9]

The fourth treatment is targeted therapy or personalised medicines. To achieve this, biomarker testing is essential, and understanding the DNA of the cancer can improve the survival rate significantly. The most common mutations occur between exon 18 and 21 of EGFR, and these mutations can confer sensitivity to EGFR tyrosine kinase inhibitors. These mutations can occur in the EGFR, as well as in genes like, KRAS, ALK and BRAF.[9] Other types of targeted therapies include immunotherapy, in which the immune system is boosted in order to target the cancer cells, by either slowing the growth or preventing the spread of the cancer.[9] A new strategy is to target the cancer cell by attacking the immune-modulating mechanisms by which the tumour protects itself against the immune system.[9]

1.5 Review of EGFR inhibitors for NSCLC

There are four types of inhibitors for targeting EGFR. The first two types are reversible ATP competitive inhibitors, type 1 and type 2, that inhibit the active and inactive conformations of the EGFR respectively.[13] The third class of inhibitors bind to the allosteric site of the kinase, offering the highest degree of selectivity due to the allosteric site being unique to each kinase.[13] The final class of inihibitors is the covalent inhibitors, also known as the second generation inhibitors. These inhibitors form covalent irreversible bonds in the active site of EGFR.[13] These molecules were designed specifically with an optimally placed electrophile that would undergo a Michael addition reaction with the solvent exposed cysteine residue at position 773.[13] Although these second generation inhibitors were designed to overcome resistance problems that will be described in the next section, the covalent binding of the inhibitor presented its own set of problems in the form of potential toxicity.[13]

1.5.1 First generation inhibitors

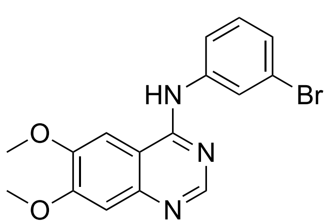

1

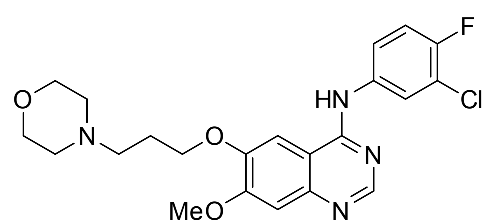

2

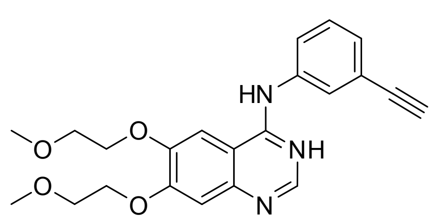

3

Figure 4: First generation tyrosine kinase inhibitors: PD153035 **1**, gefitinib **2** and erlotinib **3**.

In 1994, one of the first EGFR specific TKI, PD153035 **1** was reported (Figure 4).[21] The 4-amino quinazoline core, observed in PD153035 **1**, showed potential to be a small molecule inhibitor and so became the focus of drug development for tumors driven by EGFR with sensitising mutations.[26] From this core, two inhibitors were developed: gefitinib **2** by AstraZeneca and erlotinib **3** by OSI Pharmaceuticals.[26] Gefitinib **2** was approved by the FDA in 2003, with erlotinib **3** following close behind in 2004.[11,26] They are considered to be first generation inhibitors, and are well understood and available in many countries, as the first line of treatment for NSCLC.[11] Both of these inhibitors are taken orally, and are reversible inhibitors.[7,10] They compete with ATP for the intracellular binding site in EGFR.[7] Compared to other forms of chemotherapy, TKIs prove to have a far better response rate and progression free survival;[7] this is despite the fact that they can inhibit the "healthy" wild type EGFR.[10] The ideal situation would be to have the drugs to inhibit only the mutated form of the receptor. Although first generation inhibitors are effective, the majority of patients will develop resistance to these drugs after 10-13 months.[10,11] An overwhelming 50%-60% of patients who develop resistance do so because of the secondary point mutation, T790M, described previously.[10,11,27,28]

The substitution of a threonine for a methionine at position 790 (T790M) in the target site was discovered in 2005. This substitution is considered to be a secondary acquired mutation, usually occurring after the administration of TKIs. The T790M point mutation is observed in nearly half of all NSCLC patients that have been treated with tyrosine kinase inhibitors.[4,10,29,30] This mutation occurs at the entrance to the hydrophobic pocket at the back of the ATP binding site.[22,29,30] This "gatekeeper" position is responsible for inhibitor specificity.[29] The methionine, which has a bulkier side chain, is thought to prevent the binding of the aniline group of the TKI and hence the effectiveness of the first generation TKI is decreased.[10,30] However, this theory is disputed as the structure of the first and second generation inhibitors are so similar, particularly in the aniline region.[22] In some cases, the aniline is identical for a first generation inhibitor and a second generation inhibitor. However, if the bulky methionine group is affecting the binding of the first generation inhibitor then should not affect the initial binding of the second generation inhibitor? It was shown through direct binding assays of second generation inhibitor that the TKI binds stronger in both the L858R and the T790M mutated EGFR, compared to the binding in the wild type.[22] Crystal structures with afatinib, a second generation inhibitor, in the mutated binding site of both the active and inactive forms, show that the bulkiness of the methionine does not affect the binding of the inhibitors. All this being said, how does the presence of the T790M mutation cause resistance against first generation inhibitors? It was found that the introduction of the T790M mutation counteracts the effect of the L858R mutation by increasing the affinity for ATP to wild type levels.[7,22,29] It is therefore plausible that this is the reason the TKI is less effective against EGFR bearing the T790M mutation.

Importantly, even after developing resistance to the first generation inhibitors, the tumor is still dependent on the EGFR and so it remains the target of future drug development.[28] It was found that in some patients after a short TKI free period, the resistance due to the T790M mutation was lost.[6,29] This allowed for the patient to be treated with a second round of the first generation inhibitors, and in the majority of cases the patients did respond to this second round of treatment.[6]

1.5.2 Second generation inhibitors

BIBW2992, better known as afatinib **4** (Scheme 1), is a second generation irreversible selective inhibitor, developed in Germany by Boehringer-Ingelheim Pharma.[10] Afatinib **4** was designed to overcome the resistance observed in the first generation inhibitors. The resistance to the first generation inhibitors is due to the increased affinity for ATP in the T790M mutated enzymes, and therefore second generation inhibitors such as afatinib needed to out compete ATP for the binding site. In order to overcome this competition afatinib **4** has a Michael acceptor that forms a covalent bond with a cysteine residue (Cys- 797) in the EGFR active site **6** (Scheme 1).

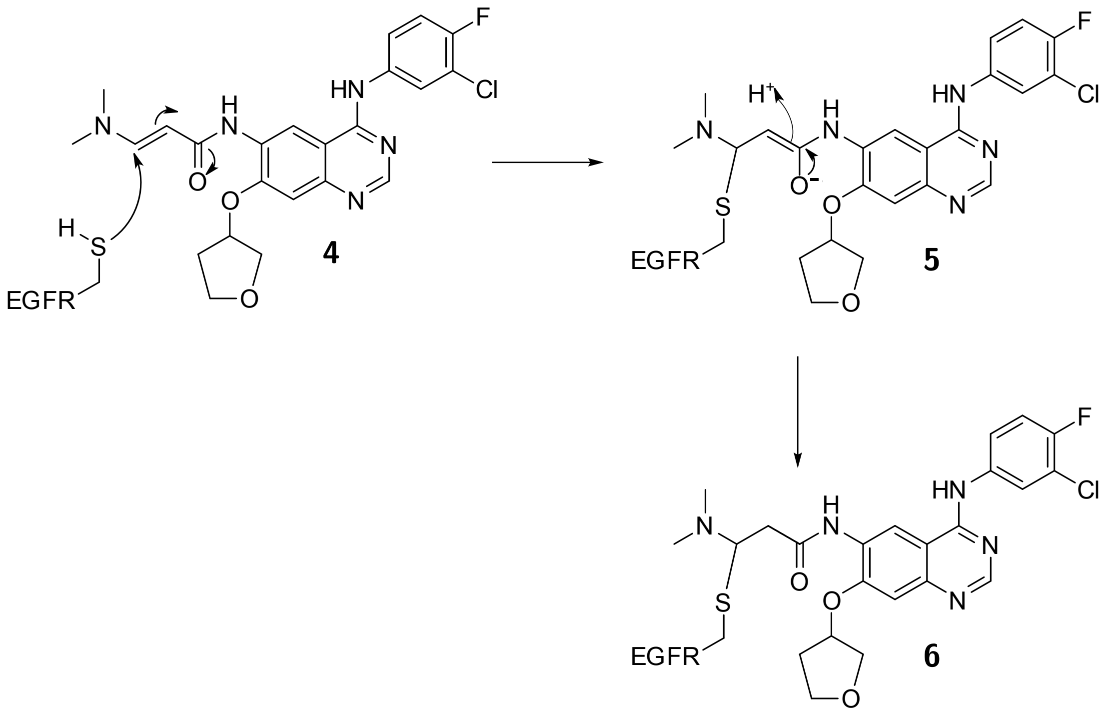

Scheme 1: Afatinib undergoing an addition to the α, β-unsaturated carboxamide to form an irreversible covalent bond with the cysteine residue in the active site.

The bond with the cysteine at position 797 is specific because of the non-covalent binding of the hydrophobic anilino group in the ATP binding pocket.[22] The crystal structure showing afatinib in the EGFR target site, shows a strong hydrogen bond with MET-793 and the covalent bond with the cysteine at 797.[15] Significantly, this covalent binding with the Michael acceptor is observed in HER2 at Cys-805 and in ErbB4 at Cys 803.[10,15] The irreversible binding to HER2 results in the inactivation of the preferred dimer partner of EGFR.[10] Afatinib was tested against 80% of the human kinome, and was shown to be highly selective, binding in the nanomolar range with EGFR, HER2 and ErbB4, while interacting in the high nanomolar range with other kinases like GAK, BLK and IRAK1, amongst others.[15] In addition, afatinib has a higher potency than the first generation inhibitors in cells with the T790M mutation.[10,15] The primary problem with second generation inhibitors is their toxicity caused in part by their irreversible nature. They also retain their affinity for the wild type EGFR, accentuating dose limiting toxicities.[11,29] The overall survival of patients who were initially treated with afatinib was improved compared to patients treated with drugs like cisplatin and pemetrexed.[7,28] Other second generation inhibitors include: dacomitinib **7** by Pfizer, pelitinib **8** and canertinib **9** (Figure 5). The latter two compounds are experimental drugs in clinical trials, while dacomitinib **7** was approved by the FDA in September 2018.[11]

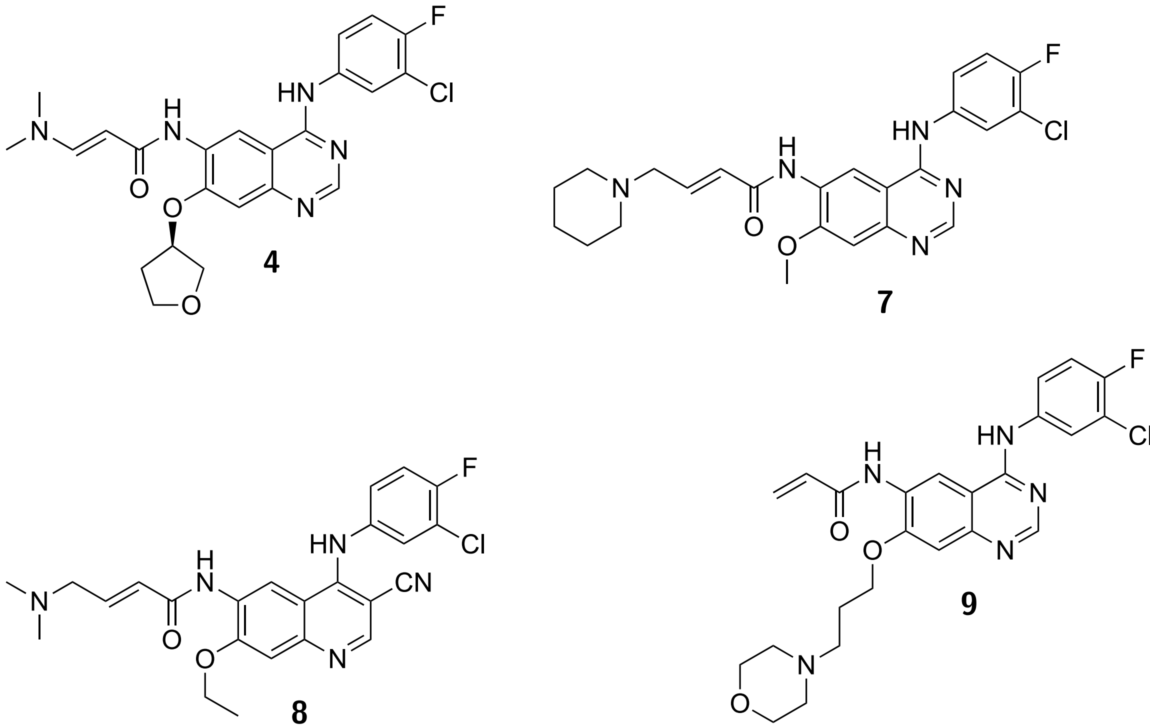

4 **7** **8** **9**

Figure 5: Second generation tyrosine kinase inhibitors: afatinib **4**, dacomitinib **7**, pelitinib **8** and canertinib **9**.

1.5.3 Third generation inhibitors

The next challenge in the quest for effective, safe TKI was to develop inhibitors with the potency of afatnib, but with improved selectivity.[27] In the development of the third generation inhibitors shown in Figure 6, the progression from the 4-amino quinazoline core to a unique anilinoopyrimidine core can be seen.[11,26] One of the first inhibitors designed with the new scaffold was WZ4002 **10**, which, based on the crystal structure, forms hydrogen bonding interaction between the anilinopyrimidine core and Met 793 of the hinge region.[26,27] The necessary covalent bond between the acrylamide and the cysteine residue which was originally used in the second generation inhibitor afatinib is also present.[26,27] The chlorine on the pyrimidine ring is thought to provide the key to the potency of this inhibitor with its interaction with the methionine at position 790.[27] Rociletinib **11**, developed by Clovis, and osimertinib **12**, developed by AstraZeneca, are another two third generation inhibitors that have received a lot of attention.[27] Osimertinib **12** in particular is an inhibitor approved by the FDA and is able to target the double mutated EGFR, L858R which is the primary, sensitising mutation combined with the T790M mutation.[27]

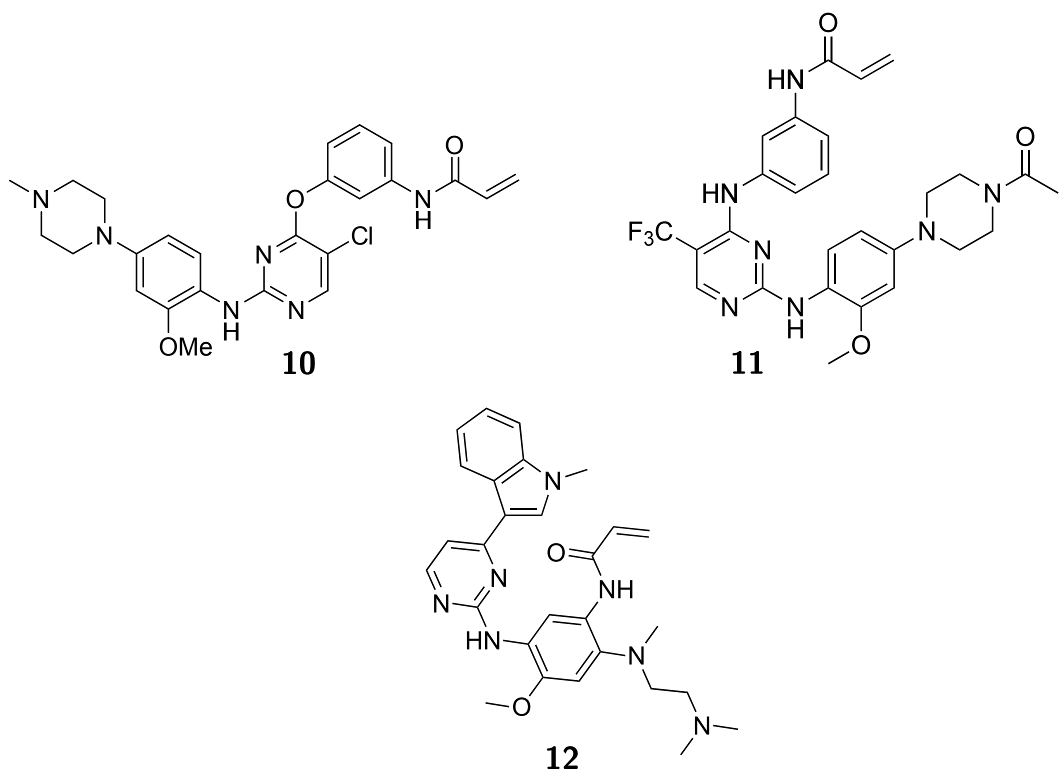

Figure 6: Third generation tyrosine kinase inhibitors: WZ4002 **10**, rociletinib **11** and osimertinib **12**.

Unfortunately as is common with any cancer therapy, once again the problem of new resistance arises, this time in the form of a tertiary substitution, namely a cysteine at position 797 to a serine.[27,28] Osimertinib **12** uses the same mode of binding as afatinib **4**, using the cysteine at 797 as a nucleophile to form a covalent bond to the inhibitor. With the conversion of the cysteine thiol to the less nucleophilic serine alcohol, this covalent bond is no longer formed, thus reducing binding in the ATP pocket to reversible competitive inhibition.[27] This resistance typically occurs within a year of the start of treatment. The mutation can occur with or without the presence of the T790M mutation and it is even probable that the T790M mutation can be lost.[27] This C797S mutation makes the target site less sensitive to any covalent inhibitors. Resistance also occurred in the rociletinib patients, the loss of the T790M mutation was observed as well as the conversion of NSCLC to SCLC.[11,27]

When designing tyrosine kinase inhibitors, it is important to carefully consider the reactivity of the warhead, (the warhead is highlighted in blue in Figure 7 for afatinib). In the design process of osimertinib **12**, the key rational came in ensuring that the reactivity of the warhead (shown in Figure 7) was decreased relative to the warhead reactivity of the second generation inhibitor, afatinib **4**.[27] The primary outcome of this reduced reactivity was that the inhibitor was far more selective compared to the earlier inhibitors.[27] However, in designing the next generation inhibitors, it is now important to fully understand the new mechanisms of resistance.

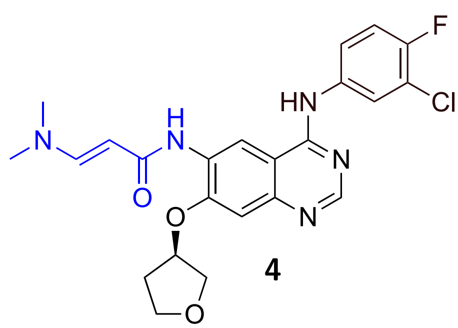

4

Figure 7: The warhead on afatinib.

Unexpectedly, although TKI's are designed to bind into the EGFR binding site, the anti-tumour activity of the TKI does not depend on the EGFR expression levels. Additionally, when the TKI's activity is compared to the activity of anti-EGFR monoclonal antibodies, it was found that the anticancer activity from the TKI's is significantly higher than the anticancer activity from the antibodies. This raised the question of specificity of the TKIs. The hetero- and homodimerisation of the receptors, described in the EGFR section, may play a role. After treatment with a TKI, a conformational change in the EGFR changes the preferred binding.[12] The previously uncommon binding of EGFR and ErbB3 now becomes common and the frequency of ErbB2-ErbB3 is significantly reduced. This suggests that the common dimers involve the EGFR which will be inhibited by the TKI, and the activity of these dimers will be blocked. In this way the TKI is able to affect the signal transduction of more than just the EGFR receptor. This may explain why the TKI can induce apoptosis of a cell.

The intention was for third generation inhibitors to have a much higher activity against mutated EGFR than against wild type EGFR.[29] There are two drugs that currently fulfill this condition, 1. osimertinib **12** and rociletinib **11**.

Cases in which there is an overexpression of EGFR, and in particular where the EGFR is affected by mutations such as L858R point mutation, respond well to these inhibitors.[8] At least 7 phase III clinical trials proved that the first generation inhibitors are the best course of action when looking at the treatment of NSCLC with mutated EGFR.[31] However, when resistance to the first generation inhibitors occurs, other avenues need to be considered. The second generation inhibitor, which is an irreversible inhibitor, works well as a combined treatment with anti-EGFR antibodies.[31]

1.6 Reversible covalent kinase inhibitors

In general, when designing inhibitors, thermodynamic affinity has been the primary focus. However, it has been found that the residence time of the drug in the target site can in fact promote pharmacodynamic activity and efficiency.[32] The most common way of prolonging the residence time of an inhibitor in the target site is to use covalent binding with a cysteine residue.[33] There are many advantages to considering a covalent binding mechanism when looking particularly at cancer treatment. One is able to target non catalytic nucleophiles which would allow for increased residence time of the inhibitor. They are also found to be highly selective if you target a poorly conserved cysteine residue.[33] This covalent mechanism is not often observed due to the potential reaction with off-target nucleophiles and hence the potential for toxicity; however, it has been fairly successful in certain cancer EGFR inhibitors, such as afatinib **4**.[32,33] The Michael acceptor on afatinib **4** undergoes an addition to an α, β unsaturated functional group at the carboxamide to form an irreversible covalent bond with the cysteine residue in the active site, as seen in Scheme 1.[33] The presence of an electrophile to react with a nucleophile in the active site is often observed in the cysteine protease inhibitors. In these cases, the electrophile is often a ketone or nitrile; however, this appear to be quite specific to the protease targets.[33] The interesting thing about this type of protease inhibitor is that they are intrinsically reversible inhibitors, even though they form a covalent bond with a cysteine residue.[33] They are considered as reversible covalent inhibitors. Non catalytic cysteines are thus an ideal target for the electrophile to react at, even though they are generally less nucleophillic than the catalytic cysteine residues.

The challenge is to find the perfect electronic balance between reactivity and reversibility.[33] Cyanoacrylamides seem to have found this balance and display an intrinsic reversibility when covalently bound to a thiol on the cysteine residue.[33] Krishnan *et al.* studied the use of novel electrophiles in the design of inhibitors that target enzymes with a significantly unconserved cysteine residue.[33] The cyanoacrylamide was also used by Bradshaw *et al.* in their design of covalent reversible inhibitors.[32] There are two important advantages of the reversible covalent bond; the first addresses the distinct disadvantage of covalent binding, toxicity. The reversible covalent inhibitors result in prolonged residence time, sought after by the covalent binding, but without the innate toxicity.[32] The second advantage identified by Bradshaw *et al.* is the potential ability to control the residence time of the inhibitor to fine tune activity, whether it be to maximise the time or to have rapid target disengagement.[32] It is noted that the maximum residence time of a covalent reversible inhibitor, like the irreversible inhibitor, is controlled by the turnover rate of the enzyme and so would still be fairly ineffective against a target with a short half-life.[33] The intention was to use the basis of the first and second generation inhibitors, together with the knowledge of the cysteine protease inhibitor, to develop a reversible covalent inhibitor such as **13** (Scheme 2). The reversible covalent inhibitor which is the focus of this MSc, is intended to bind to the sulfur in the cysteine residue within the EGFR active site, and to form a reversible covalent bond as seen in **14**.

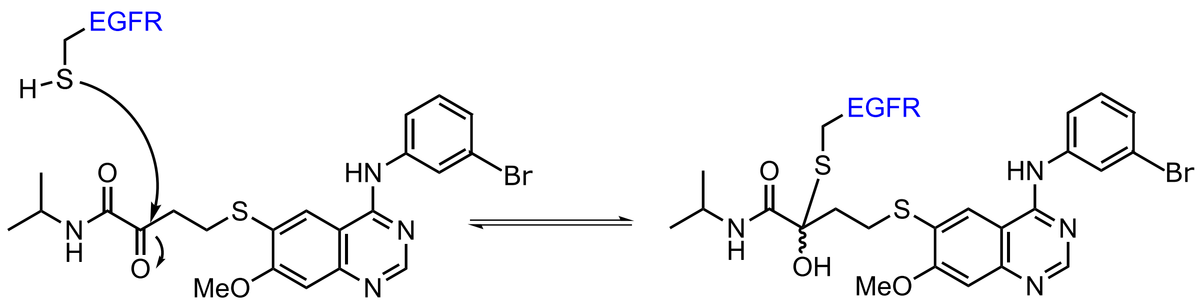

13 **14**

Scheme 2: Rational for reversible covalent kinase inhibitor.

1.7 Phenylamino-quinazolines

Heterocyclic compounds are a popular scaffold within the pharmaceutical industry; in particular, quinazolines and quinazolinones represent an important privileged pharmacological scaffold.[34,35] These fused heterocycles are present in many natural products and their similarity to ATP makes them an interesting starting point for pharmaceuticals in the agrochemical industry, as well as medicines for both humans and animals.[34] The therapeutic and pharmacological properties of quinazolines offer a diverse range of applications. They have been known to be involved in treatments that include antimicrobial, anticancer and anti-diabetic.[34,35] However the synthesis of the quinazoline core is often time consuming and low yielding.[34] The quinazolines can also be formed as salts, which improves the aqueous solubility of the compounds vital for bioavaliability and oral absorption.[36]

The synthesis of these compounds has been widely reported in literature. For example Knesl *et al.* have reported a synthesis for both erlotinib **3** and gefitinib **2**.[37] For erlotinib, the starting material, ethyl 3,4-dihydroxy-benzoate **15**, was alkylated twice with 1-chloro-2-methoxyethane to produce **16** (Scheme 3). The intermediate was then nitrated regioselectively at position 6 to form ethyl 4,5-bis(2-methoxyethoxy)-2-nitrobenzoate **17**. The nitro group was then reduced to an amine **18**, which was reacted with formamide to undergo a ring closure reaction, with the elimination of ethanol, to form **19**. The chlorination was performed using phosphoryl chloride and *N,N*-diethylaniline to afford **20**, which when reacted with 3-ethynylaniline gave erlotinib **3**.

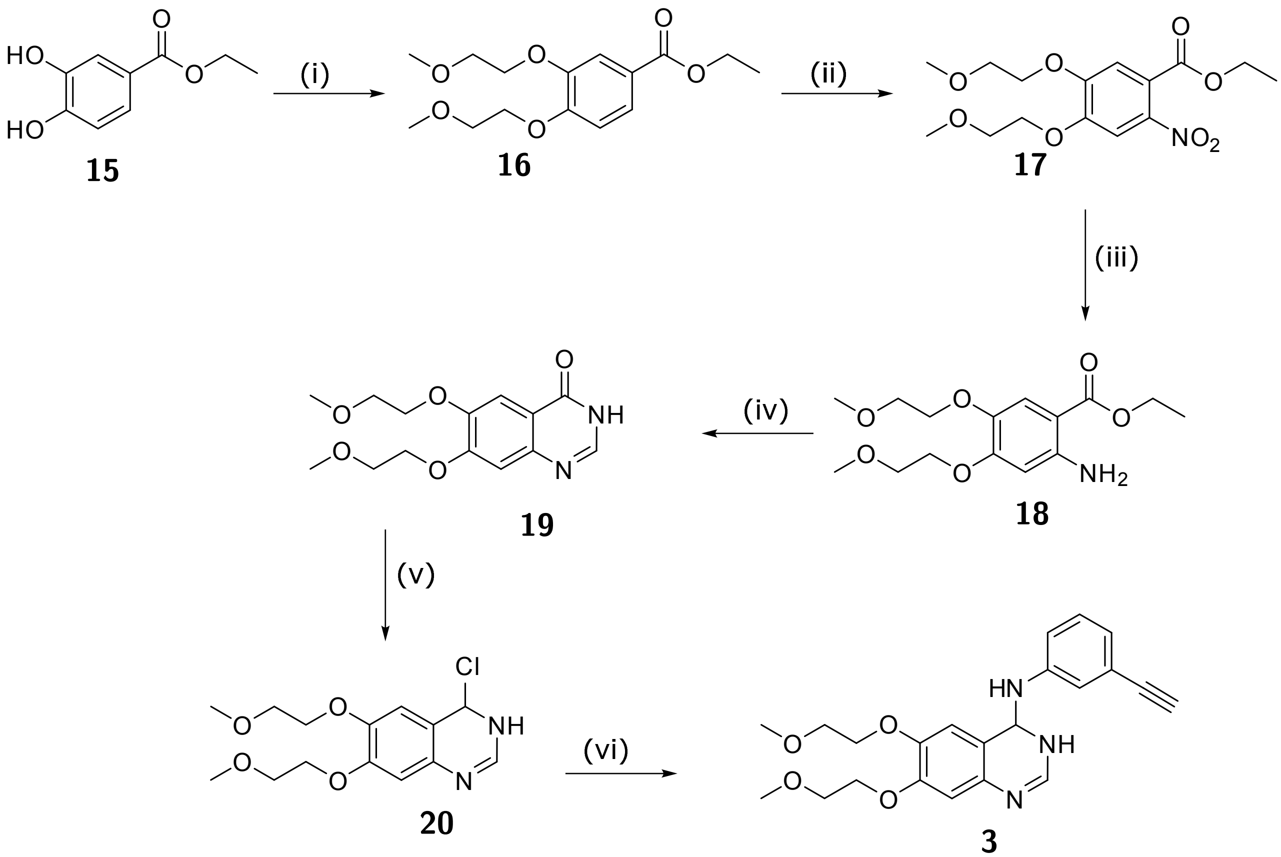

Scheme 3: The synthesis of erlotinib **3** followed by *Knesl et al.* .[37]
Conditions: i) 1-Chloro-2-methoxyethane; K_2CO_3, $Bu_4N^+Br^-$, acetone; ii) AcOH, HNO_3, 0 – 5 °C; iii) $PtO_2.H_2O$, H_2; iv) Formamide, 165 – 170 °C; v) $POCl_3$, *N,N*-diethylaniline; vi) 3-ethynylaniline, pyridine, *i*-PrOH, NH_4OH/H_2O. Overall yield: 56%

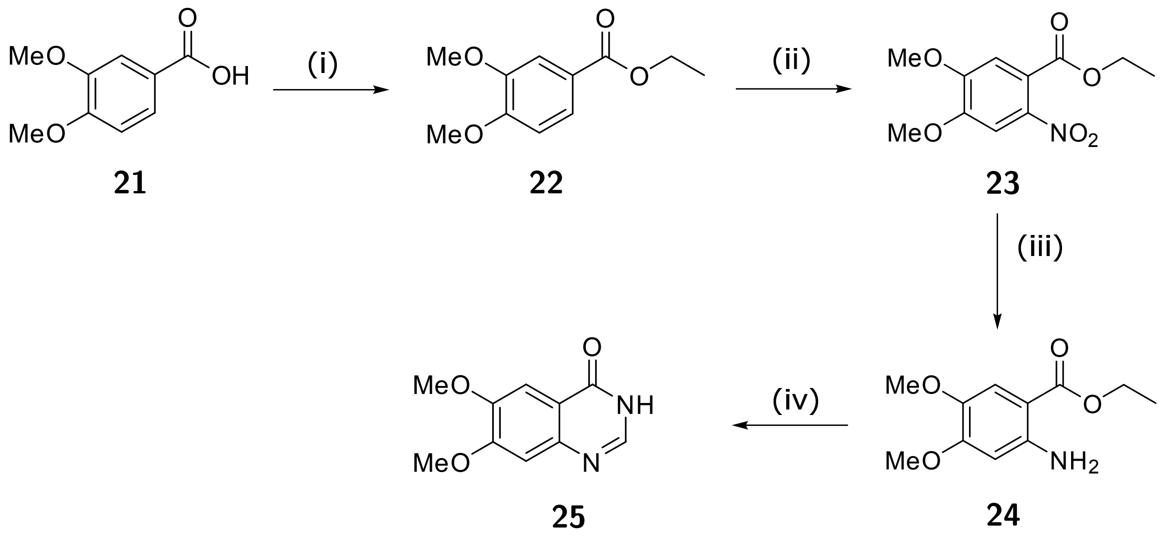

Scheme 4: The synthesis of the intermediate used by Knesl *et al.* for gefitinib; 6,7-dimethoxy-3*H*-quinazolin-4-one **25**.[38] Conditions: i) CH_3CH_2OH, H_2SO_4, reflux; ii) AcOH, HNO_3, $0-5\,°C$; iii) Pd/C, H_2; iv) formamide, $160-170\,°C$.

In 2012, Chen *et al.* synthesised **25** (Scheme 4) on route to three novel ^{18}F labelled 4-aminoquinazoline derivatives.[38] The purpose of this study was to track the potential inhibitors in an *in vitro* study using mice and determine it's route and destination.[38] The compounds possessed the same overall structure as gefitinib. Chen *et al.* described the synthesis of the starting material **25** used by Knesl *et al.* and Chandregowda *et al.* (Scheme 4).[38,39] The commercially available 3,4-dimethoxybenzoic acid **21** first underwent an acid-mediated esterfication using ethanol to afford **22**, which was then nitrated to give **23** and reduced to **24**. The compound **24** then underwent a ring closure with formamide to produce 6,7-dimethoxy-3*H*-quinazolin-4-one **25**.

This starting material **25** was used by Knesl *et al.* in the synthesis of gefitinib **2** (Scheme 5). The methoxy in position 6 on **25** was regioselectively demethylated using L-methionine and methanesulfonic acid to produce an alcohol **26**. The phenol was then protected using an acetyl group to yield **27**; this compound underwent a chlorination to give **28** and aniline substitution (S_NAr) at the chlorine to afford **29**. Once the aniline (3-chloro-4-fluoro aniline) had been added, the acetate group was removed to reveal the phenol again in **30** and the required linker [4-(3- chloropropyl)morpholine] was added to reveal the final product, gefitinib **2**.

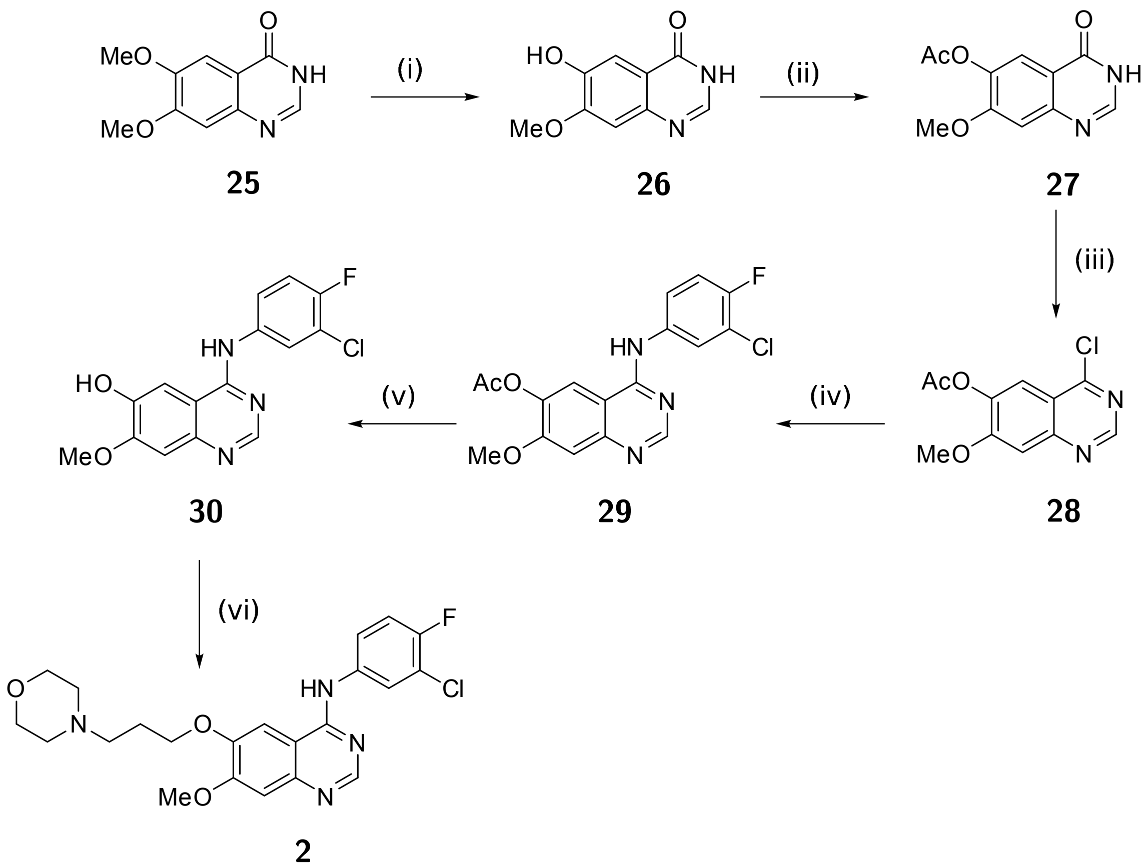

Scheme 5: The synthesis of gefitinib **2** followed by Knesl *et al.*.[37] Conditions: i) Methansulfonic acid, L-methionine, reflux; ii) Ac_2O, pyridine, DMAP; iii) $POCl_3$, Et_2NH; iv) 3-chloro-4-fluorophenylamine, *i*-PrOH; v) NH_3/MeOH, H_2O; vi) 4-(3-chloropropyl)morpholine, K_2CO_3, DMF. Overall Yield: 33%.

The work described in this introduction and the steps towards the synthesis of erlotinib **3** and gefitinib **2** form the basis synthesis in this Master's dissertation. In the next chapter the synthesis plan will be outlined. This will include looking at work previously done in the University of Witwatersrand laboratories by Dr A. M. Prior. The successful synthesis of a reversible covalent inhibitor as well as the obstacles towards the optimal chain length on the quinazoline core. The key step, the

Miyazaki-Newman-Kwart rearrangement will also be introduced. This step will be expanded further in Chapter 3.

Chapter 2

Previous Work and Synthesis plan

In the first chapter, the experimental work performed by Knesl and coworkers was described. The rational behind the covalent-reversible kinase inhibitors was also detailed. In this chapter, the focus will be on the synthesis plan for this MSc. Previous work done in our laboratory at the University of the Witwatersrand by Dr A.M Prior has been focused on the concept of the reversible covalent kinase inhibitor. An initial target molecule **31** (Figure 8) was designed using molecular modeling, with the ketoamide placed in the same position as the Michael acceptor in afatinib **4**, to bind to Cys 797 in the same way as afatinib does.[40] However, owing to complications in the synthesis of **31**, the second CH_2- extended compound **32** was successfully synthesised at Wits.[40]

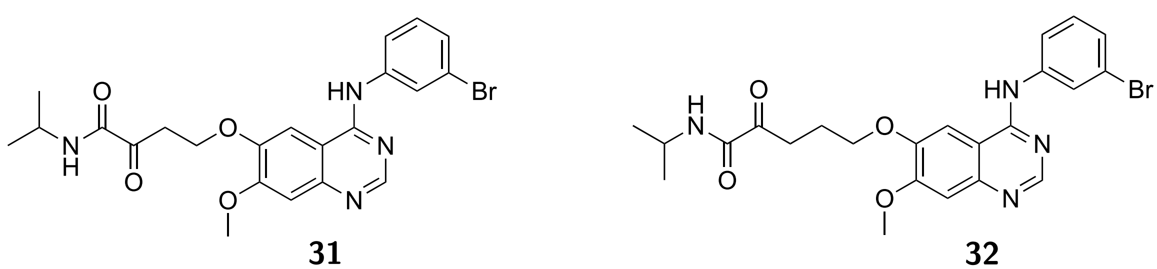

Figure 8: Reversible covalent inhibitors **31** and **32**

In the project by Dr A. M Prior, the phenol **33** was reacted with 3-bromopropanol **34** to form the intermediate **35** with a terminal OH group Scheme 6. The terminal alcohol was then oxidised with Dess-Martin periodinane (DMP) to give the aldehyde **36**. Although this aldehyde formed, it was highly unstable due to a reverse Michael reaction and so could not be isolated in reasonable yields. Because the aldehyde would undergo a reverse Michael addition reaction to give back compound **33**, the final the synthesis of **31** was not achieved. The reverse Michael addition can be seen in Scheme 7.

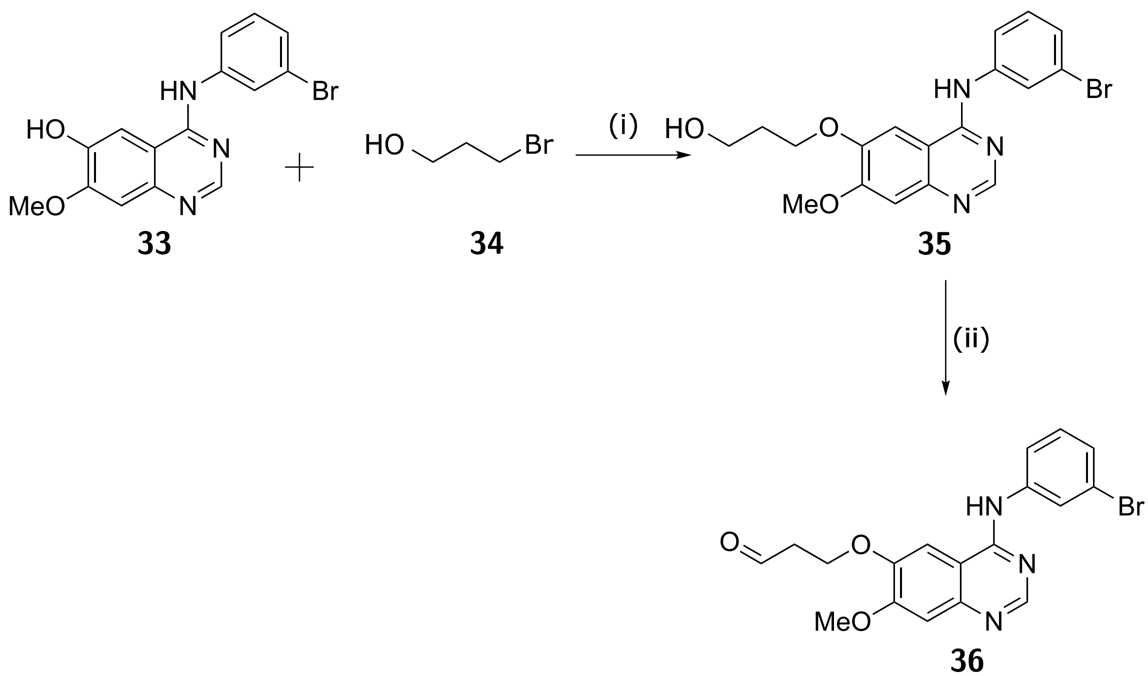

Scheme 6: Synthesis of **36** Conditions: i) K_2CO_3/ DMF, 80 °C, Yield: 60%, ii) DMP, DCM/DMF, Yield: 50%

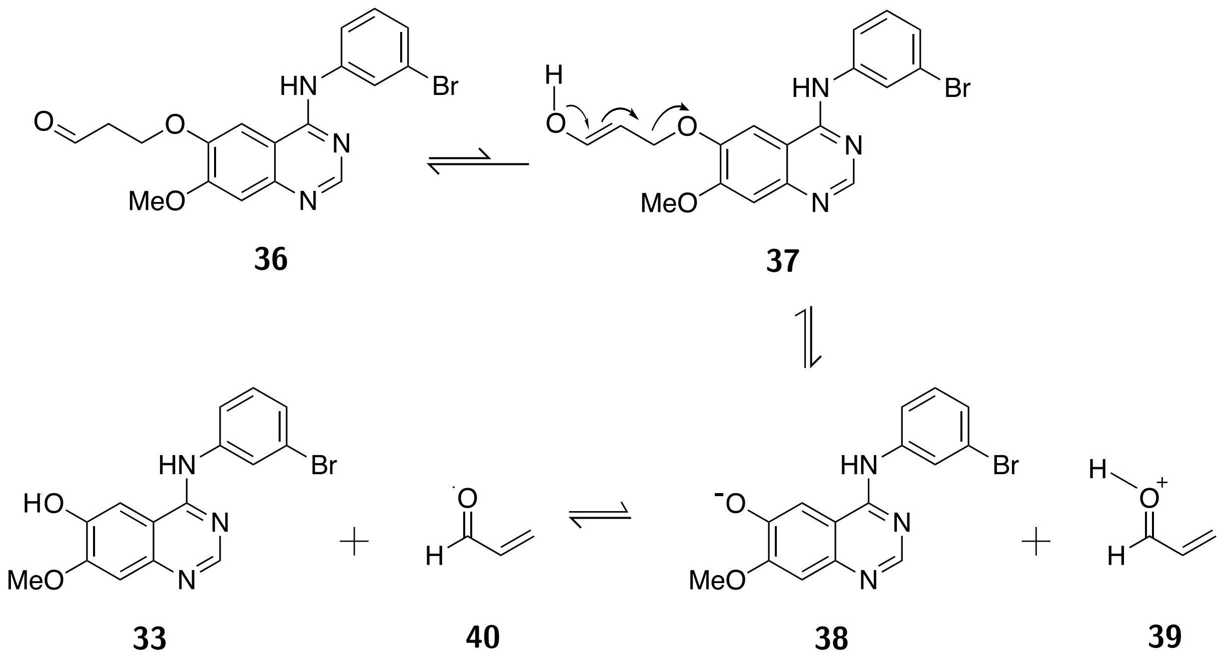

Scheme 7: Reverse Michael addition of **36**

It was at this point that an extra carbon was added to the chain by replacing 3-bromopropanol with 4-bromo-1-butanol **41**. As shown in Scheme 8, the phenol **33** was reacted with 4- bromo-1-butanol **41** to form the phenol **42** with an extra carbon. This extra carbon prevented the reverse Michael from occurring and so the phenol **42** could be oxidised to form the aldehyde **43**. From here the isocyanide could be added to the aldehyde **43** to form **44** and the oxidation to the ketoamide could occur, hence successfully making the final compound **32**. However in the computational modeling it was seen that the extra carbon in **32** caused the chain to bend slightly and so the binding with the Cys 797 was not ideal.

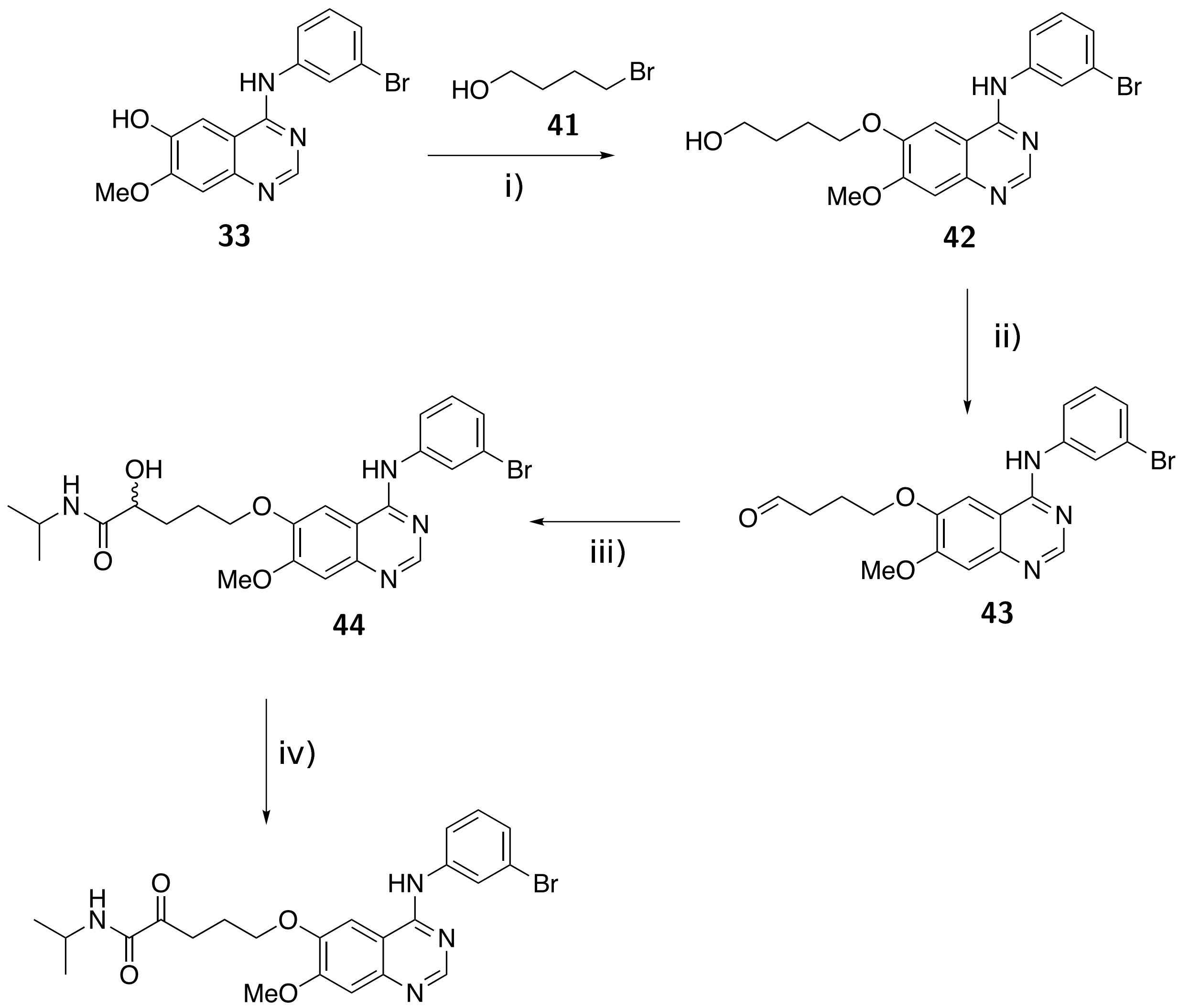

Scheme 8: The route towards the synthesis of **32**. Conditions: i) K_2CO_3, DMF, 120 °C; ii) DMP, DCM/DMF, RT; iii) CN-i-Pr, MeOH/water, K_2CO_3, AcOH; iv) DMP, DCM, RT.

The focus of this MSc was therefore to produce a reversible covalent inhibitor with good potential to bind to Cys 797, but that would be more stable than compounds formed during the synthesis of **31**. We hoped the introduction of a sulfur atom instead of the oxygen atom at the 6$^{\text{th}}$ position (example: **13**), would accomplish this. In terms of overcoming the reverse Michael Addition on the alcohol it was hypothesised that instead of starting with an alcohol, we would attempt to start with a thiol, the SH. According to the hard soft acid base (HSAB) theory, acrolein which is a soft electrophile would prefer to react with a thiol, a soft nucleophile, compared to a reaction with an alcohol which is a hard nucleophile.[41]

In our retro-synthetic strategy (Scheme 9), towards the target compound **13** we took advantage of the work done towards the synthesis of **32** (Scheme 8). Therefore we envisaged that the target compound **13** could be obtained from the amide **45** through an oxidation reaction. In turn, the amide **45** could be accessed by an addition reaction of isopropylisocyanide to the aldehyde **46**.

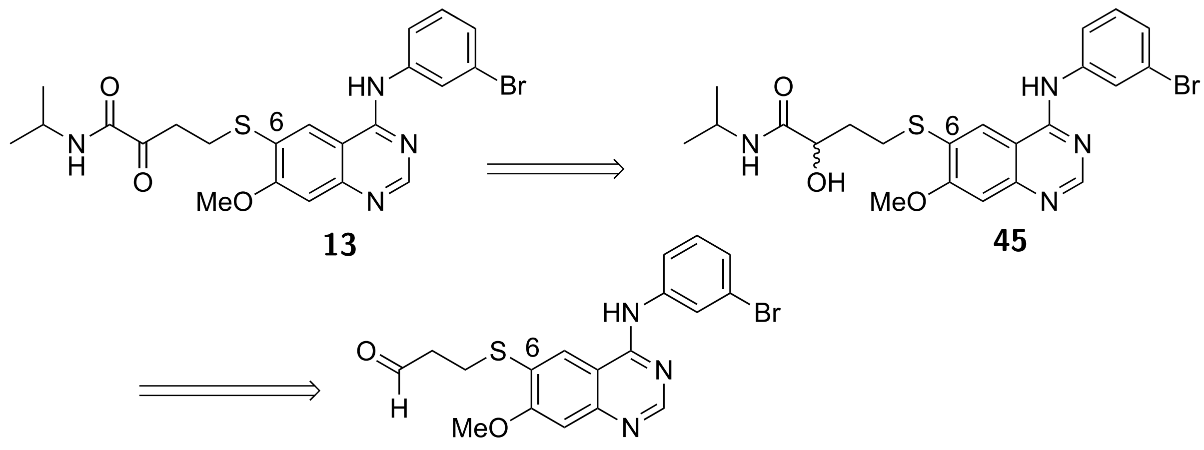

13 **45** **46**

Scheme 9: The retrosynthetic route of the target molecule **13**.

The goal was to now find a way to replace the alcohol with a thiol in position 6 on the quinazoline core of **13**. The retro-synthetic strategy for this can be seen in Scheme 10. From the hypothetic retrosynthesis we should be able to achieve aldehyde **46** through the addition of acrolein **40** to the thiol **47**. The thiol **47** is obtained through the elimination of the carbomoyl group on **48**. The synthesis of **48** can be achieved through a rearrangement. The most common rearrangement in which to achieve this conversion is the Miyazaki-Newman-Kwart (MNK) rearrangement, in which first a carbamothioyl group is added to the alcohol **33** to form the precursor **49**. This is then rearranged at high temperatures to form **48**. The Miyazaki-Newman-Kwart rearrangement will be discussed in detail in the next section.

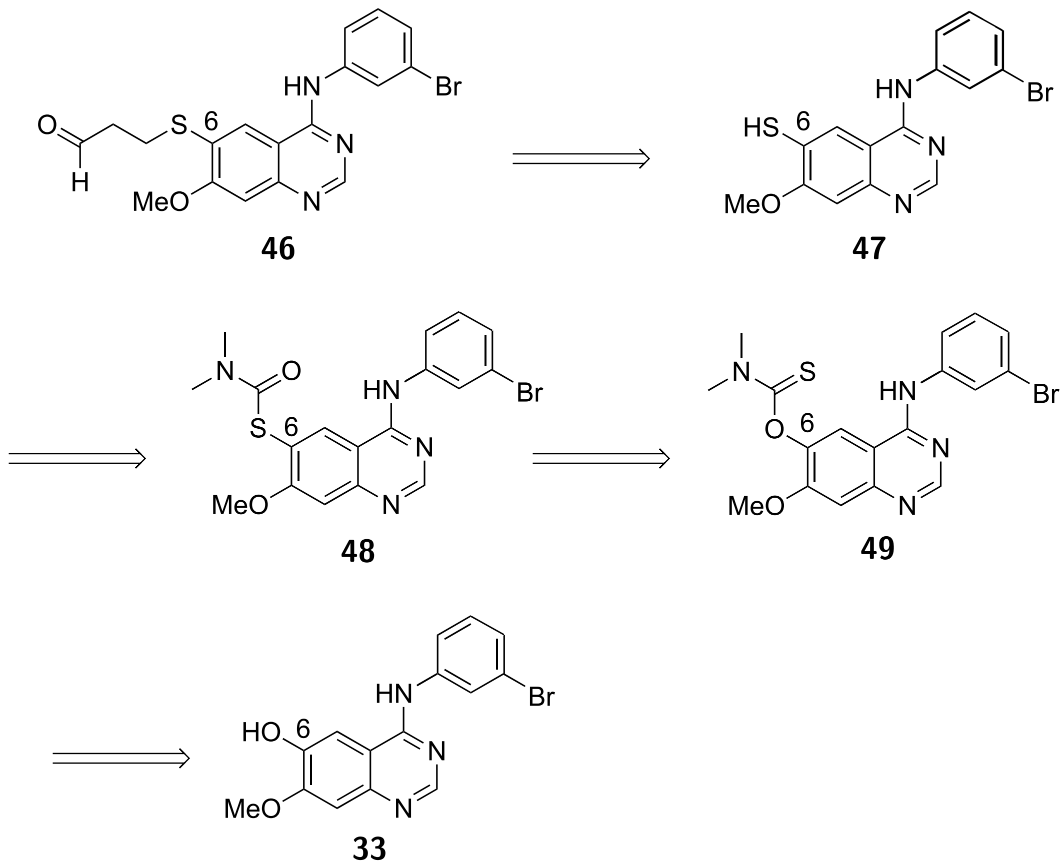

Scheme 10: The retrosynthetic route of **46**.

Chapter 3

Miyazaki-Newman-Kwart Rearrangement

As discussed in 2 the key step in the synthesis of the target molecules (**13** and **70**) of this project requires the conversion of an aromatic alcohol into a thiol. In order to achieve this we used the Miyazaki-Newman-Kwart (MNK) rearrangement

The Newman-Kwart rearrangement (NKR) is named after Harold Kwart[42] and Melvin S. Newman.[43] They discovered the NKR reaction in 1965[43] and 1966[42] respectively. It was not until later that it was observed that Koshin Miyazaki of Osaka, Japan also discovered the reaction in 1965.[44] It has thus become accepted to refer to the rearrangement as the Miyazaki-Newman-Kwart (MNK) rearrangement.[45]The MNK rearrangement is a reaction in which an oxygen and sulfur are mutually exchanged. The MNK rearrangement allow researchers to access many sulfur-containing aromatic compounds. These range from thiols to sulfonic acids.[46] The rearrangement is commonly used to convert a phenol into a thiol on aromatic rings. In Scheme 11, the phenol **50** is converted into **51** by the addition of carbamothioyl chloride. Compound **51** is then subjected to extreme conditions, either very high temperatures or microwave conditions to rearrange the oxygen and the sulfur on the benzene ring to afford **52**. The carbamoyl group is then removed to expose the thiol **53**. This can be further reacted to remove the thiol using Raney Nickel to give **54** and so the overall effect would be the removal of a phenol group.[45,46]

However, there are also many industrial applications that make this an interesting reaction, for example, in the preparation of chiral ligands, dyestuffs, agrochemicals, as well as making a big impact in the field of supramolecular chemistry.[47,48] The application that we are most interested in is that for the pharmaceutical industry.

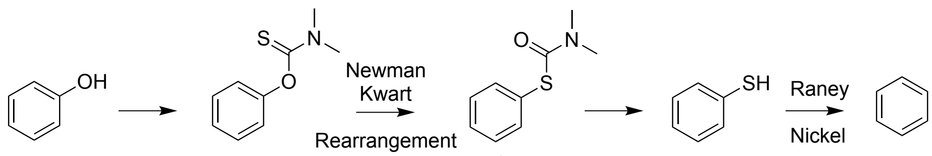

50 51 52 53 54

Scheme 11: The Miyazaki-Newman-Kwart rearrangement on a simple benzene ring.

The MNK rearrangement was not the first rearrangement like this, it was in 1930 that Schönberg first observed the thione-thiol rearrangement, now commonly known as the Schönberg rearrangement (Scheme 12).[45,49] Schönberg's starting material was a symmetrical xanthate **55**. He then rearranged the sulfur and oxygen, under thermal heating, to form a carbonyl-type compound **56**, which was then further reacted to afford the thiol **53**. It can be seen that this is not an efficient rearrangement as the highest possible yield of product is 50%. It was not until the introduction of a nitrogen atom by Miyazaki that we saw the efficiency improve dramatically (Scheme 13).[45] Miyazaki was able to increase the yields by including a nitrogen into the starting material **57** and by rearranging at high temperatures to form **58**.[50]

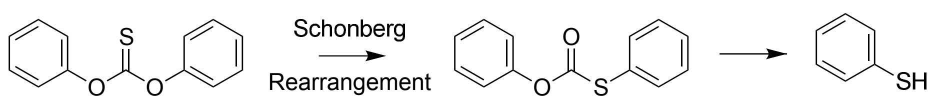

55 56 53

Scheme 12: The Schönberg rearrangement.

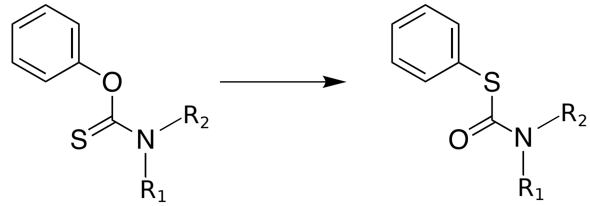

57 **58**

Scheme 13: Miyazaki included the nitrogens as an extension of the Schönberg rearrangement.

The currently accepted mechanism for the MNK rearrangement is via a four membered cyclic transition state as can be seen in Scheme 14.[45] The mechanism is thought to proceed by attack of the sulfur in **51** on the aromatic ipso carbon to give **59** with a negative charge on the adjacent carbon on the benzene ring, and a positive charge on the non-aromatic carbon. The negative charge can then be delocalised on the benzene ring and the positive charge situated on the nitrogen atom of **60**. Finally, the electrons are transferred onto the oxygen to form a carbonyl group of the favourable structure **52**. This mechanism has been investigated and scrutinised by many researchers over the years. A brief history and summary of this research is given below.

Kwart and Evans used the Schönberg Rearrangement as the basis for their hypothe-

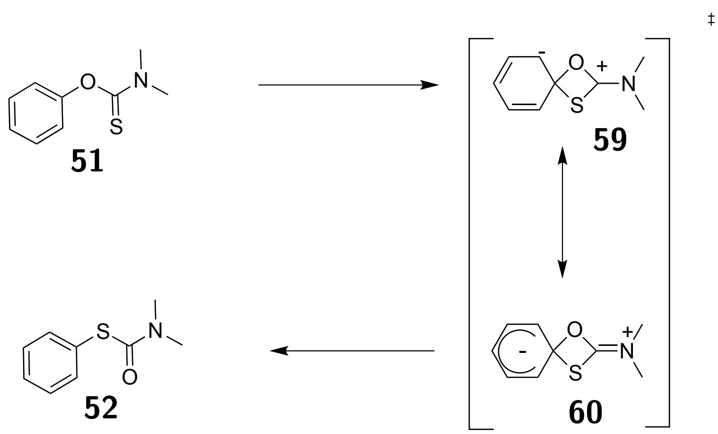

Scheme 14: The currently accepted mechanism of the Miyazaki-Newman-Kwart rearrangement.

sis. The Schönberg rearrangement, which can be seen in Scheme 12, was the original method of converting a phenol to a thiol.[43] However with a maximum yield of 50%, the scope of the reaction was limited. Electron-withdrawing groups on the aromatic ring were found to accelerate the rearrangement, which occurs due to the nucleophilic character of the sulfur group and the fact that the oxygen is a good leaving group.[42] If the Schönberg rearrangement does in fact occur via a four membered cyclic transition state, then there would be no need for solvation. Kwart and Evans thus used this knowledge to test the proposed intramolecular mechanism.

Newman and Barnes expanded on the work done by Kwart and Evans by exploring the generality of the still unnamed reaction.[43] They determined that both time and temperature were important and that if the reaction ran for a longer time, then the temperature of the reaction could be lowered.[43] The use of boron trifluoride and hydrogen chloride as catalysts allowed for the temperature to be dropped by at least 60 °C.[43] It was further found that the R groups on the nitrogen had little to no effect on the reaction, but that it was not ideal to have a NHR substituted nitrogen (where $R \neq H$) as the heating of the reaction resulted in the cleavage to an isothiocyanate and a phenol.[43] Newman agreed with Kwart and also predicted that the rearrangement occurred via a nucleophilic attack at the aromatic carbon bearing the oxygen substituent. Evidence to suggest this includes the fact that electron-withdrawing groups on the aromatic ring favour the reaction, smaller groups on the nitrogen promote the reaction and that the rearrangements of trifluoride and hydrogen chloride salts of the reagents occur at room temperature.[43]

In 1967, Miyazaki explored the kinetics of the rearrangement in an attempt to determine the mechanism of the rearrangement.[51] He conducted his rearrangements neat at 170 °C and 190 °C, and monitored them using UV spectroscopy. Through these experiments of fifteen different compounds, he concluded that the reactions were first order reactions.[51] He corroborated Newman's findings that electron-withdrawing groups allowed the reaction to proceed at a faster rate, and that this was due to the fact that the transition state of the rearrangement was stabilised by the resonance effects of aromatic substituents, particularly than in the *para* position. Miyazaki also concluded that the R group of the carbamothioyl moiety had little effect on the rearrangement. Finally and probably most importantly in later debates, Miyazaki determined that the reaction occurred via an intramolecular pathway. Cross-over reactions, between molecules with different substituents on the aromatic ring were performed, but no cross-over products were observed.[51]

Overall, the three scientists came to the same conclusions about the rearrangement between 1965 and 1968. The intramolecular four membered cyclic transition state was confirmed by Miyazaki's cross-over reactions. Although the intramolecular mechanism was agreed on by all three of the above chemists, this has been disputed over the years ,with some researchers claiming that the reaction in fact occurs via an intermolecular transition state.

In 1968, Relles focused on proving Kwart's theory that the rearrangement occurred via the four membered transition state, and that the substituents in the *ortho* position assisted the rearrangement by reducing the freedom of rotation. This hinderance of rotation is known as the SAHR (steric acceleration due to hindered rotation) effect. By decreasing the freedom of rotation, you will decrease the change in entropy from the starting material to the transition state.[52] However, if a group in the *ortho* position is too bulky, then it will hinder the rearrangement reaction.[52] It should be noted that if the reaction proceeds by an intermolecular mechanism, the presence of *ortho* substituents would hinder the reaction rather than assist it. In some cases it proved to be difficult to determine if the reaction was enhanced by the *ortho* substituents or by the electronic factors caused by the electron-withdrawing groups. Thus in order to prove the SAHR effect in this reaction, electron-donating groups were placed in the *ortho* position to determine if the rate of rearrangement increased. Because electron-donating groups destabilise the transition state, an increase in the rate would suggest that the *ortho* substituents do in fact have this SAHR effect. When one methyl was placed in the *ortho* position, the rate increased by 16%. If only polar and steric decelerating effects were to be considered, we would expect the rate to decrease. A 61% increase was observed when two methyl groups were in the *ortho* positions either side of the *ipso* carbon. In the case of the methyl groups, the second methyl exhibits a much larger effect than we would have expected from the initial 16% increase. While this evidence does prove that the restricted free rotation due to the *ortho* substituents increases the rate of reaction, it was also observed that larger groups, such as *t*-butyl groups can cause steric compression and hinder the rearrangement.[52] Interestingly, if there is a halogen in the *ortho* position, there is a chance of competing reaction pathways. The sulfur is able to attack the carbon attached to the halogen, resulting in a substitution reaction of the aromatic ring rather than the desired rearrangement.[53]

As previously stated, the four membered cyclic transition state was questioned by some researchers. In particular in 2008, Gilday *et al.* observed during rearrangements under microwave heating that as the concentration of the arylthiocarbamates was increased, the reaction rate increased disproportionately.[54] It was proposed at this point that the eight-membered transition state, showing an intermolecular reaction was kinetically significant for concentrations above 2M. In 2010, Burns *et al.* decided to investigate this further, as although the four-membered transition state had become so well accepted, the idea of a new mechanism was important to follow up on.[48] Burns *et al.* followed the footsteps of Miyazaki, as they wanted to use the same idea of cross over reactions used in 1967. Taking it one step further, they prepared isotopically labelled reagents.[48] Mass spectroscopy was then used to determine if cross-over reactions had occurred; however, in their experiments no cross-over products were found. As an intramolecular reaction in which no cross over occurs is not easily rationalised, the proposed intermolecular mechanism was reconsidered. Burns *et al.* looked at how the microwave results could have been misinterpreted to appear as if a mixed order reaction was taking place. A commonly used term in microwave reactions is "hunting", when a balancing loop is used to modulate the microwave irradiation power in response to the effective reaction temperature. This correction can lead to an oscillation in temperature.[48] The thick pyrex vessel also causes a lag time in the internal temperature vs the external temperature.[48] After investigation, Burns *et al.* found that the amplitude of hunting was greater with an increased concentration of starting material, and that this could be due to more efficient energy conversion by the concentrated solution. This accounts for the observation that there is a disproportionate increase in the reaction rate when the concentration of the starting material is increased.

In 2016, a research group in Germany investigated the potential of conducting the rearrangement in the microwave using water as a solvent.[46] The MNK reaction performs better under polar solvents as the solvent is able to stabilise the transition state. The question was then raised, to what extent can water stabilise the transition state? The benefits of water, particularly in an age of green chemistry, are obvious, from it being non-flammable to being non-toxic.[46] The rearrangement in water was successful, in particular when looking at substrates with electron-withdrawing substituents. However, a limitation of water was observed when the pressure build-up was too significant for substrates with electron-donating groups, as these required much higher temperatures to facilitate the reaction.[46]

Electron-withdrawing groups are known to stabilise the four membered transition state, and hence favour the rearrangement. The presence of electron-donating groups on the aromatic ring require higher temperatures, longer times or catalysts in order to promote rearrangement.[55] Perkowski *et al.* looked at mediating the rearrangement using organic photoredox catalysis. They hypothesised that the single electron oxidation of the O-aryl carbamothioate would lower the activation energy of the sulfur attack on the *ipso* carbon and hence increase the rate of the rearrangement.[55] In their findings they were able to conclude that an ambient temperature MNK rearrangement is possible through organic redox catalysis using triarylpyrylium salts.[55]

It is important to note that although the rearrangement is a useful route to the thiol derivative of many molecules, the potential for decomposition of sensitive molecules is a genuine concern. Above this, even molecules which are stable at such high temperatures can be charred by the temperature gradient observed when using heating sources like oil baths and heating mantles.[48] Ideally having high temperature for a shorter time period would be ideal.

This chapter provided an overview of the MNK rearrangement, the focus on this rearrangement was important because it is an unusual reaction and a key step in the synthesis. The next chapter will look at the experiments conducted in this MSc towards the final target molecules.

Chapter 4

Results and Discussion

4.1 Attempted synthesis of 4-chloro-6-nitroquinazoline-4(3*H*)-one - 63

In the first attempt to synthesise the desired final product **13**, the starting material was the commercially available 2-amino-4-chlorobenzoic acid **61** (Scheme 15). For the first step, the work done by Buha *et al.* was followed, the same starting material was reacted with formamide. The desired ring closure product **62** was obtained in a yield of 96% compared to the yield of 58% obtained by the research group.[56] The ^{1}H NMR spectrum shows the NH peak at 12.45, and 4 signals integrating for 1 proton each. The sharp peak at about 3.5 ppm is due to water. The next step was to nitrate at the C6 position on the quinazolinone core **62**. This step was also completed by Buha *et al.* with a yield of 92%, no issues were expected with this step.[56] Buha *et al.* added the quinazoline **62** portion-wise to a mixture of nitric acid and sulfuric acid at a maximum temperature of 50 °C. Once the addition was complete the reaction temperature was raised to 90 °C for 45 minutes. Initially this method was followed exactly. The quinazolinone was added portion-wise to a mixture of nitric acid and sulfuric acid, and after complete dissolution of the compound, the solution was orange in colour. The temperature was then raised to 90 °C for 45 minutes. The reaction was poured onto ice and allowed to precipitate. After filtration and drying, the ^{1}H NMR spectrum indicated a mixture of starting material and desired product. In order to ensure the completion of the reaction, it was attempted to monitor it using TLC and allowed the reaction to proceed for 2.5 hours, unfortunately an unidentified contaminant was obtained. The time was then increased to 18 hours, and the reaction yielded only starting material. With the hypothesis that the reaction was reversing, the reaction was preformed under inert conditions, as well as adding acid at various time points during the reaction. It was found that, if the temperature was too high or the time too long, the contaminant was present. However, a full conversion of the **62** to **63** was not achieved without producing the the third unidentified product and unfortunately the three materials were not separate-able using column chromatography.

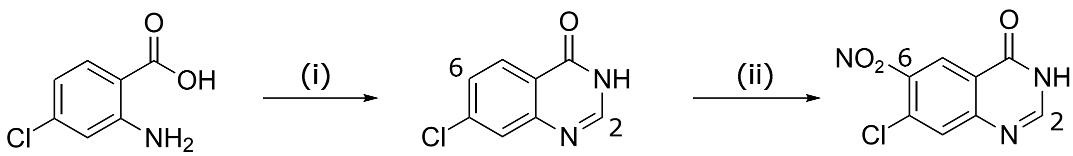

61 **62** **63**

Scheme 15: i) Formamide, reflux for 2 hours. Yield: 96% ; ii) conc. nitric acid, conc. sulfuric acid, 90 °C, 45 min.

4.2 Synthesis of the intermediate 4-chloro-7-methoxyquinazoline-6-yl acetate - 28

An alternative synthetic route to the target quinazoline core was identified. For this synthesis, work done previously in the laboratories at Wits University were followed as well as work reported by Knesl *et al.* and Chen *et al.* in their synthesis of erlotinib **3** and gefitinib **2**.[37,38] In the discussion of the synthesis towards compound **13**, the synthesis of common intermediate **28** Scheme 16 will be discussed. The synthetic route was then split into two, for the synthesis of the two target molecules.

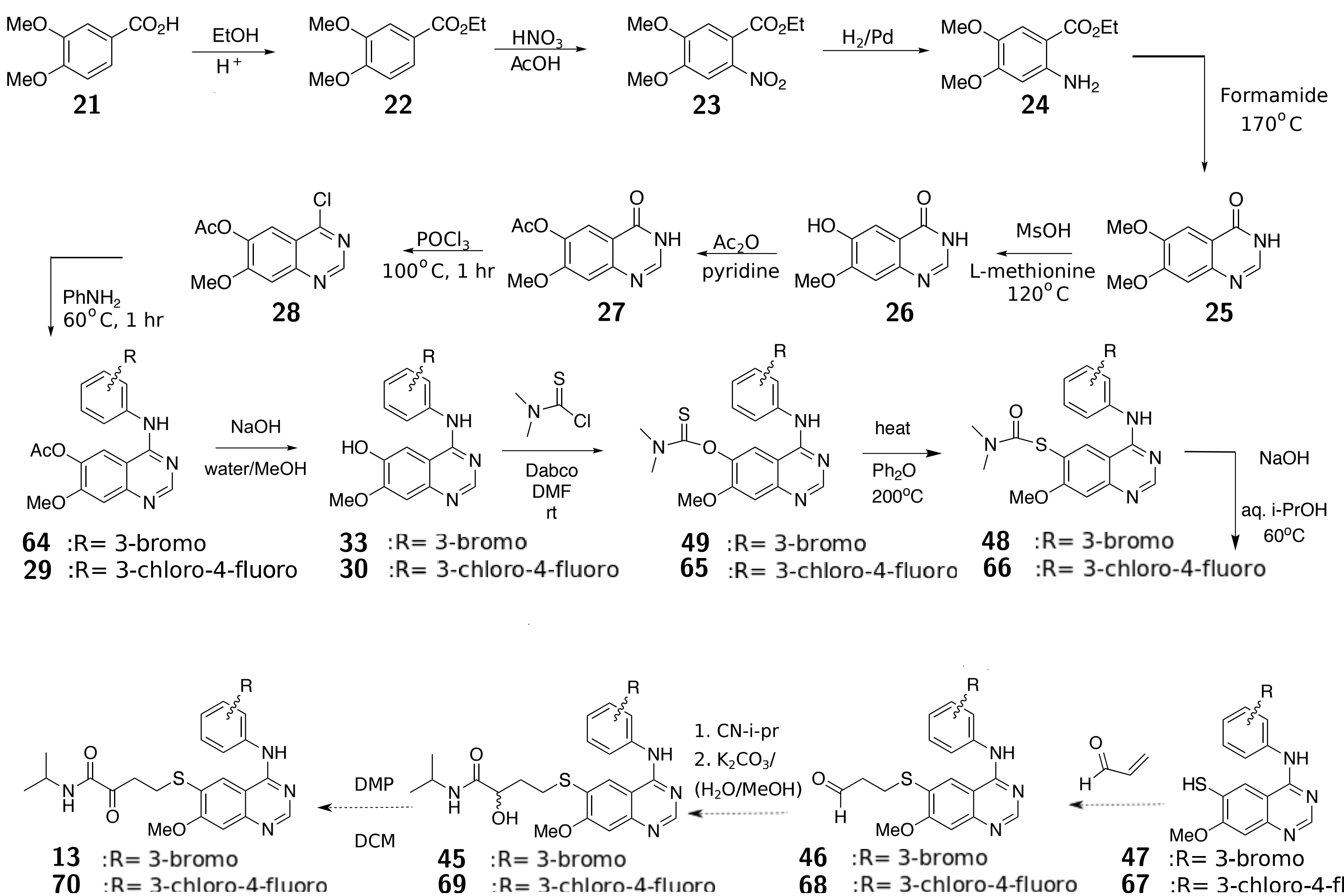

Scheme 16: The full synthesis scheme.

4.2.1 Synthesis of ethyl-3,4-dimethoxybenzoate - 22

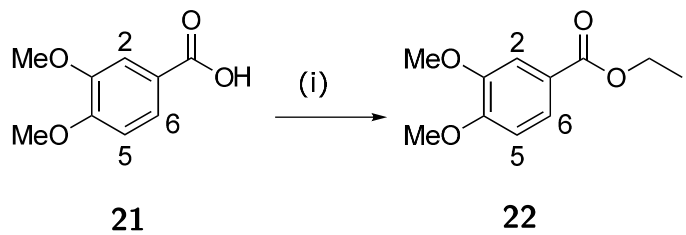

Scheme 17: i) EtOH, H_2SO_4, toluene, reflux for 72 hours. Yield: 85%.

The synthesis of the first intermediate started with the commercially available 3,4-dimethoxybenzoic acid **21**. The acid was converted into the ethyl ester using ethanol and H_2SO_4 (as the catalyst) and could be done a large scale (100 g). The reaction was allowed to go for 72 hours due to the large quantity of starting material, and H_2O was removed using a Dean Stark apparatus. The esterfication was completed successfully on large scales and with a good yield of 85%. The reaction was followed by TLC and only worked up once the starting material was consumed. The reaction yielded a single product was clean and no further purification was required.

From the ^{1}H NMR spectrum, the success of the reaction was confirmed by the quartet at 4.35 ppm due to the CH_2 and the new triplet at 1.38 ppm due to the CH_3 group. In the ^{13}C NMR spectrum 10 signals were observed, the methoxy carbons were in equivalent environments and so were found under one signal at 55.9 ppm. In the ^{1}H NMR spectrum, the methoxy peaks were observed as signals at 3.93 ppm, which integrated for 6 protons. The three aromatic signals show the expected splitting pattern with H6 a doublet of doublets at 7.68 ppm with coupling constants of 8.4 Hz and 2.0 Hz, which correspond to the J values of the H2 and H5 doublet coupling constants. The low resolution mass spectrometer (LRMS) was used to confirm this, a m/z peak was observed at 211.1. The melting point of 42 °C also corresponded with the literature value of the known compound.[57]

4.2.2 Synthesis of ethyl-4,5-dimethoxy-2-nitobenzoate - 23

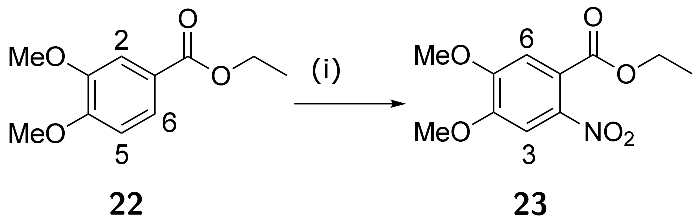

Scheme 18: i) AcOH, HNO_3, RT for 48 hours. Yield: 97%.

The next step in the synthetic route was to nitrate at position 6 on the ring of the ester **22**. This reaction was completely selective. The methoxy groups at position 3 and 4 were electron-donating groups activating position 2, 6 and 5 respectively. So with position 2 and 6 being activated twice, it could be expected that there would be a 50:50 split of products nitrated at these positions. However, no nitration occurs at position 2 or 5. The most electronically favourable product was where the nitro was substituted at position 6, this was because the resulting product **23** had a 1, 2, 4, 5 substitution pattern avoiding the sterics observed in the alternative substitution patterns 1, 2, 5, 6 and 1, 3, 5, 6 on compounds **71** and **72** respectively.

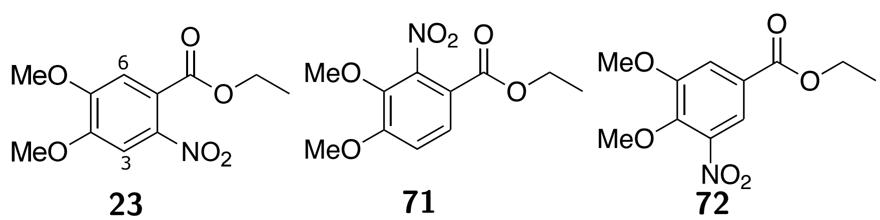

Figure 9: The alternate substitution patterns for the nitration of **22**.

The nitrated compound **23** was successfully synthesised, in a yield of 97%, by dissolving the precursor ethyl-3,4 dimethoxybenzoate **22** in acetic acid at room temperature; this dissolution occurred over a few hours. Once the dissolution was complete, the reaction was cooled down to between $0-5\,°C$. The nitric acid was added drop-wise to the stirring solution. Once all the nitric acid had been added, the reaction was allowed to warm to room temperature and was stirred for a further 48 hours. The reaction was followed by TLC. Upon completion the reaction mixture was diluted with ethyl acetate and washed with saturated sodium bicarbonate solution to remove any excess acid. The ethyl acetate was removed under vacuum to produce a light yellow powder. The product did not require any further purification as it was found to be sufficiently pure using ^{1}H NMR spectroscopy.

The ^{1}H NMR spectrum of **23** indicated that the nitration reaction had been successful and the nitro group was added selectively to the desired position. The two remaining aromatic protons gave rise to singlet signals and showed no coupling to one another, indicating that they were arranged *para* to each other. If the nitro group had added at position 6 of **23**, coupling between the two remaining aromatic proton would have been observed. In the ^{13}C NMR spectrum, the shift of the signal due to the carbon attached to the nitro group from 123.5 ppm to 141.3 ppm with a lower intensity was indicative of a quaternary carbon. The methoxy groups were no longer equivalent, in the ^{1}H NMR spectrum, and the OMe singlet at 3.96 ppm for **22** was split into two signals at 3.96 and 3.97 ppm integrating for 3 protons each. Finally in the ^{13}C NMR spectrum the single peak at 55.87 ppm for **22** now appeared as two peaks at 56.72 and 56.76 ppm, the two OMe groups in **23**.

4.2.3 Synthesis of ethyl-2-amino-4,5-dimethoxybenzoate - 24

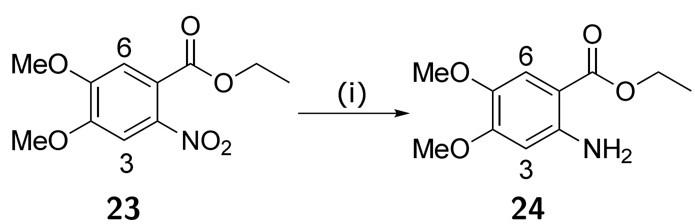

Scheme 19: i) MeOH, 10% Pd/C, $H_{2\,(g)}$, RT for 36 hours. Yield: 98%.

The reduction of the nitro-containing compound **23** to an amine-containing compound **24** was successfully completed under inert conditions. The nitro benzoate **23** was dissolved in methanol, and the whole system was then degassed. In a separate flask, the palladium on carbon was weighed out and that flask was degassed before adding methanol. Once the Pd/C was completely immersed in methanol, the solution of **23** in methanol was transferred to the reaction vessel. A balloon was used to provide a constant supply of hydrogen gas to the reaction and the reaction proceeded for 36 hours. Once completed, the Pd/C was removed by filtration over celite. The methanol was then removed under vacuum and a white solid was obtained in a 98% yield.

The primary evidence for the success of this reaction could be seen in the ^{1}H NMR spectrum, with a new broad peak at 5.2 ppm integrating for 2 protons appearing, indicative of the NH_2 group. The remainder of the peaks in the ^{1}H NMR spectrum remained relatively unchanged by this reduction. In the ^{13}C NMR spectrum it could be seen that majority of the aromatic carbons had shifted downfield with the conversion of the nitro group into an amine group. Although the shift for the peak for C2 on **24** was not significant, the relative intensity did increase.

4.2.4 Synthesis of 6,7-dimethoxyquinazolin-4(3*H*)-one - 25

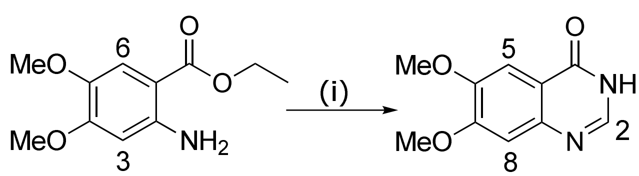

24 **25**

Scheme 20: Formamide, $Ar_{(g)}$, 170 °C for 12 hours. Yield: 90%.

The formation of the quinazolinone was achieved by reacting the amino benzoate **24** with formamide at 170 °C for 12 hours. After approximately 10 hours, a solid was precipitate out of the reaction mixture, and the progress of the reaction was monitored using low resolution mass spectrometry, to ensure completion. It was not possible to check the reaction progress using TLC as the product was insoluble in most solvents. Once the reaction was complete, the reaction was allowed to cool to room temperature; the product was then isolated by filtration and washed with water to remove any excess formamide in the filtration process. Initially as much as 500 mL of water was added to the reaction, and the solid was also washed with acetonitrile and acetone; however, the volume of water was decreased when the yield of the isolated producted was seen to be low. It was also found that washing with acetonitrile and acetone proved to be unnecessary, and only about 20 mL of water was necessary to remove the excess formamide. This resulted in an increase in the yield of product from 60% to 88%. The reaction was allowed to dry in the desiccator overnight and did not require any further purification.

The solubility of this product, even in DMSO, was incredibly low, and so it was necessary to make the NMR spectroscopic sample concentrated and to use the 500 MHz NMR spectrometer at a reduced number of scans, in order to obtain the ^{13}C NMR spectrum before the product precipitated out of the deuterated solvent. The ^{1}H spectrum showed that the CH_2 and the CH_3 of the ester group were no longer present, and a new singlet at 7.98 ppm corresponding to the CH (C2) of the newly formed ring on the quinazoline core **25** was observed. The NH could also be seen as a broad singlet at 12.05 ppm as a broad singlet integrating for 1 proton. It is possible for this molecule to have multiple tautomers, two NH forms and an OH form. However, only one form is observed in the ^{1}H NMR spectrum. The only signals in the aliphatic region of the ^{13}C NMR spectrum corresponded to the two methoxy groups at around 56 ppm. In the ^{13}C NMR spectrum, the signal due to the ketone carbon (C4) can be seen at 160.5 ppm. All of these features confirmed the formation of the quinazoline core. The mechanism of this reaction can be seen in Scheme 21. The amine group on the formamide attacks the electrophilic carbon of **24**. This was followed by the removal of ethanol and the intramolecular reaction of the amine and the ester carbonyl from the formamide. The elimination of water results in the quinazolinone core **25**

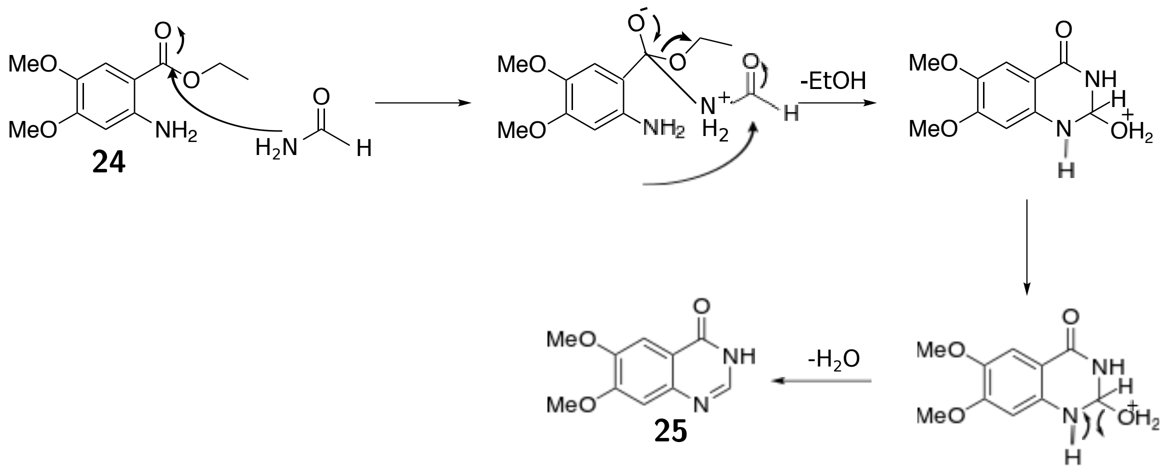

Scheme 21: Mechanism of the formamide ring-closure to obtain **25**.

4.2.5 Synthesis of 6-hydroxy-7-methoxyquinazolin-4(3*H*)-one - 26

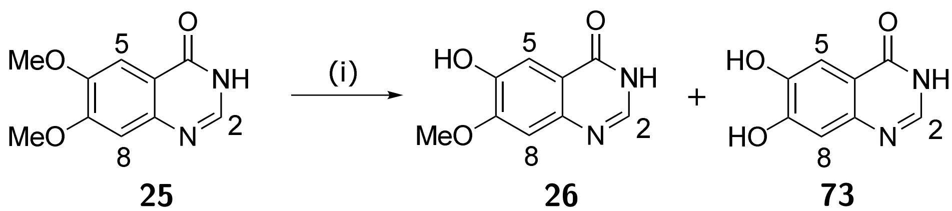

Scheme 22: i) $_{\text{DL}}$-methionine, MSOH, 110 °C for 12 hours.

The next step of the synthesis involved selectively deprotecting the methoxy group at position 6 using $_{\text{DL}}$-methionine and methane sulfonic acid. This has been reported in literature, namely by Knesl *et al.* and Chen *et al.*.[37,38] Although Knesl *et al.* reported selective deprotection, in all the experiments that were conducted 3 products were always, namely the starting material **25**, the desired product **26** and a side-product **73**. The relative amounts of these compounds was dependent on the time and temperature of the reaction. The experiment was conducted a number of times at various temperatures and for different lengths of time. It was observed that the reaction was more sensitive to temperature than to time. The optimal time and temperature was found to be 110 °C for 12 hours. However, the desired product was not isolated free of either **25** or **73**, and as such, the mixture containing **26** as the major product (estimated 90% yield) was carried through into the subsequent step of the synthesis. In the work done by Knesl *et al.*, the desired compound **26** was not characterised. Although the reaction was monitored by HPLC and they obtained 95% purity the reason for not characterising the product was not provided. The compound was carried through to the next step.

DL-methionine is an amino acid that plays an important role in the metabolism of humans and other species. The role the DL-methionine plays in the demethylation reaction is not detailed in literature. The reason it was used in this experiment is because it was used by both Knesl *et al.* and Chen *et al.*, the mechanism was not described in either of these two papers.[37,38]

4.2.6 Synthesis of 7-methoxy-4-oxo-3,4-dihydroquinazolin-6-yl acetate - 27

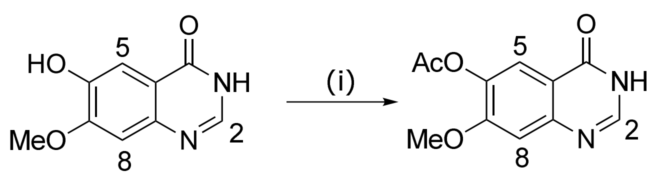

26 **27**

Scheme 23: i) Acetic anhydride, DMAP (catalytic), pyridine, 100 °C for 36 hours.

The phenol in the mixture was then protected with an acetyl group, using a catalytic amount of DMAP and acetic anhydride. The reaction temperature was increased to 80 °C and then heated with pyridine under inert atmosphere. It was important that this mixture was completely dry, or it may boil over when the pyridine was added to the reaction. After addition of the pyridine, the reaction was heated up to 100 °C. Once completed the reaction was quenched by pouring it onto ice, and the product was isolated by filtration to afford a white powder. The product isolated was the single desired product **27**, in a moderate yield of 66%. It was thought that the minor compounds from the mixture, **25** and **73** were removed during the work-up of the reaction. The yield was improved from the literature yield of 56%.[37]

The ^{1}H NMR spectrum of compound **27** clearly showed the acetate protecting group with a singlet signal visible at 2.29 ppm. The signal at 3.91 ppm ,which was due to the methoxy group, shows that the other two products were removed during the work up. The signal due to the NH was still present at 12.18 ppm. In the ^{13}C NMR spectrum the acetate group could be observed as two signals at 20.8 ppm and 169.2 ppm. The signal at 56.9 ppm corresponded to the methoxy group at position 7 of the quinazoline core. And finally the peak at 169.4 ppm indicated the presence of the carbonyl on the quinazoline core. The ^{1}H NMR spectrum corresponds to the literature spectrum,[37] and although the ^{13}C NMR does not align exactly to the literature spectrum,[37] the peaks are all in similar environments.

Due to the correlation with the ^{1}H NMR spectrum in the paper by Knesl *et al.*, there is confidence that the correct compound **26** was carried through from Scheme 22.

4.2.7 Synthesis of 4-chloro-7-methoxy-3,4-dihydroquinazolin-6-yl acetate - 28

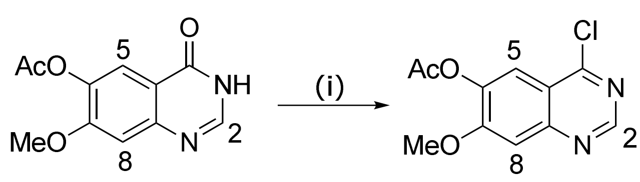

Scheme 24: $POCl_3$, diethylaniline, $Ar_{(g)}$, 80 °C for 3 hours. Yield: 79%.

The synthesis of compound **28** provided us with many challenges, despite reported accounts in the literature.[37,38] The optimised synthesis of **28** involved the addition of $POCl_3$ to a mixture of 7-methoxy-4-oxo-3,4-dihydroquinazolin-6-yl acetate **27** and *N,N*-diethylaniline. The reaction was then heated up to 80 °C, under inert conditions. It was important that the starting material was dry as any moisture present promoted the reverse reaction. The reaction was allowed to run for 3 hours, as analysis by TLC or low resolution mass spectrometry was difficult. After 3 hours, the hot reaction mixture was poured into a conical flask, cooled on liquid nitrogen. When the reaction mixture had been cooled below room temperature the solution became a solid. The flask was then vigorously shaken with the ice to quench the $POCl_3$, as in our experience any "hot spots" would cause the reverse reaction to afford the starting material. After a few minutes of shaking, a solid material formed in the melted ice. When majority of the ice was melted the product was filtered and washed with samll amounts of cold water to remove excess acid. Unfortunately, the reaction reversed in deuterated DMSO, making characterisation difficult. The NMR spectroscopic sample had be prepared and run immediately in order to observe only the desired product. The yield of 79% was lower than the 92% yield reported by Knesl *et al.*.

The ^{1}H NMR spectrum of **28** showed the three aromatic protons shifting downfield due to the deshielding nature of the chlorine in position 4 on the quinazoline core. The observed loss of the signal due to the NH group shows the full aromatisation of the ring, while the acetate and the methoxy signal shifts remain relatively unchanged.

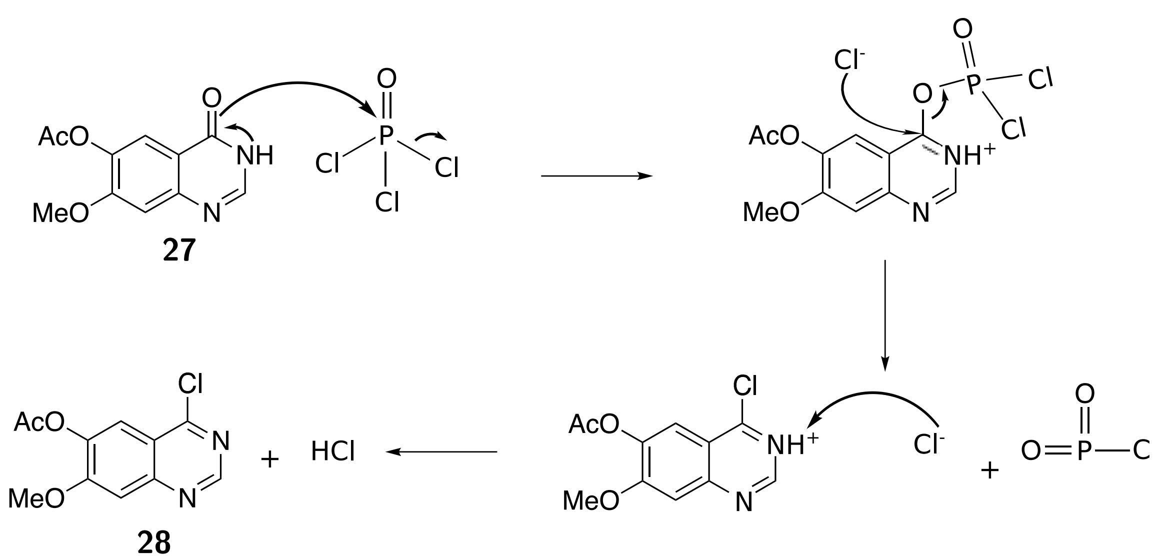

Scheme 25: Mechanism of the ring-closure to obtain **28**.

4.3 Synthesis of the target molecules 13 and 70

With the key intermediate **28** in hand, the analogueswe with different functionality in the hydrophobic portion of the inhibitor were synthesised. This involved the addition of 3-bromoaniline, and 3-chloro 4-fluoroaniline, to obtain the two target compounds **13** and **70**.

4.3.1 Synthesis of 4-[(3-bromophenyl)amino]-7-methoxyquinazolin-6-yl acetate - 64

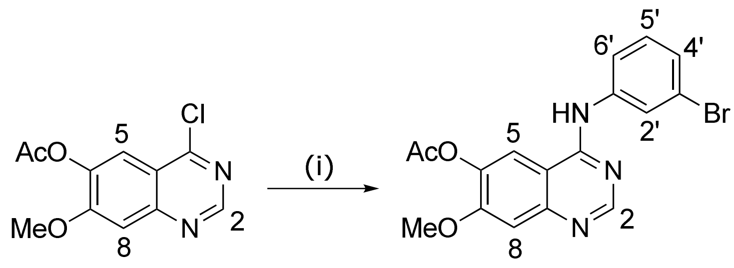

Scheme 26: i) 3-Bromoaniline, DMF, 80 °C for 2 hours. Yield: 73%.

In order to facilitate substitution of the chloro substituent in compound **28** with the 3-bromoaniline, it was important that the starting material was dry to prevent hydrolysis to **27**. The 3-bromoaniline was added to the starting material **28** in DMF, and then heated to 80 °C for 2 hours. The reaction was then cooled in ice, and diluted with diethyl ether. After cooling in ice for half an hour a solid precipitated out, which was filtered and washed with cold diethyl ether. The resulting product was a brown powder in a yield of 73%.

The addition of the aniline to **28** was immediately obvious when looking at the ^{1}H NMR spectrum. There were additional peaks in the aromatic region, accounting for an additional 4 hydrogens. There was also an additional NH peak accounting for the NH from the aniline at 11.59 ppm. The proton at position 5 on the quinazoline core was most affected by the addition of the aniline and experienced a large shift from 7.79 ppm in the spectrum of **28** to 8.86 ppm in **64**.

4.3.2 Synthesis of 4-[(3-chloro-4-fluorophenyl)amino]-7-methoxy-3,4-dihydroquinazolin-6-yl acetate - 29

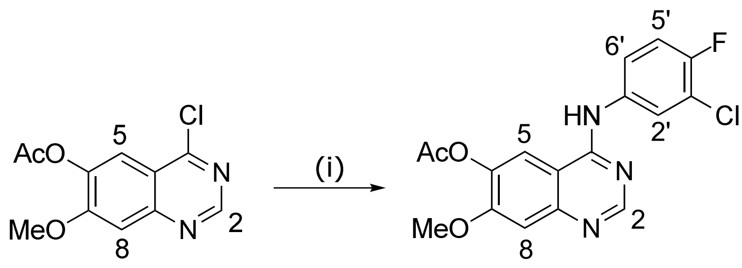

28 **29**

Scheme 27: i) 3-chloro-4-fluoroaniline, DMF, 80 °C for 2.5 hours. Yield: 68%.

The substitution of 3-chloro-4-fluoroaniline onto the quinazoline **28** was approached in a similar fashion to the reaction seen in Scheme 26. The starting material **28**, was added to DMF and treated with the 3-chloro-4-fluoroaniline. The reaction was then heated to 80 °C for 2.5 hours. Once the reaction had cooled, it was seen that the product started to precipitate out of solution. A small amount of diethyl ether was added, and the reaction was cooled in an ice bath. The reaction mixture was then filtered to afford the product which was washed with diethyl ether.

The ^{1}H NMR spectrum of product **29** clearly shows that the addition of the aniline was successful, as the NH peak from the aniline was visible as a signal at 11.63 ppm. There were also an additional three peaks in the aromatic region of the ^{1}H NMR specturm accounting for the 3 hydrogens on the aniline aromatic ring. The signal splitting from the fluorine could also be observed. The doublet of doublets at 8.05 ppm was due to the proton on carbon 5 (H-5'); here the coupling to the proton at position 6 (H-6') and the fluorine on carbon 4 could be seen. The doublet of doublets of doublets (ddd) at 7.75 ppm was due to the proton (H-6'); and the coupling to the protons on carbon 2' and carbon 5' and the fluorine on carbon 4' was observed. The signal at 7.55 ppm in the ^{1}H NMR spectrum was for a combination of two signals the first being the proton on carbon 2 and the second being the proton on carbon 8. The methoxy group and acetate group signals were at 4.00 ppm and 2.38 ppm respectively. The ^{1}H NMR spectrum is comparable to that of the spectrum found in the literature.[37] The ^{13}C NMR spectrum was not obtained due to the poor solubility of the product.

4.3.3 Synthesis of 4-[(3-bromophenyl)amino]-7-methoxyquinazolin-6-ol - 33

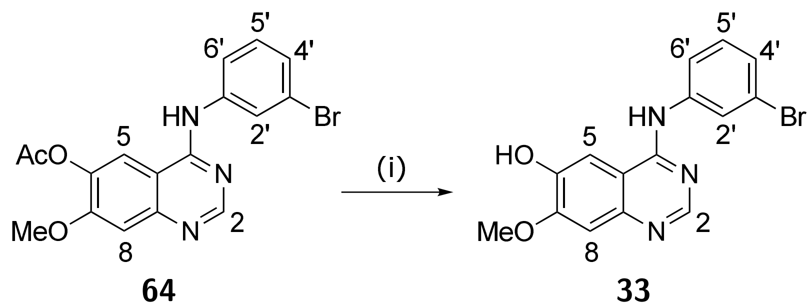

Scheme 28: i) 7 N NH_3/MeOH, RT for 48 hours. Yield: 84%.

The acetate-protecting group could now be removed in order to functionalise the chain at position 6. This was an easy reaction where the acetate-protected compound was suspended in a methanolic ammonia solution. The reaction was tracked via TLC and once the reaction was complete, the methanolic ammonia solution was removed under vacuum and the residue washed with a small amount of cold water. The same method was followed by Knesl *et al.* who obtained a yield of 90% of the desired product compared to our yield of 84%.[37]

The proton NMR spectrum showed that the acetate peak was no longer present at 2.39 ppm and a new signal due to the OH group at 9.61 ppm had appeared, which was not previously present. The proton at position 5 on the quinazoline core was once again the most affected, being shifted upfield to 7.81 ppm from 8.86 ppm.

4.3.4 Synthesis of 4-[(3-chloro-4-fluorophenyl)amino]-7-methoxy-3,4-dihydroquinazolin-6-ol - 30

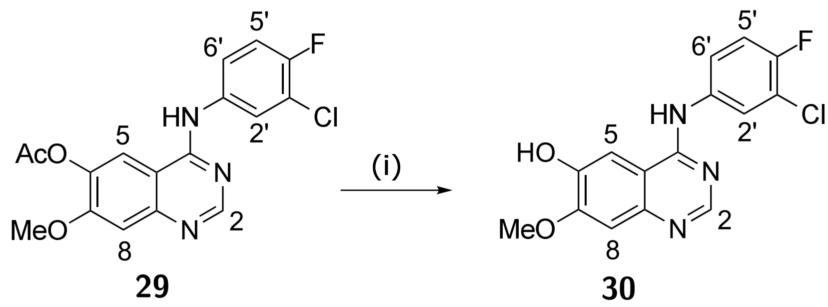

Scheme 29: i) 7 N NH_3/MeOH, RT for 48 hours. Yield: 73%.

The acetate-protected compound **29** was suspended in a methanolic ammonia solution for 48 hours. The reaction was tracked via TLC, once the reaction was complete, the methanolic ammonia solution was removed under vacuum and the residue washed with small amount of cold water. The reaction was successful with a yield of 73%.

The acetate peak that was at 2.38 ppm was no longer present in the ^{1}H NMR spectra for **30**, this showed the success of the reaction. At 9.70 ppm the the alcohol peak was observed. It was also seen that the proton at position 5 was affected by the removal of this group, this was evident by the shift from 8.83 ppm to 7.82 ppm. This was also observed in the experiment for **33**, Scheme 28. This provided evidence that the phenol in **26** and the acetate in **27** was at position 6 as required.

The next step in the synthesis plan is the addition of the thiocarbamoyl group. Initially, the addition of this group and subsequent rearrangement was tested on two test reactions before conducting the reactions on **33** and **30**. This was done in order to better understand the reactions.

4.3.5 MNK rearrangement on model systems

In an effort to understand the Miyazaki-Newman-Kwart reaction better, two test reactions were preformed. The first one was on 2-methoxy phenol **78** and the second was on the 6-hydroxyquinoline **83**. The reason for choosing **78** was due to the methoxy substituent being in a similar position to the methoxy substituent *ortho* to the phenol on the target product. This methoxy group was hypothesised to be able to assist in the rearrangement due to restricting the rotation of the carbamoyl group. The second compound **83** was selected as it contained a double ring system which included a nitrogen.

The synthesis followed work done by Ochiai *et al.* in 2012. In this work the Miyazaki-Newman-Kwart rearrangement was preformed on a single ring system.[58] In the first step a phenol **74** was stirred in DMF, adding DABCO and dimethylthiocarbamoyl chloride. The reaction was allowed to stir for 12 hours at room temperature. The reaction was then concentrated *in vacuo* and extracted the product using ethyl acetate. Finally the solid was triturated with diisopropyl ether and obtained the final product **75** by filtration. This then underwent a rearrangement reaction with diphenyl ether at 200 °C for 30 minutes to give **76**, and finally the carbamoyl group was removed to give **77**.

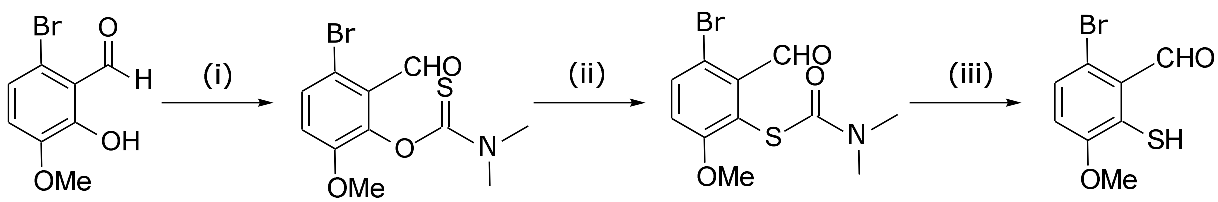

74 **75** **76** **77**

Scheme 30: i) Dimethylthiocarbamoyl chloride, DABCO, DMF, RT, 12 hours; ii) Ph_2O, 200 °C, 30 minutes; iii) NaOH, aq/*i*-PrOH, 60 °C, 30 minutes.

In our hands, it was found that both of the model systems behaved very differently and required different conditions to achieve the rearrangement (Scheme 42 and Scheme 43 respectively.)

Synthesis of *O*-(2-methoxyphenyl)-dimethylcarbamothioate -79

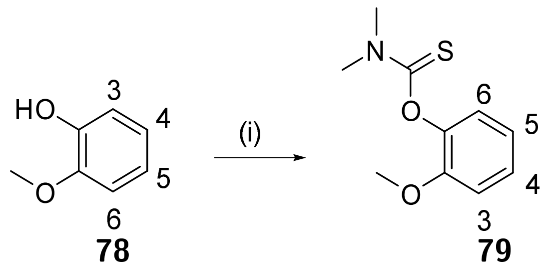

Scheme 31: i) Dimethylthiocarbamoyl chloride, DABCO, DMF, RT, 12 hours. Yield: 44%.

Compound **78** was treated with dimethylthiocarbamoyl chloride, DABCO and DMF as described by Ochiai *et al.* in the first step (Scheme 30. From the work up this reaction, a yellow oil was obtained. The oil was cooled overnight, and the final product crystallised out. In the ^{1}H NMR spectrum, it was clear that compound **79** had been synthesised, the defining signals were due to the two methyl groups on the nitrogen were visible at 3.34 and 3.29 ppm. The methyls on the nitrogen were not equivalent due to the restricted rotation. In ^{13}C NMR spectrum, the C=S signal can be seen at 186.8 ppm as well as the two N-CH_3 signals at 43.0 and 38.5 ppm.

Synthesis of *S*-(2-methoxyphenyl)-dimethylcarbamothioate -80

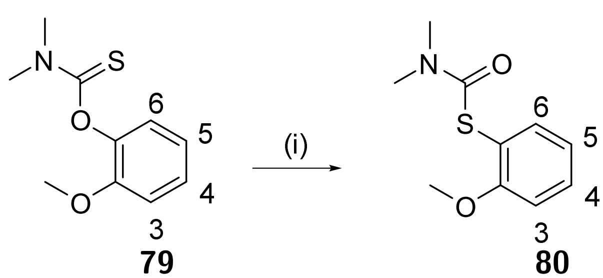

Scheme 32: i) *N*-methyl-2-pyrrolidone (NMP), microwave (160 °C, 150 Watts, 15 minutes (×3). Yield: 56%.

The initial MNK reactions done on **79** employed conventional heating as described by Ochiai *et al.* However, no success was found with this approach. After multiple attempts, including trying to heat **79** neat at 220 °C, a new approach of using microwave irradiation was considered. Here the solvent used was NMP and the optimal conditions were found to be 3 consecutive reactions in the microwave at 160 °C for 15 minutes at a time. The overall reaction was successful and the rearranged product **80** was isolated. It was noted that the sharp peaks integrating for 3 protons at 3.34 and 3.29 ppm were no longer present, and instead broader peaks at 3.01 and 2.89 ppm also integrating for 3 protons each were observed. The reason for this broad peak compared to the sharp peaks in Scheme 31, is due the equilibrium that can be seen in the Figure 10. In this equilibrium to the right, the predominant bond is a double bond which restricts the rotation and allows the methyls to be observed in separate environments as two sharp peaks integrating for three protons. How ever in the case of the amide, we see that the equilibrium in rather in the middle of the two and so we see some restricted rotation due to the double bond and the free rotation around the single bond. The rotation is at a similar frequency to the NMR time scale and so a single state is not observed. This leads to the signals being broad and of lower intensity. In addition, in the ^{13}C NMR spectrum the C=S signal at 186.8 was replaced by the carbonyl signal at 164.6 ppm.

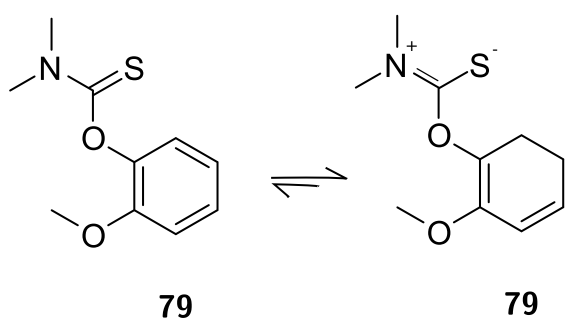

Figure 10: Equilibrium for **79**

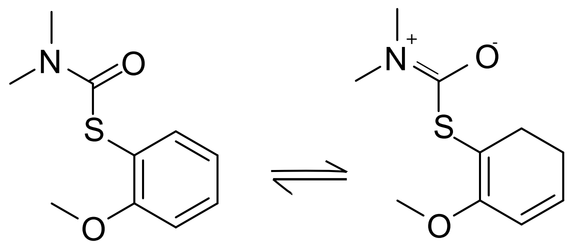

80 **80**

Figure 11: Equilibrium for **80**

4.3.6 Synthesis of 2-methoxybenzenethiol -81

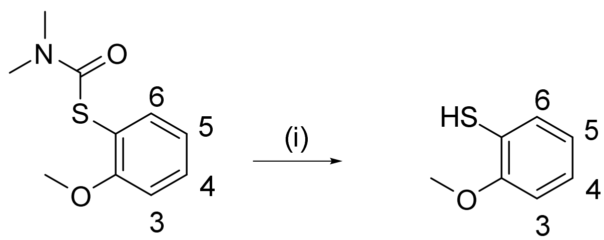

80 **81**

Scheme 33: i) NaOH, aq. *i*-PrOH, 60 °C, Ar_g, 30 minutes.

The removal of the carbamoyl group to expose the thiol at position 6, **80** proved to be more challenging than expected. The rearranged product *S*-(2-methoxyphenyl)-dimethylcarbamothioate **80** was added to a mixture of NaOH and *iso*-propyl alcohol, this was heated to 60 °C for 30 minutes. In the same reaction was conducted by a colleague in the Wits Laboratory.[59] The ^{1}H NMR spectrum for the product isolated from this reaction indicated that bis(2-methoxyphenyl)disulfide **82** was formed. The ^{1}H NMR spectrum shows the aromatic peaks for the benzene rings, and it shows one peak for the methyl. However, there is no peak for the thiol group, or the previously present methyl groups on the nitrogen. From this we have concluded that a disulfide bond has formed causing the benzene rings to be in equivalent environments and thus giving only one set of peaks. Unfortunately, the thiol **81** was not successfully isolated.

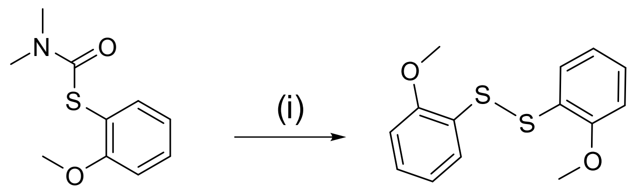

80 **82**

Scheme 34: i) NaOH, aq. *i*-PrOH, 60 °C, Ar_g, 3 days

Having successfully performed the MNK rearrangement on the simple substrate **79**, the same rearrangement could be preformed on the fused bicyclic system **83**. This required the initial synthesis of the thiocarbamate (Scheme 35)

4.3.7 Synthesis of *O*-(7-methoxyquinolin-6-yl)-dimethylcarbamothioate -84

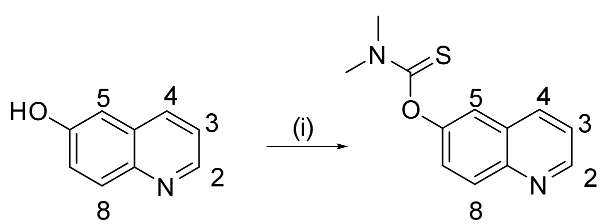

83 **84**

Scheme 35: i) Dimethylthiocarbamoyl chloride, DABCO, DMF, RT, 12 hours. Yield: 20%.

The first step was conducted in the same manner as described previously (Scheme 31). The only difference was that the final product **84** was triturated with diethyl ether to remove some of the dimethylthiocarbamoyl chloride from the final product. The yield was not good at 20%, however there was sufficient product to test the MNK rearrangement. The ^{1}H NMR spectrum showed the two new methyl peaks at 3.48 and 3.40 ppm and no alcohol peak from the starting material was observed. In the ^{13}C NMR spectrum, the C=S signal was observed at 187.2 ppm, and the two N-CH_3 groups at 43.1 ppm and 38.6 ppm.

4.3.8 Synthesis of *S*-(7-methoxyquinolin-6-yl)-dimethylcarbamothioate -85

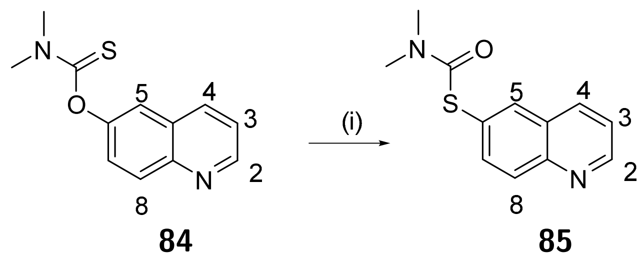

Scheme 36: i) Diphenyl ether, 210 °C, 12 hours. Yield: 36%.

In this reaction (Scheme 43) the synthesis set out by *Ochiai et al.* was followed. Compound **84** was heated in diphenyl ether at 210 °C for 12 hours. As with the ^{1}H NMR spectrum of **80**, after the rearrangement the methyl peaks were present in the ^{1}H NMR spectrum of **85**, not as sharp singlets but broad singlets overlapping slightly. However, they did integrate for 6 protons, which aligns to the expected assignment. And so the rearrangement to **85** was successful under conventional heating. A reaction using microwave irradiation was attempted, however, this was not successful.

4.3.9 Synthesis of *O*-4-[(3-bromophenyl)amino]-7-methoxyquinazolin-6-yldimethylcarbamothioate - 49

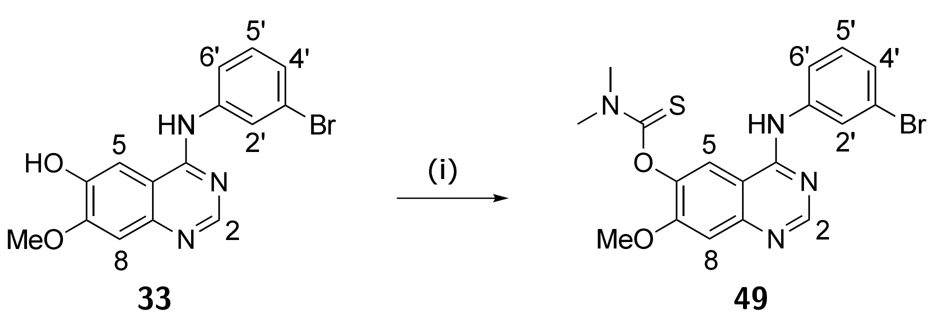

Scheme 37: i) Dimethylcarbamoyl chloride, DABCO, DMF, Ar_g, RT for 24 hours. Yield: 36%.

From the above successful reaction it was not possible to prepare the MNK precursor of the target quinazolines. To this end, **33** was dissolved in DMF and treated with the dimethylcarbomoyl chloride and DABCO for 24 hours at room temperature. After completion of the reaction, which was monitored by NMR spectroscopy, the reaction mixture was diluted with DCM, washed with water and brine and the concentrated down. The product was purified by heating the crude mixture in water, to effect precipitation of the desired product.

The ^{1}H NMR spectrum for this product, shows two clearly defined peaks in the aliphatic region at 3.38 and 3.39 ppm, both integrating for three protons. These two peaks account for the methyl groups from the dimethylthiocarbamoyl group in **49**. Once again, the biggest peak shift could be seen for the signal due to the proton at position 5 on the quinazaline core; here the peak moved downfield from 7.81 ppm to 8.28 ppm. In the ^{13}C NMR spectrum, the defining features were C=S signal at 186.7 ppm and two N-CH_3 signals at 43.5 ppm and 38.6 ppm respectively. In Figure 12, the ORTEP of **49** can be seen, this structure confirms that the correct methyl was removed in Scheme 22. It also confirms the addition of the thiocarbamoyl group onto the exposed phenol. It can also be seen that the sulfur group is out of the plan of the aromatic rings, this provides the sulfur group the opportunity to attack the ipso carbon in an intramolecular fashion in order for the MNK rearrangement to occur in the next reaction.

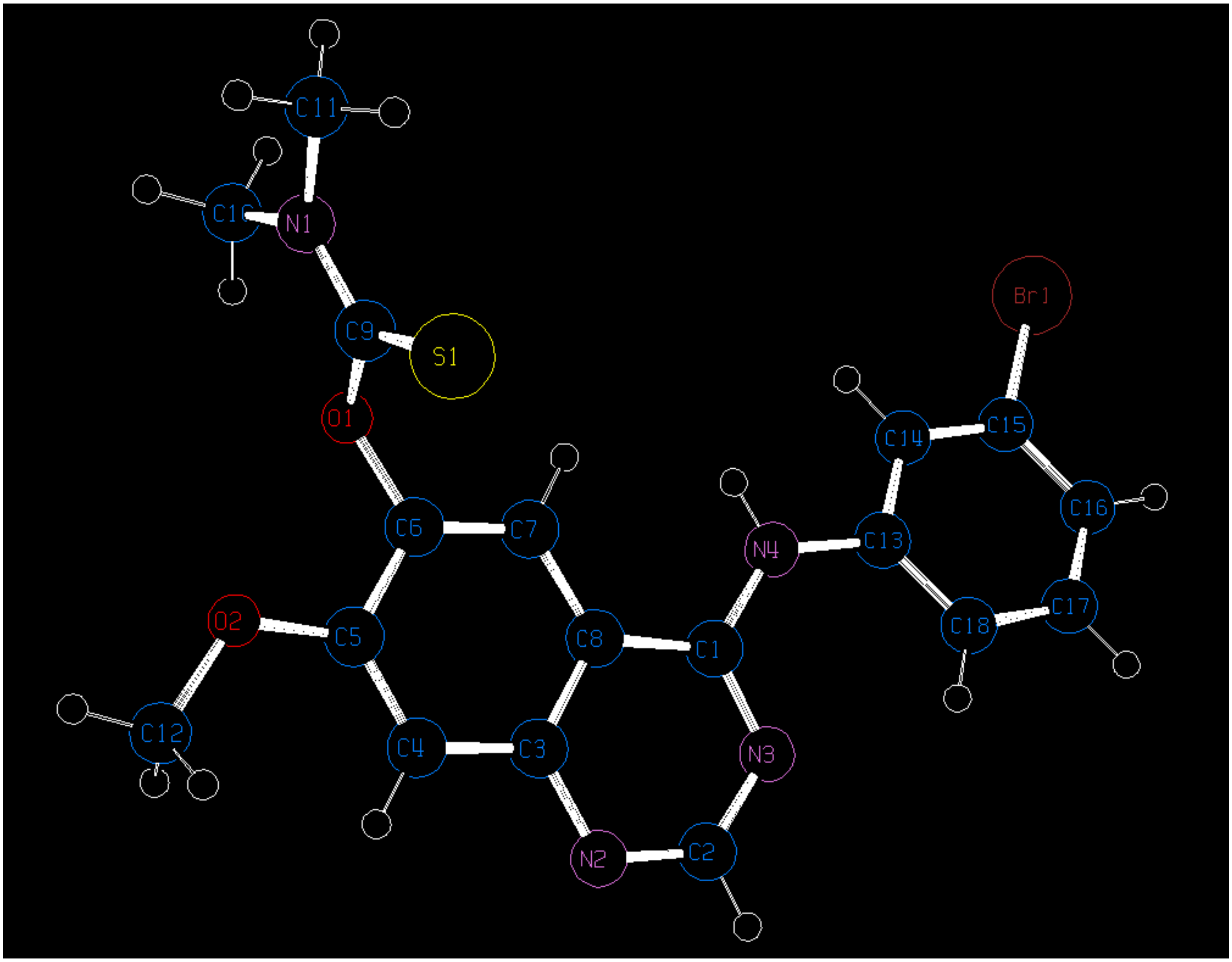

Figure 12: The crystal structure of **49**.

4.3.10 Synthesis of *O*-4-[(3-chloro-4-fluorophenyl)amino]-7-methoxyquinazolin-6-yldimethylcarbamothioate - 65

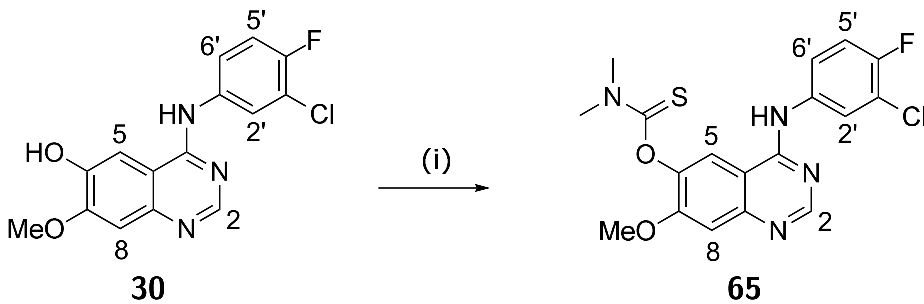

Scheme 38: i) Dimethylcarbamoyl chloride, DABCO, DMF, Ar_g, RT for 48 hours. Yield: 68%.

This reaction was completed in the same way as the synthesis of **49**, in that the starting material **30**, dimethylthiocarbomoyl chloride and DABCO were dissolved in DMF and stirred at room temperature for 42 hours. After this time, it was observed that starting material was still present. Additional reagents were therefore added and allowed to react for a further 6 hours. The final product **65** was easier to work up than the bromine analogue **49**. The DCM was added, and washed with brine and water. The DCM was then removed under vacuum and the product remained.

In the ^{1}H NMR spectrum, the two additional methyl peaks were easily identified at 3.38 ppm and 3.40 ppm, with both the peaks integrating for three protons each. The alcohol peak observed at 9.70 ppm was no longer present, and the shift in the proton at position 5 from 7.82 ppm to 8.24 ppm was observed. In the ^{13}C NMR spectrum the thion peak at 186.69 ppm, the three peaks in the aliphatic region accounting for the methoxy and two methyl groups on the nitrogen were all present.

4.3.11 Synthesis of *S*-4-[(3-bromophenyl)amino]-7-methoxyquinazolin-6-yldimethylcarbamothioate - 48

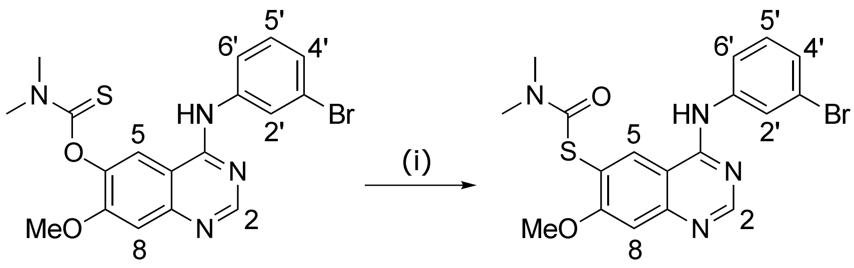

49

48

Scheme 39: i) Diphenyl ether, 210 °C, 12 hours. Yield: 24%.

With **49** in hand, the MNK rearrangement on the target quinazoline substrate could be preformed. Here, the work done by Ochiai *et al.* was followed (Scheme 30). The reaction followed the exact path, however for the work up, it was found that purification using column chromatography was not successful, as the product **48** was unstable on silica gel. Fortunately, adding hexane to the reaction mixture caused the desired product **48** to precipitate out of solution, and the product was isolated by filtration and washed with hexane to remove any additional diphenyl ether. The challenge was to now characterize the product, as the only difference that should be observed in the ^{1}H NMR spectrum was the possible movement of the methyl peaks attributed to the dimethylcarbonylcarbamoyl group at position 6. In the ^{1}H NMR spectrum the broad, low intensity peaks at 3.13 ppm and 2.94 ppm, seen in the test reactions on **80** and **85**, were observed. Both peaks integrated for 3 hydrogens each, and the peaks had shifted upfield from 3.38 and 3.39 ppm, as they were no longer as shielded by the sulfur as they were by the oxygen.

4.3.12 Synthesis of *S*-4-[(3-chloro-4-fluorophenyl)amino]-7-methoxyquinazolin-6-yldimethylcarbamothioate - 66

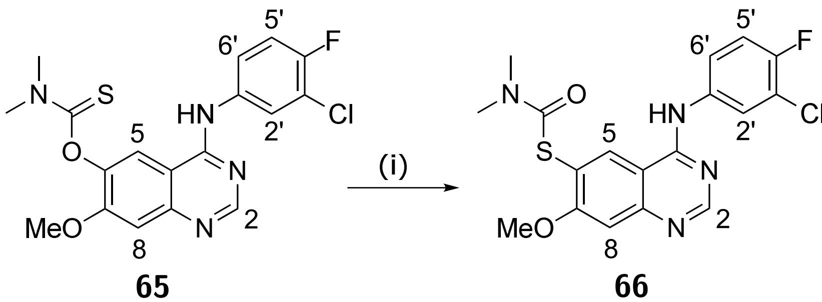

Scheme 40: i) Diphenyl ether, 210 °C, 12 hours.

The *O*-4-[(3-chloro-4-fluorophenyl)amino]-7-methoxyquinazolin-6-yldimethylcarbamothioate **65** was added to diphenyl ether and heated at 210 °C for 12 hours, the progress of the reaction was determined using TLC, with the confirmation using ^{1}H NMR spectroscopy. Upon completion of the reaction, the reaction was worked up by adding hexane to the reaction mixture and as a result the product precipitated out of solution. The precipitate was isolated by filtration and washed with hexane. In the ^{1}H NMR spectrum of **66**, it was observed that there was full conversion to the desired product, with the identifiable broad peaks in below 3.38 ppm. However, there was diphenyl ether present. After a few attempts at washing the diphenyl ether out with hexane, it was decided to attempt to remove it using silica gel column chromatography. The diphenyl ether was identified, and the yellow band corresponding to the dimethylthiocarbamoyl group. Unfortunately, the product **66** was not isolated from this column, and so additional characterisation of this product was not possible.

Although, the products **48** and **66** were synthesised successfully, the limited quantity of material in hand and time constraints prevented further route scouting towards the synthesis of **13** and **70**.

4.3.13 Attempted synthesis of *S*-4-[(3-bromophenyl)amino]-7-methoxyquinazolin-6-yldimethylcarbamothioate - 47

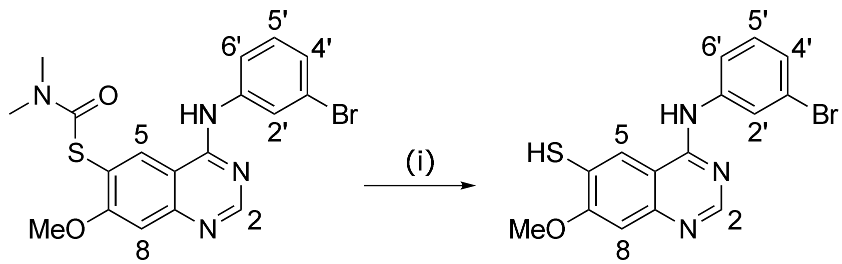

48 **47**

Scheme 41: i) NaOH, aq.*i*-PrOH, 60 °C, Ar_g, 30 minutes.

In an attempt to obtain the thiol **47**, *S*-4-[(3-bromophenyl)amino]-7-methoxyquinazolin-6-yldimethylcarbamothioate was added to a mixture of *iso*-propanol and NaOH under argon at 60 °C for 30 minutes, upon work up it was found that the solid was not soluble in any solvents and so characterisation was not possible. An attempt to obtain an IR spectrum of the solid was also unsuccessful. It was hypothesised that the thiols formed a disulfide bond as was the case with the model reaction Scheme 44. Due to low yields of the **48**, this reaction was not completed.

Chapter 5

Conclusion and Future Work

5.1 Conclusion

The focus of this body of research was to design and synthesise novel EGFR inhibitors. The full synthesis plan seen in Scheme 16 was based on work previously done in the Wits Chemistry laboratories[40] as well as work done by Chen *et al.*, Knesl *et al.*, Chandregowda *et al.* and Oshiai *et al.*

The work performed during this MSc was split up into three phases: 1. the synthesis of **28**, 2. the MNK rearrangement of **49** and **65**, and finally 3. the development of the chain on the thiol group at position 6.

In phase 1, the synthesis of **28** was predominately based on work done by Chen *et al.*[38] as well as work done previously in the Wits laboratories.[40] The synthesis of intermediate **28** was overall successful despite the challenges already discussed.

Phase 2 entailed functionalising two positions on this quinazolinone core Figure 13. The first position was at carbon 4, two different anilines were added here; the 3-bromoaniline and the 3-chloro-4-fluoroaniline. The second position that was functionalised, was the carbon 6 on the quinazolinone core. Here the chain was used to get into the EGFR site and bond in a reversible covalent fashion.

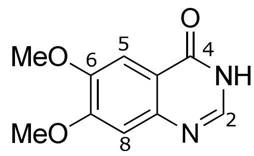

25

Figure 13: Position 4 and 6 on the quinazolinone core- **25**

The final step towards the intermediate **28**, turned out to be one of the more challenging steps. The challenge came from the fact that the product **28** easily and relatively quickly reversed in the presence of any water to form **27**. This lead to a large amount of product being lost due to forcing the reaction to go too long, working up the reaction inefficiently and believing a reaction was unsuccessful when in fact it was. The product would reverse in the DMSO-d6 while a ^{1}H NMR spectrum was being run. It was also noted that keeping the reaction as close to 0 °C during the work-up as possible was important. This reaction was optimised with yields of 79% and we obtained the fully aromatic system that would allow us to introduce the different anilines.

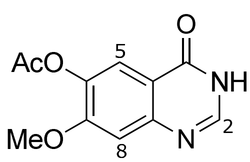

27

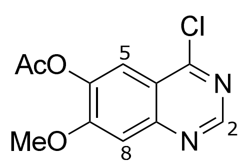

28

Figure 14: 7-methoxy-4-oxo-3,4-dihydroquinazolin-6-yl acetate- **27** and 4-chloro-7-methoxy-3,4-dihydroquinazolin-6-yl acetate- **28**

In phase 2, we functionalised at carbon 4 with our two anilines to form **33** and **30** and started the process of functionalising at position 6. In order to achieve functionalisation at position 6 we needed to obtain a thiol in place of the phenol at this position. This was a key step; the MNK rearrangement. This required us to add the dimethylthiocarbamoyl chloride to the phenols **33**, **30** to form **49**, **65** respectively. Then to finally use the MNK rearrangement to obtain **48** and **66**

This rearrangement was initially based on work done by Oshiai *et al.*, and it was observed in the test reactions Scheme 42 and Scheme 43 that the rearrangement

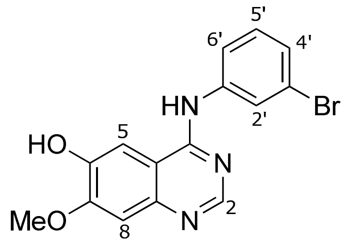

33

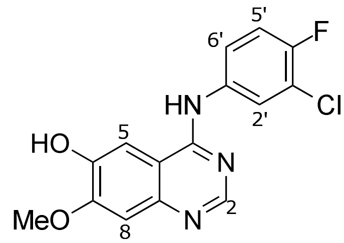

30

Figure 15: Functionalised compounds at position 4: 4-((3-bromophenyl)amino)-7-methoxyquinazolin-6-ol- **33** and 4-[(3-chloro-4-fluorophenyl)amino]-7-methoxy-3,4-dihydroquinazolin-6-ol- **30**

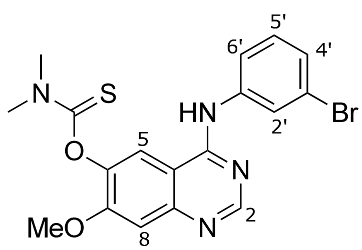

49

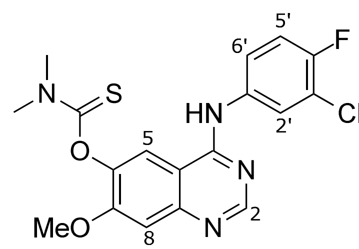

65

Figure 16: MNK precursors: *O*-4-[(3-bromophenyl)amino]-7-methoxyquinazolin-6-yldimethylcarbamothioate- **49** and *O*-4-[(3-chloro-4-fluorophenyl)amino]-7-methoxyquinazolin-6-yldimethylcarbamothioate- **65**

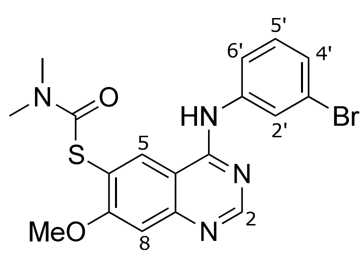

48

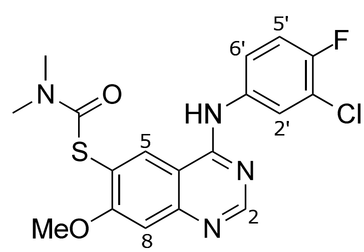

66

Figure 17: MNK precursors: *S*-4-[(3-bromophenyl)amino]-7-methoxyquinazolin-6-yldimethylcarbamothioate- **48** and *S*-4-[(3-chloro-4-fluorophenyl)amino]-7-methoxyquinazolin-6-yldimethylcarbamothioate- **66**

could occur under different conditions for example conventional heating vs microwave heating. It was also noted that although there were two types of heating available, the rearrangement on different structures would would occur exclusively under one set of reaction conditions. This was observed when the rearrangement of **79** was performed under conventional heating, as no matter how long the reaction was heated and the solvent in which the reaction took place, no rearrangement would occur. However, under microwave heating a full conversion of the **79** to **80** was observed. For the second test reaction, described in Scheme 43, the best route to the MNK rearrangement product was through conventional heating in diphenyl ether as was done by Oshiai *et al.*.[58]

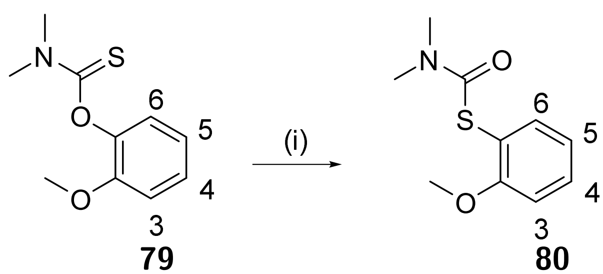

Scheme 42: i) *N*-methyl-2-pyrrolidone (NMP), microwave (160 °C, 150 Watts, 15 minutes (×3)). Yield: 56%.

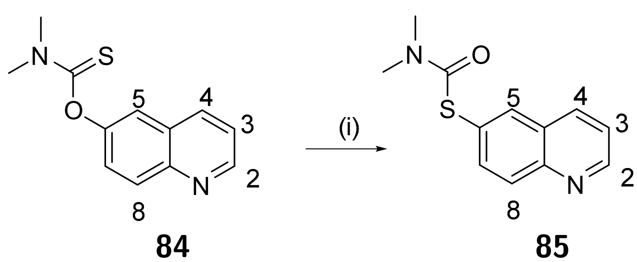

Scheme 43: i) Diphenyl ether, 210 °C, 12 hours. Yield: 36%.

It was found that after performing the reaction on **49** that the best route for the compound was conventional heating. The rearrangement was successful, and the product obtained was uniquely identifiable by the unusual broad peaks below 3 ppm in the ^{1}H NMR spectrum integrating for 3 protons each belonging to the methyl groups on the nitrogen. These unusual peaks were observed in all 4 of the MNK rearrangements performed. For the characterisation of **48**, the ^{13}C NMR spectrum was not obtained due to the low solubility of the product in the deutrated solvent. With the success of the MNK rearrangement, we looked at removing the carbamoyl group to expose the thiol group. This presented its own set of challenges as when attempting this on the test reaction compound **80** we saw that the thiols reacted with each other in a intermolecular fashion to form a disulfide bond, as well as a benzenethiosulfonic acid-type bond. An attempt on this reaction on **48**, an uncharacterisable solid was obtained. In an attempt to successfully remove this group, we placed the reaction under inert conditions and tried again. Unfortunately, this was not successful and due to time constraints, we were unable to continue with the total synthesis of **13** and **70**.

5.2 Future work

Following the initial success of the MNK rearrangement on **49** and **65**, we would first like to optimize this step for both **49** and **65**. The isolation of these two compounds in better yields would allow us to experiment with the removal of the carbamoyl group to obtain the thiol **48** and **66**. We would repeat the initial reaction (Scheme 33) using degassed solvents (nitrogen or argon) in order to remove any oxygen. This would prevent the initial formation of the disulfide observed in the MNK test reaction as shown in Scheme 44. Further options include using a reducing agent (e.g: lithium aluminum hydride ($LiAlH_4$)) to reduce the disulfide **82** back to a thiol **81**. The successful isolation of the thiol **81** would allow us to use our knowledge to continue with the synthesis of **13** and **70**.

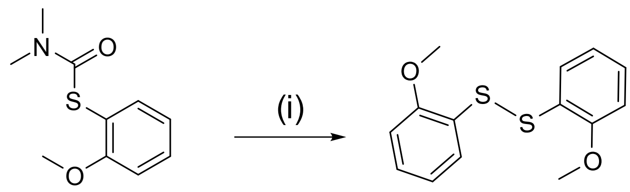

80 **82**

Scheme 44: i) NaOH, aq. i-PrOH, 60 °C, Ar_g, 3 days

Once the thiols **47** & **67** are isolated, the acrolein can be added. This step would test the hypothesis of the sulfur preventing the reverse Michael Addition. Assuming the acrolein addition is successful, a CN-i-pr will be added to **46** & **68** to give **45** & **69**. This will then be reduced using DMP in DCM to give the final target molecules **13** and **70**. With the target molecules in hand, we would test the biological activity of **13**, **70** and be able to compare the activity to that of **32**. This would allow us to better understand the interaction of the chain at position 6 in the EGFR site.

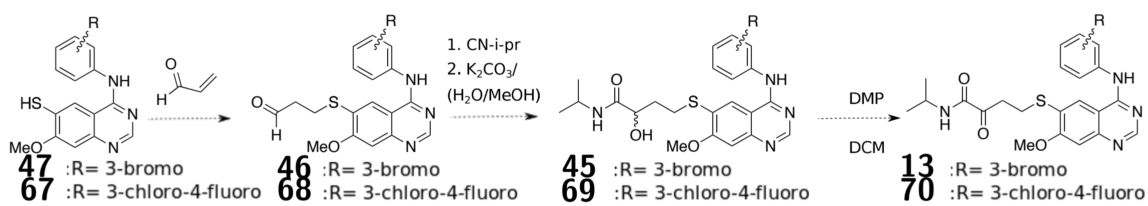

Scheme 45: The final steps in the synthesis plan.

Once the synthesis of **13** and **70** has been optimised. Further work could be done in order to assess the important features on the molecules in their contribution to the binding within the EGFR site. The three components that could be considered are

1. Aniline
2. Length of the side chain
3. Oxygen vs sulfur at position 6

In order to achieve this comparison, additional molecules would need to be synthesised. Compounds that are on the market and comparable to the structure in this MSc can be seen in Figure 18.

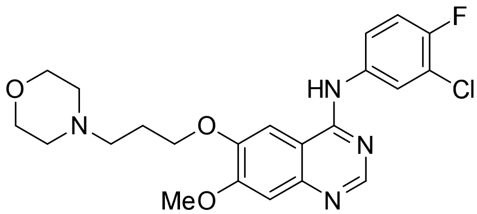

2

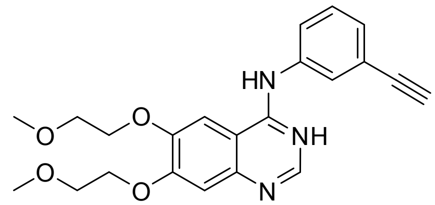

3

Figure 18: Literature compounds

The compounds that were successfully synthesised in the Wits Laboratories or where the synthesis was attempted in the Wits laboratories can be seen in Figure 19.

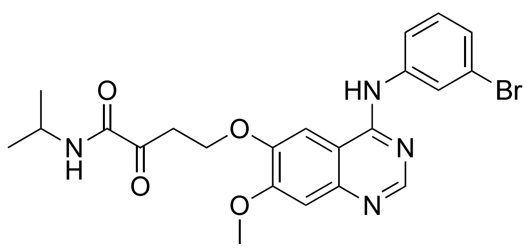

31

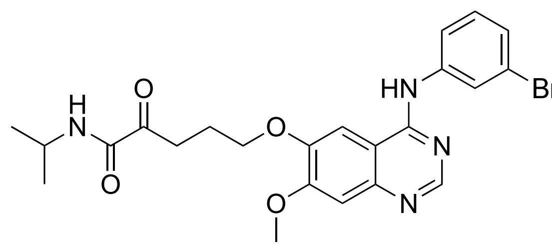

32

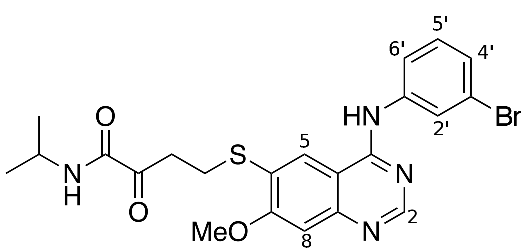

13

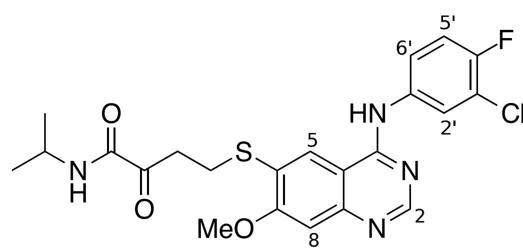

70

Figure 19: Compounds successfully synthesised in the Wits laboratories and compounds attempted in Wits laboratories

The first compound synthesised in the Wits laboratories **32** has the 3-bromoaniline- changing this aniline to the 3-chloro-3-fluoroaniline to make **86** and the 3-ethynylaniline to make **87**. Additionally adding the 3-ethynylaniline to make **88**. Having these 6 compounds in place would allow for the determination of two factors, first being the aniline and second the chain length. This would allow us to evaluate the chain length by comparing **13** to **32**, **70** to **86** and **88** to **87**. Finally, changing the oxygen at position 6 on **32** to a sulfur group **89** would allow us to determine if the sulfur group adds any additional biological value to the compounds. This comparison can be extended to compare **86** to **90** and **87** to **91**

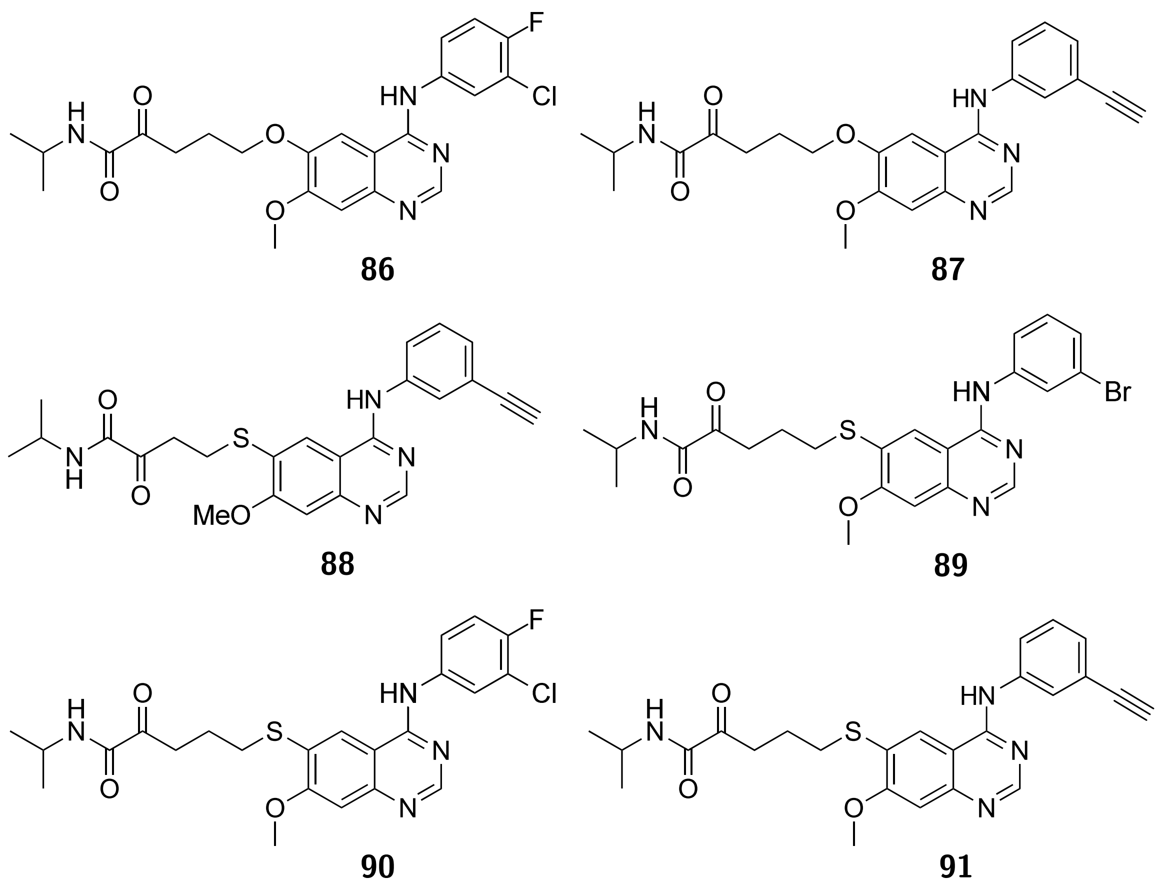

Figure 20: The future compounds to be synthesised to assess the important features in binding in the EGFR active site.

The successful synthesis of these future compounds would allow the full understanding of the chain length, the aniline and finally the sulfur vs oxygen at position 6 on the quinazoline core.

Chapter 6

Experimental

6.1 General procedures

All reagents were purchased from Sigma-Aldrich (South Africa) and were used as received. All solvents for reactions were of analytical grade quality purchased from Sigma-Aldrich (South Africa), Merck KGaA (South Africa). Solvents for column chromatography (ethyl acetate and hexanes) and acetone for cleaning were purchased from Protea Chemicals (South Africa) and were distilled before use to remove non-volatiles. Column chromatographic purification was done on Macherey-Nagel silica gel 60 (particle size 0.063 mm to 0.200 mm). Thin Layer Chromatographic analysis was done on Merck Aluminium foil backed plates coated with silica gel 60, F254. Melting points were recorded on a Stuart Smp10 apparatus. ^{1}H Nuclear Magnetic Resonance (NMR) data were acquired on a Bruker 300 or 500 MHz spectrometer at room temperature, using the specified deuterated solvent. For those compounds soluble in deuterated chloroform ($CDCl_3$), the solvent contained tetramethylsilane (TMS, 0.05 % v/v) as internal standard. For others, the residual solvent signal was used for referencing. ^{13}C Nuclear Magnetic Resonance (NMR) data were acquired on the same instrument. Data processing was done using MestreNova Software under license from Mestrelab Research, CA, USA. The following abbreviations are used to designate the multiplicity: s = singlet, d = doublet, t = triplet, q = quartet, p = pentet, m = multiplet, dd = doublet of doublets. When an assignment is marked with a *- this indicates that the two signals are not equivalent but are not distinguishable from eachother in the NMR spectra. DMF was distilled from calcium hydride and stored over molecular sieves. Dichloromethane, chloroform, ethanol and methanol were purchased and used as is.

6.2 Synthesis of of intermediate 4-chloro-7-methoxyquinazoline-6-yl acetate - 28

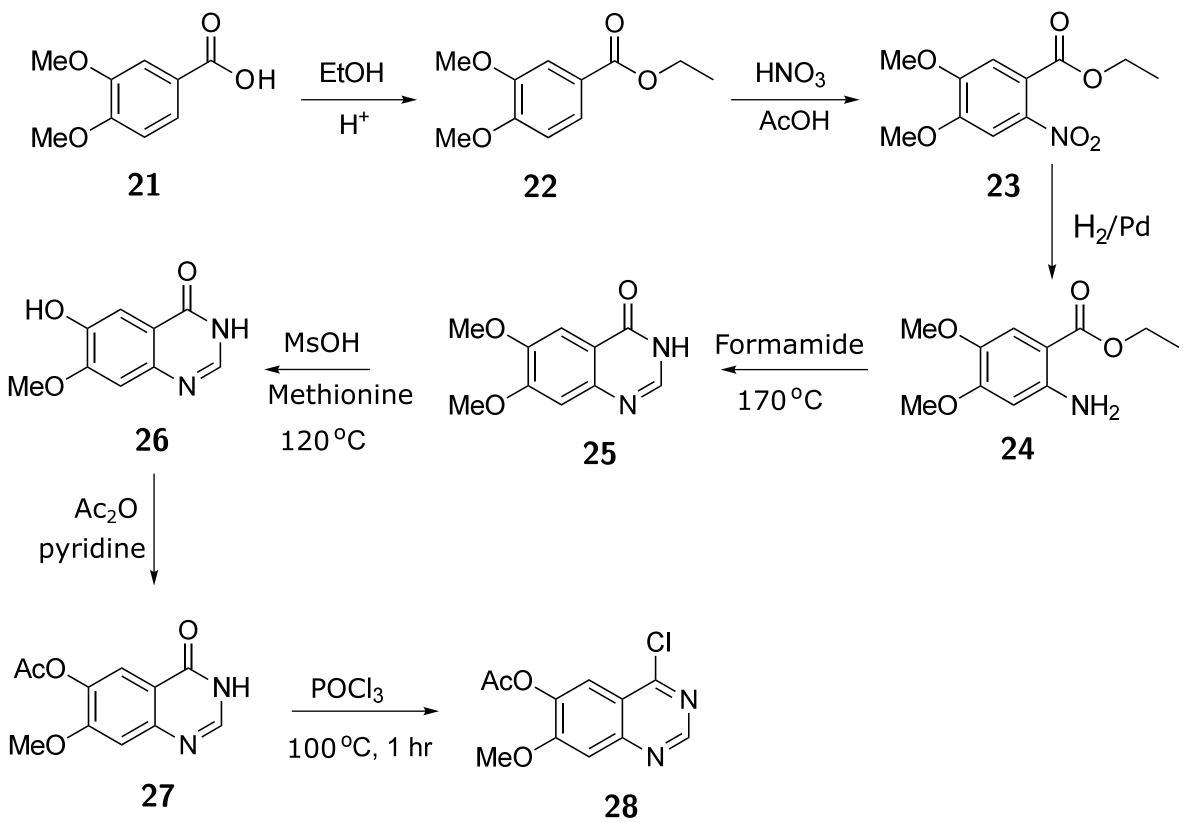

Scheme 46: Synthesis path to **28**

6.2.1 Synthesis of ethyl-3,4-dimethoxybenzoate - 22

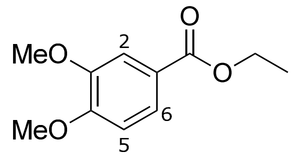

22

3,4-Dimethoxybenzoic acid **21** (100 g, 0.551 moles) was added to a mixture of toluene (600 mL) and ethanol (90 mL). The reaction was then heated to 60 °C, under argon, conc. H_2SO_4 (10 mL) was added. The reaction was further heated to 80 °C and allowed to reflux for 72 hours. Dean Stark apparatus was used to remove water produced in the reaction. The reaction was followed using TLC. On completion, the reaction mixture was diluted using ethyl acetate (800 mL). The organic layer was then washed with 2 M NaOH (200 mL) (×3), water and finally with brine (150 mL). The organic layer was dried using $MgSO_4$. The solvent was then removed under vacuum to give a white solid (98.8 g, 0.470 moles, 85%).

$\mathbf{R_f}$: 0.79 (50% EtOAc: Hexane); **M.p:** 42 – 43 °C ; **LRMS** $(M+H)^+$= 211.1;
^{1}H NMR (500 MHz, $CDCl_3$) δ 7.68 (dd, J = 8.4, 2.0 Hz, 1H, H-6), 7.54 (d, J = 2.0 Hz, 1H, H-2), 6.87 (d, J = 8.4 Hz, 1H, H-5), 4.35 (q, J = 7.1 Hz, 2H, O-$\mathbf{CH_2}$-CH_3), 3.93 (s, 6H, 2 × O-CH_3), 1.38 (t, J = 7.1 Hz, 3H, O-CH_2-$\mathbf{CH_3}$);
^{13}C NMR (126 MHz, $CDCl_3$) δ 166.3 (Ar-**C**(O)-O-CH_2), 152.8 (C-4), 148.5 (C-3), 123.4 (C-6), 122.9 (C-1), 111.9 (C-2), 110.1 (C-5), 60.7 (O-$\mathbf{CH_2}$-CH_3), 55.9 (O-CH_3), 14.3 (O-CH_2-$\mathbf{CH_3}$).

6.2.2 Synthesis of ethyl-4,5-dimethoxy-2-nitobenzoate - 23

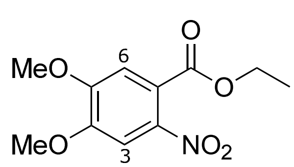

23

Ethyl 3,4-dimethoxybenzoate **22** (50.5 g, 0.241 moles) was dissolved in acetic acid (200 mL) at room temperature. Nitric acid 60% (60 mL, 6 eq) was added dropwise to the stirring solution at $0 - 5\,°C$. The reaction was then stirred at room temperature for 48 hours. The reaction was monitored using TLC. On completion, the reaction was dissolved in ethyl acetate (200 mL), and washed with sodium bicarbonate (50 mL)(×3) and water (×2). The organic layer was dried using $MgSO_4$. The solvent was then removed under vacuum to give a pale yellow solid (60.1 g, 0.235 moles, 97%). The ^{1}NMR spectrum compared well to the literature NMR for the same compound.[60]

$\mathbf{R_f}$: 0.73 (50% EtOAc: Hexane); **M.p:** $98 - 99\,°C$; **LRMS** $(M+H)^+$= 256.1;
^{1}H NMR (300 MHz, CDCl$_3$) δ: 7.45 (s, 2H, H-6), 7.07 (s, 1H, H-3), 4.37 (q, J= 7.2 Hz, 2H, O-**CH$_2$**-CH$_3$), 3.97 (s, 3H, *O-CH$_3$), 3.96 (s, 3H, *O-CH$_3$), 1.34 (t, J = 7.2 Hz, 3H, O-CH$_2$-**CH$_3$**);
^{13}C NMR (75 MHz, CDCl$_3$) δ: 165.8 (Ar-**C**(O)-O-CH$_2$), 152.5 (C-4), 150.3 (C-5), 141.2 (C-2), 122.1 (C-1), 110.8 (C-3), 106.9 (C-6), 62.5 (O-**CH$_2$**-CH$_3$), 56.7 (*O-CH$_3$), 56.6 (*O-CH$_3$), 13.8 (O-CH2-**CH$_3$**).

6.2.3 Synthesis of ethyl 2-amino-4,5-dimethoxybenzoate - 24

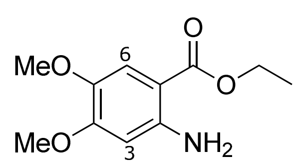

24

Ethyl 4,5-dimethoxy-2-nitrobenzoate **23** (40.0 g, 0.157 moles) was dissolved in methanol (100 mL). Once all the material was completely dissolved, 10% Palladium/C (7.3 g) was added to the reaction. The reaction was then stirred at room temperature. Balloons were used to supply $H_{2(g)}$ to the reaction. The reaction was monitored using TLC. Once all starting material was reacted, the reaction was filtered using a celite column in order to remove the Pd/C. The methanol was removed under vacuum to yield an off-white solid (34.2 g, 0.152 moles, 97%), which was used without further purification.

$\mathbf{R_f}$: 0.66 (50% EtOAc: Hexane); **M.p:** 86 – 88 °C; **LRMS** $(M+H)^+$= 226.1;

^{1}H NMR (300 MHz, CDCl$_3$) δ 7.32 (s, 1H, H-6), 6.15 (s, 1H, H-3), 5.24 (s, 2H, NH_2), 4.32 (q, J = 7.1 Hz, 2H, O-$\mathbf{CH_2}$-CH_3), 3.86 (s, 3H, *O-CH_3), 3.83 (s, 3H, *O-CH_3), 1.38 (t, J = 7.1 Hz, 3H, O-CH_2-$\mathbf{CH_3}$);

^{13}C NMR (75 MHz, CDCl$_3$) δ 167.8 (Ar-**C**(O)-O-CH_2), 154.8 (C-4), 147.1 (C-5), 140.6 (C-2), 112.9 (C-6), 102.4 (C-1), 99.4 (C-3), 60.1 (O-CH_2-CH_3), 56.5 (*O-CH_3), 55.8 (*O-CH_3), 14.5 (O-CH_2-CH_3).

6.2.4 Synthesis of 6,7-dimethoxyquinazolin-4(3*H*)-one - 25

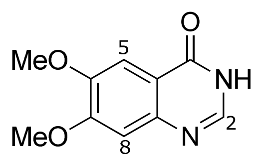

25

Ethyl-2-amino-4,5-dimethoxybenzoate **24** (32.5 g, 0.144 moles) was suspended in formamide (90 mL) at 170 °C under argon for 12 hours. After 12 hours, a solid was seen to precipitate out. The progress of the reaction was checked using TLC (1:1 EtOAc: Hexane). Water (20 mL) was added to the cooled reaction mixture. The solid was filtered and washed with small amounts of cold water. The solid was left in the desiccator overnight, giving a light brown solid (26.8 g, 0.130 moles, 90%) and did not require further purification. The ^{1}NMR spectrum compared well to the literature NMR for the same compound.[37]

$\mathbf{R_f}$: 0.86; **M.p:** 297 – 298 °C;

^{1}H NMR (500 MHz, DMSO) δ 12.05 (s, 1H, N-H), 7.98 (s, 1H, H-2), 7.44 (s, 1H, H-8), 7.12 (s, 1H, H-5), 3.90 (s, 3H, *O-CH_3), 3.86 (s, 3H, *O-CH_3);

^{13}C NMR (126 MHz, DMSO) δ, 160.5 (C-4), 154.9 (C-7), 149.0 (C-6),145.3 (C-9), 144.3 (C-2), 116.1 (C-10), 108.5 (C-5), 105.4 (C-8), 56.4 (*O-CH_3), 56.2 (*O-CH_3).

6.2.5 Synthesis of 6-hydroxy-7-methoxyquinazolin-4(3*H*)-one - 26

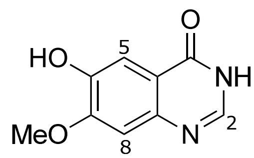

26

Dimethoxyquinazolin-4(3*H*)-one **25** (25.1 g, 0.122 moles) and DL-methionine was added to methane sulphonic acid (140 mL). The reaction was heated to 110 °C for 12 hours. Once completed, the reaction was neutralized using 6 M NaOH. At pH 7 the product precipitated out of solution. The solid was filtered and dried in a desiccator. An off white solid was produced (23.4 g). This solid was a mixture of products; the desired product, the starting material and the dihydroxy product, this was determined by NMR spectroscopy. The products could not be separated, but the major product was the desired one. The mixture was carried through to the next reaction.

^{1}H NMR (300 MHz, DMSO) δ 7.90 (s, 1H, H-2), 7.38 (s, 1H, H-8), 7.09 (s, 1H, H-5), 3.90 (s, 3H, O-CH_3).

6.2.6 Synthesis of 7-methoxy-4-oxo-3,4-dihydroquinazolin-6-yl acetate - 27

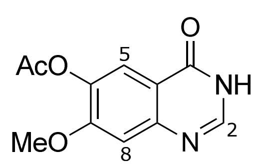

27

The mixture from the previous reaction, (5.60 g) and a catalytic amount of DMAP was added to acetic anhydride (80 mL). The reaction was heated to 80 °C under argon. Pyridine (10 mL) was added to the reaction and then the temperature was raised to 100 °C. The reaction stirred for 36 hours. Upon completion the reaction was cooled to room temperature and then poured onto ice. The solid **27** was filtered and dried to give a pure white solid (4.20 g, 0.0181 moles) which did not require further purification. The ^{1}NMR spectrum compared well to the literature NMR for the same compound.[37]

M.p: 292 – 294 °C;
^{1}H NMR (300 MHz, DMSO) δ 12.18 (s, 1 H, NH), 8.07 (s, 1H, H-2), 7.75 (s, 1H, H-8), 7.27 (s, 1H, H-5), 3.91 (s, 3H, O-CH_3), 2.29 (s, 3H, OAc);
^{13}C NMR (126 MHz, DMSO) δ, 169.2 (C-15), 160.4 (C-4), 156.6 (C-7),149.3 (C-2), 146.3 (C-9), 139.3 (C-6), 119.6 (C-10), 116.0 (C-5), 109.6 (C-8), 56.9 (O-CH_3), 20.85 (C(O)**C**H_3).

6.2.7 Synthesis of 4-chloro-7-methoxy-3,4-dihydroquinazolin-6-yl acetate - 28

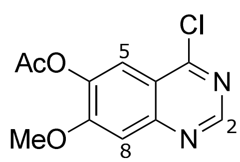

28

$POCl_3$ (30 mL) was added to a mixture of 7-methoxy-4-oxo-3,4-dihydroquinazolin-6-yl acetate **27** (5.0 g, 0.022 moles) and diethylaniline (5.1 g, 0.034 moles). The reaction was heated to 90 °C under argon for 3 hours. The reaction was poured into three conical flasks and liquid nitrogen was used to freeze the product (this was done to prevent any hotspots that may cause the reaction to reverse). Ice was then added to the reaction and it was stirred for a few minutes, until all the $POCl_3$ was quenched. The solid was filtered and allowed to air dry. The product was a brown solid (4.3 g, 0.017 moles, 79%) which did not require further purification. The ^{1}NMR spectrum compared well to the literature NMR for the same compound.[37]

^{1}H NMR (300 MHz, DMSO) δ 8.37 (s, 1H, H-2), 7.79 (s, 1H, H-8), 7.31 (s, 1H, H-5), 3.93 (s, 3H, O-CH_3), 2.30 (s, 3H, OAc);

^{13}C NMR (75 MHz, DMSO) δ 168.5 (C-15), 158.9 (C-7), 156.6 (C-4), 148.2 (C-2), 147.4 (C-9), 139.4 (C-6), 119.7 (C-10), 114.8 (C-5), 106.0 (C-8), 56.6 (O-CH_3), 20.3 (OAc).

6.3 Towards the synthesis of *S*-4-[(3-bromophenyl)amino]-7-methoxyquinazolin-6-yldimethylcarbamothioate 48 and *S*-4-[(3-chloro-4-fluorophenyl)amino]-7-methoxyquinazolin-6-yldimethylcarbamothioate 66

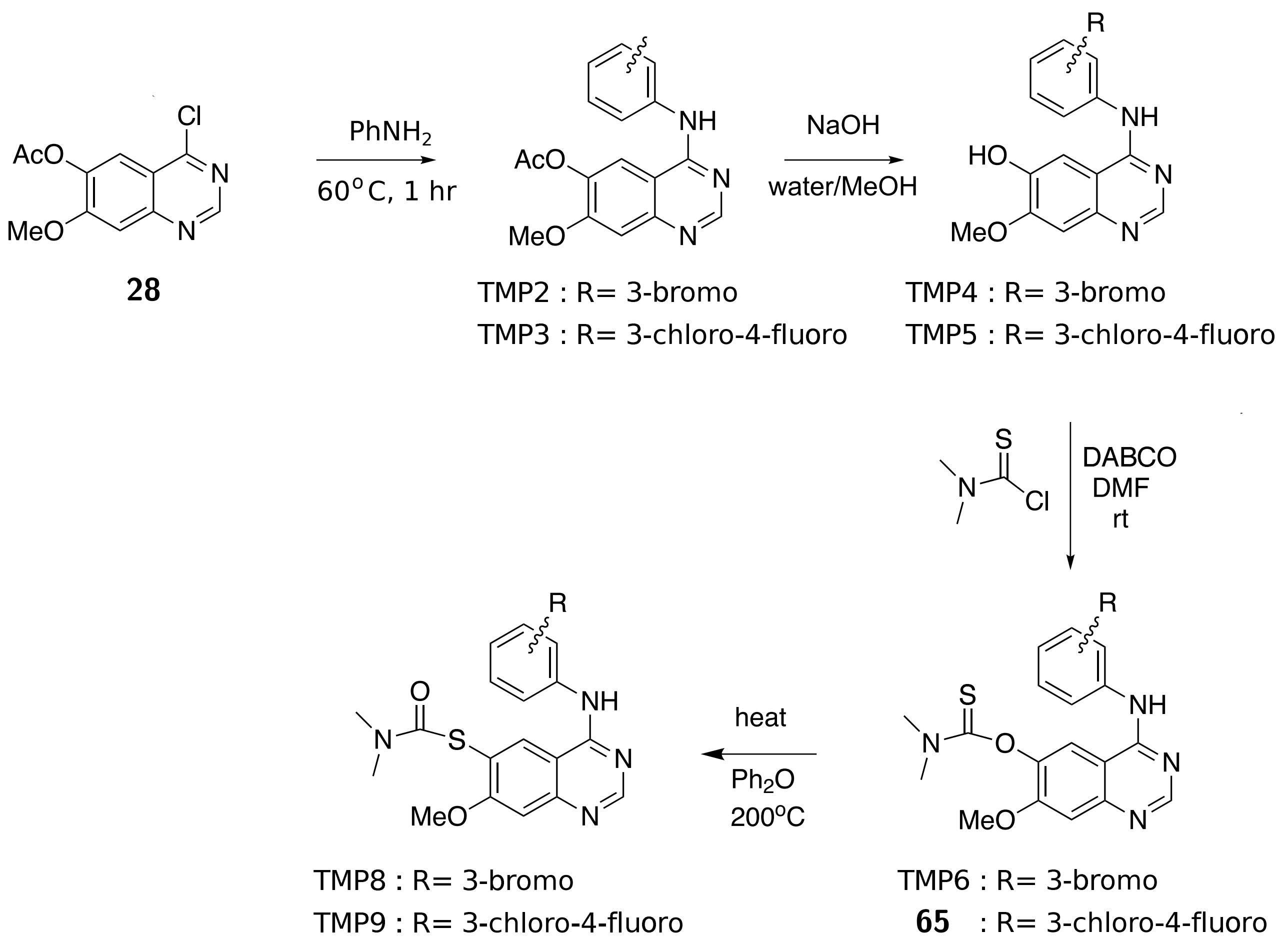

Scheme 47: Synthesis path to **48** and **66**

6.3.1 Synthesis of 4-[(3-bromophenyl)amino]-7-methoxyquinazolin-6-yl acetate - 64

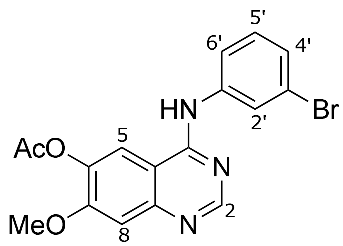

64

4-Chloro-7-methoxyquinazolin-6-yl acetate **28** (4.2 g, 0.017 moles) and *m*-bromoaniline (2.0 mL, 0.017 moles) was added to DMF (100 mL) at room temperature. The reaction was heated to 80 °C under argon, and allowed to stir for 2 hours. The reaction was then cooled to room temperature and diethyl ether (200 mL) was added to the cooled reaction mixture. The solution was cooled to 5 °C for half an hour. The solid that precipitated out was then filtered and air dried to yield a light brown solid (4.7 g, 0.012 moles, 73%) which was used without further purification.

R$_f$: 0.61 (20:1 DCM:MeOH); **M.p:** 321 – 322 °C; **LRMS** $(M+H)^+$= 364.0;
^{1}H NMR (300 MHz, DMSO) δ 11.59 (s, 1H, NH), 8.96 (s, 1H, H-2), 8.86 (s, 1H, H-5), 8.06 (s, 1H, H-2'), 7.78 (d, J = 7.9 Hz, 1H, H-4'), 7.58 (s, 1H, H-8), 7.53 7.40 (m, 2H, H-6' & 5'), 4.01 (s, 3H, O-CH_3), 2.39 (s, 3H, OAc).

6.3.2 Synthesis of 4-[(3-chloro-4-fluorophenyl)amino]-7-methoxyquinazolin-6-yl acetate- 29

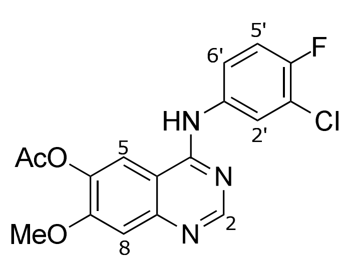

29

4-chloro-7-methoxyquinazolin-6-yl acetate **28** (3.6 g, 0.014 moles) and 3-chloro, 4-fluoroaniline **92** was added to DMF (110 mL) at room temperature. The reaction was heated to 80 °C under argon, and allowed to stir for 2.5 hours. The reaction was then cooled to room temperature and diethyl ether (200 mL) was added to the cooled reaction mixture. The solution was cooled to 5 °C for half an hour. The solid that precipitated out was then filtered and air dried to yield a light brown solid (3.5 g, 0.0097 moles, 68%) and used without further purification.

M.p: 270 – 271 °C;
^{1}H NMR (300 MHz, DMSO-d6) δ 11.63 (s, 1H, NH), 8.95 (s, 1H, H-2), 8.83 (s, 1H, H-5), 8.05 (dd, J = 6.8, 2.6 Hz, 1H, H-5'), 7.75 (ddd, J = 9.0, 4.3, 2.6 Hz, 1H, H-6'), 7.59 7.49 (m, 2H, H-8 & H-2'), 4.00 (s, 3H, O-CH_3), 2.38 (s, 3H, OAc) and was used without further purification. The ^{1}NMR spectrum compared well to the literature NMR for the same compound.[37]

6.3.3 Synthesis of 4-[(3-bromophenyl)amino]-7-methoxyquinazolin-6-ol - 33

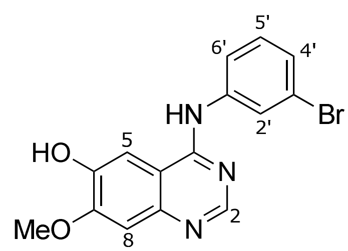

33

4-[(3-Bromophenyl)amino]-7-methoxyquinazolin-6-yl acetate **64** (4.7 g, 0.012 moles) was suspended in a 7N NH_3/MeOH solution (300 mL). The reaction was allowed to stir for 48 hours at room temperature. The reaction was monitored using TLC. The NH_3/MeOH was removed under vacuum, the solid was filtered and washed using small amounts of cold water. The solid was then placed in the desiccator. The product was a light brown solid (3.5 g, 0.010 moles, 84%) and was used without further purification.

R$_f$: 0.34 (9:1 DCM:MeOH); **M.p:** 248 °C;

^{1}H NMR (300 MHz, DMSO) δ 9.61 (s, 1H, OH), 9.45 (s, 1H, NH), 8.49 (s, 1H, H-2), 8.24 (dd, J= 2.0 Hz, 1H, H-2'), 7.90 (ddd, J= 8.1, 2.0, 1.1 Hz, 1H, H-4'), 7.81 (s, 1H, H-5), 7.31 (dd, J= 8.1 Hz, 1H, H-5'), 7.24 (dd, J= 2.0, 1.1 Hz, 1H, H-6), 7.21 (s, 1H, H-8), 3.98 (s, 3H, O-CH_3);

^{13}C NMR (126 MHz, DMSO) δ 155.8 (C-4), 153.9 (C-7), 151.9 (C-2), 146.7 (C-6), 146.3 (C-9), 141.6 (C-1'), 130.2 (C-5'), 125.1 (C-3'), 123.4 (C-4'), 121.1 (C-6'), 120.0 (C-2'), 109.7 (C-10), 107.2 (C-8), 105.3 (C-5), 55.9 (O-CH_3).

6.3.4 Synthesis of 4-[(3-chloro-4-fluorophenyl)amino]-7-methoxyquinazolin-6-ol- 30

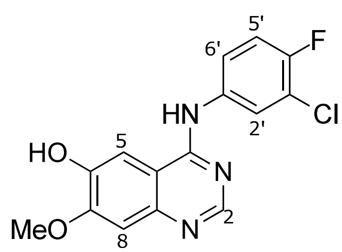

30

4-[(3-chloro-4-fluorophenyl)amino]-7-methoxy-3,4-dihydroquinazolin-6-yl acetate **29** (3.4 g, 0.0093 moles) was suspended in a 7N NH_3/MeOH solution (200 mL). The reaction was allowed to stir for 48 hours at room temperature. The reaction was monitored using TLC. The NH_3/MeOH was removed under vacuum, the solid was filtered and washed using small amounts of cold water. The solid was then placed in the desiccator. The product was a brown solid (2.2 g, 0.0068 moles, 73%), which was used without further purification. The ^{1}NMR spectrum compared well to the literature NMR for the same compound.[37]

R$_f$: 0.58 (9:1 DCM; MeOH); **M.p:** 314 – 316 °C;

^{1}H NMR (300 MHz, DMSO) δ 9.70 (s, 1H, OH), 9.47 (s, 1H, NH), 8.47 (s, 1H, H-2), 8.22 (dd, 1H, H-6'), 7.86 7.78 (m,1H, H-5'), 7.77 (s, 1H, H-5), 7.39 (t, 1H, H-2'), 7.21 (s, 1H, H-8), 3.97 (s, 3H, O-CH_3);

^{13}C NMR (75 MHz, DMSO) δ 155.8 (C-4), 153.9 (C-7), 152.81 (d, J = 242.3 Hz, C-4'), 146.7 (C-2), 146.2 (C-6), 137.14 (d, J = 3.0 Hz, C-2'), 122.7 (C-1'), 120.6 (C-9), 118.61 (d, J = 18.3 Hz, C-5'), 116.38 (d, J = 21.4 Hz, C-3'), 109.5 (C-8), 107.1 (C-5), 105.3 (C-10), 55.9 (O-CH_3). 152.81 (d, J = 242.3 Hz), 137.14 (d, J = 3.0 Hz), 118.61 (d, J = 18.3 Hz), 116.38 (d, J = 21.4 Hz)

6.4 MNK rearrangement on model systems

6.4.1 Synthesis of *O*-(2-methoxyphenyl)-dimethylcarbamothioate -79

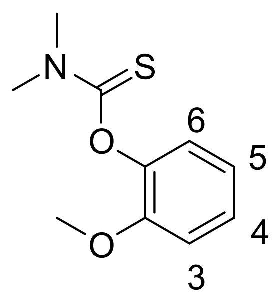

79

2-Methoxy phenol **78** (1.2 g, 0.010moles), DABCO (1.2 g, 0.010 moles) and dimethylthiocarbamoyl chloride (1.1 g, 0.010 moles) was mixed in DMF (40 mL) at room temperature under argon for 12 hours. The reaction was monitored by TLC, (4:1 hexane:EtOAc). Once the reaction was completed the reaction mixture was dissolved in ethyl acetate (80 mL) and then washed with water (40 mL) (×3) and brine (20 mL) (×2). The reaction was then dried using Na_2SO_4. The solvent was removed under vacuum and a yellow oil remained. This was placed in the freezer overnight, at which point the material crystallised. This solid was washed with cold diethyl ether to give the desired product; a yellow solid (0.9 g, 0.004 moles, 44%) which was used without further purification.

R_f: 0.68 (4:1 hexane:EtOAc); **M.p:** 56 – 59 °C;
^{1}H NMR (500 MHz, DMSO) δ 7.20 (dd, J= 7.8 Hz, 1H, H-6), 7.09 (d, J= 8.2

Hz, 1H, H-5), 7.00 (d, J= 7.8 Hz,1H, H-4), 6.93 (t, J= 7.8 Hz, 1H, H-3), 3.74 (s, 3H, O-CH_3), 3.34 (s, 3H, N-Me*), 3.29 (s, 3H, N-Me*);
^{13}C NMR (126 MHz, DMSO) δ 186.8 (C=S), 151.4 (C-2), 142.6 (C-1), 126.9 (C-5), 124.2 (C-4), 120.5 (C-3), 113.1 (C-6), 55.9 (O-CH_3), 43.0 (N-CH_3*), 38.5 (N-CH_3*).

6.4.2 Synthesis of *S*-(2-methoxyphenyl)-dimethylcarbamothioate -80

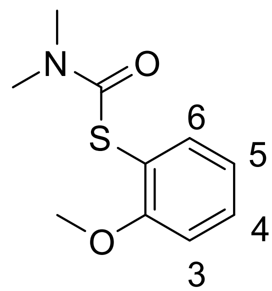

80

The rearrangement was conducted under microwave conditions. The starting material **79** (0.5 g, 0.002 moles) was dissolved in *N*-methyl-2-pyrrolidone (0.7 g, 0.007 moles). This reaction was then heated in the microwave at 160 °C for 15 minutes, this cycle was repeated 3 times. The reaction was followed using TLC (1:1 hexane: EtOAc), upon completion of the reaction, the reaction was dissolved in ethyl acetate (20 mL) and washed with water (5 mL) (×3) and brine (10 mL) (×2). The reaction was then dried and the excess solvent removed under vacuum. The final product **80** was obtained as a brown solid (0.3 g, 0.001 moles, 56%). This product was used without further purification.

R_f: 0.35 (1:1 hexane:EtOAc); **M.p:** 56 – 57 °C;
^{1}H NMR (500 MHz, DMSO) δ 7.42 (t, 1H, H-6), 7.37 (d, J= 7.6 Hz, 1H, H-5), 7.08 (d, J= 8.3 Hz, 1H, H-4), 6.96 (t, J= 7.6 Hz, 1H, H-3), 3.77 (s, 3H, O-CH_3), 3.01 (s, 3H, N-CH_3*), 2.89 (s, 3H, N-CH_3*);
^{13}C NMR (126 MHz, DMSO) δ 164.6 (C=O), 159.8 (C-2), 137.8 (C-1), 131.5

(C-5), 120.6 (C-4), 116.3 (C-3), 111.8 (C-6), 55.8 (O-CH_3), 39.1 (N-CH_3*), 36.5 (N-CH_3*).

6.4.3 Synthesis of *O*-(7-methoxyquinolin-6-yl)-dimethylcarbamothioate -84

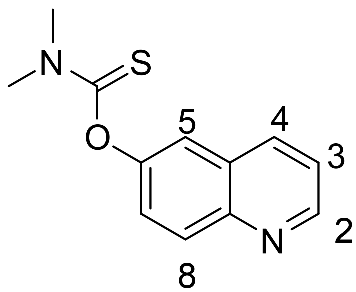

84

6-hydroxyquinol **83** (2.1g, 0.0144 moles), DABCO (1.7 g, 0.0148 moles) and dimethylthiocarbamoyl chloride (1.8 g, 0.0149 moles) was mixed in DMF (70 mL) at room temperature under argon for 12 hours. The reaction was monitored by TLC, (9:1 DCM: MeOH). Once the reaction was completed the reaction mixture was dissolved in ethyl acetate (10 mL) and then washed with water (5 mL) (×3) and brine (5 mL)(×2). The reaction was then dried using Na_2SO_4. The solvent was removed under vacuum, the solid was then titurated with ether and placed on high vac for 2 hours. The final product was obtained (0.6 g, 0.00288 moles, 20%) and was used without further purification.

R$_f$: 0.69 (9:1 DCM: MeOH); **LRMS** $(M+H)^+$= 233.1;
^{1}H NMR (300 MHz, CDCl$_3$) δ 8.90 (dd, J = 4.2, 1.7 Hz, 1H, Ar-H), 8.23 7.99 (m, 2H, Ar-H), 7.50 7.45(m, 2H, Ar-H), 7.40 (dd, *J*= 8.3, 4.2 Hz, 1H, Ar-H), 3.48 (s, 2H, N-Me*), 3.40 (s, 2H, N-Me*);
^{13}C NMR (75 MHz, CDCl$_3$) δ 187.2 (C=S), 151.4 (C-7), 149.9 (C-2), 146.1 (C-6), 135.5 (C-9), 130.3 (C-4), 128.1 (C-10), 125.9 (C-3), 121.2 (C-5), 119.1 (C-8), 43.1 (N-CH_3*), 38.6 (N-CH_3*).

6.4.4 Synthesis of *S*-(7-methoxyquinolin-6-yl)-dimethylcarbamothioate -85

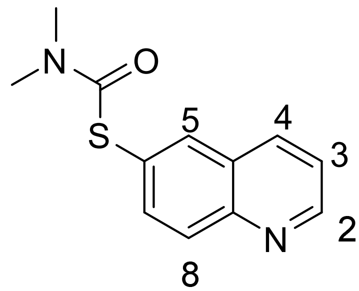

85

Compound **84** (0.2 g, 0.0009 moles) was dissolved in diphenyl ether (1.8 mL) at 60 °C. The reaction was then heated upto 206 °C in a silicon bath for 7 hours. The reaction was followed by TLC using 80% EtOAc: hexane. The reaction was then dissolved in ethyl acetate (10 mL) and worked up by washing with water (5 mL) and brine (5 mL). The solvent was then dried and removed under vacuum to give a white solid (72 mg, 0.00032 moles, 36%) and was used without further purification.

$\mathbf{R}_f$: 0.22 (80% EtOAc: hexane.);
¹H NMR (300 MHz, $CDCl_3$) δ 8.93 (dd, J= 4.3, 1.7 Hz, 1H, Ar-H), 8.15 8.07 (m, 2H, Ar-H), 8.01 (d, J=1.7 Hz, 1H, Ar-H), 7.77 (dd, J= 8.8, 1.9 Hz, 1H, Ar-H), 7.41 (dd, J= 8.3, 4.3 Hz, 1H, Ar-H), 3.12 (s, 3H, N-CH_3*), 3.05 3.12 (s, 3H, N-CH_3*).

6.4.5 Synthesis of *O*-4-[(3-bromophenyl)amino]-7-methoxyquinazolin-6-yldimethylcarbamothioate - 49

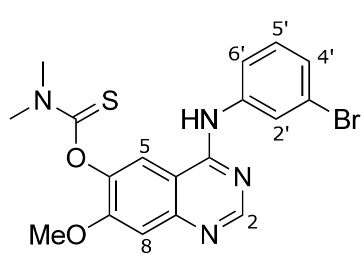

49

DMF (80 mL) was added to a mixture of 4-[(3-bromophenyl)amino]-7-methoxyquinazolin-6-ol **33** (1.9 g, 0.0057 moles), DABCO (1.4 g, 0.013 moles) and dimethylthiocarbamoyl chloride (1.3 g, 0.011 moles). The reaction was stirred at room temperature under argon for 24 hours. The reaction was monitored via NMR. When all the starting material was used up, the reaction was diluted using DCM (15 mL). The Organic layer was washed three times with water (10 mL) and once with brine (10 mL). The organic layer was then dried using MgSO4, the solvent was removed under vacuum. An oil was found. Overnight some of the solid crystalized out, these crystals were washed using EtOAc (5 mL). Water (5 mL) was added to the remainder of the oil and then heated, at which point a solid crashed out. This solid was also washed with EtOAc (5 mL). The washings were collected, and the EtOAc was removed under vacuum. This produced an oil, the same procedure was repeated again. The product was a white solid (1.6 g, 0.0039 moles, 68%) and was used without further purification.

M.p: 216 – 218 °C; **LRMS** $(M+H)^+ = 433.3$;
^{1}H NMR (500 MHz, DMSO) δ 9.64 (s, 1H, NH), 8.62 (s, 1H, H-2), 8.28 (s, 1H, H-5), 8.24 (s, 1H, H-2'), 7.90 (d, J= 8.0 Hz, 1H, H-4'), 7.35 7.31 (m, 2H, H-8 & H-5'), 7.27 (d, J= 8.0 Hz, 1H, H-6'), 3.92 (s, 3H, O-CH_3), 3.40 (s, 3H, N-CH_3*), 3.38 (s, 3H, N-CH_3*);
^{13}C NMR (126 MHz, DMSO) δ 186.7 (C=S), 157.3 (C-4), 156.5 (C-7), 155.0 (C-2), 150.6 (C-6), 142.7 (C-9), 141.6 (C-1'), 130.9 (C-5'), 126.2 (C-3'), 124.2 (C-4'), 121.7 (C-6'), 120.7 (C-2'), 117.6 (C-10), 109.2 (C-8), 108.8 (C-5), 56.8 (O-CH_3), 43.5 (N-CH_3*), 38.6 (N-CH_3*).

6.4.6 Synthesis of *S*-4-[(3-bromophenyl)amino]-7-methoxyquinazolin-6-yldimethylcarbamothioate - 48

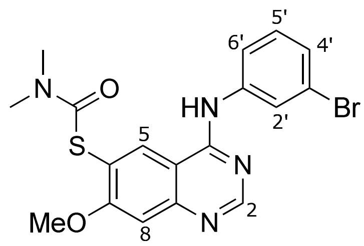

48

A mixture of *O*-4-[(3-bromophenyl)amino]-7-methoxyquinazolin-6-yldimethylcarbamothioate **49** (0.024 g, 5.5 x 10^{-5} moles) and diphenyl ether (1.3 mL) was heated to 210 °C in a silicon bath for 12 hours. The reaction can be followed by TLC using 20:1 DCM: MeOH. And completion was confirmed using NMR. Once completed, hexane (10 mL) was added to the reaction, this caused the product to precipitate out and allowed the removal of the diphenyl ether which was soluble in the hexane. The remaining solid was used without further purification.

M.p: 336 °C;

^{1}H NMR (500 MHz, DMSO) δ 9.85 (s, 1H, NH), 8.74 (s, 1H, H-2), 8.64 (s, 1H, H-5), 8.23 (dd, J= 1.9 Hz, 2H, H-2'), 7.94 7.88 (m, 2H, H-4'), 7.35 (d, J= 8.0 Hz, 1H, H-6'), 7.32 7.27 (m, 3H, H-5'), 3.95 (s, 3H, O-CH_3), 3.13 (s, 3H, N-CH_3*), 2.94 (s, 3H, N-CH_3*).

6.4.7 Synthesis of *O*-4-[(3-chloro-4-fluorophenyl)amino]-7-methoxyquinazolin-6-yldimethylcarbamothioate - 65

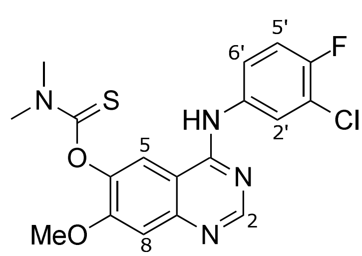

65

A mixture of 4-[(3-chloro-4-fluorophenyl)amino]-7-methoxyquinazolin-6-ol **30** (2.1 g, 0.0055 moles), DABCO (1.4 g, 0.012 moles) and dimethylthiocarbamoyl chloride (1.5 g, 0.012 moles) was mixed in DMF (70 mL) at room temperature under argon for 48 hours. A mini work up was conducted and starting material was found to still be present. After this time, additional DABCO (0.1 g, 0.001 moles) and dimethylthiocarbamoyl chloride (0.2 g, 0.001 moles) was added to the reaction. After an additional 6 hours, the reaction was complete and was worked up in the same way as the synthesis of **49**. However the product **65** was obtained after the DCM was removed under vacuum. The product was a white solid (0.7 g, 0.002 moles, 34%). This was carried through without further purification

M.p: 254 – 255 °C;

^{1}H NMR (500 MHz, DMSO) δ 9.66 (s, 1H, NH), 8.60 (s, 1H, H-2), 8.24 (s, 1H, H-5), 8.22 (dd, J= 6.8, 2.7 Hz, 1H, H-6'), 7.86 7.80 (m, 1H, H-5'), 7.42 (t, J= 9.1 Hz, 1H, H-2'), 7.33 (s, 1H, H-8), 3.92 (s, 3H, O-CH_3), 3.40 (s, 3H, N-Me*), 3.38 (s, 3H, N-Me*);

^{13}C NMR (126 MHz, DMSO) δ 186.7 (C=S), 157.3 (C-4), 156.5 (C-7), 154.9 (C-2), 153.64 (d, J = 242.9 Hz, C-4'), 150.6 (C-6), 142.7 (C-9), 137.1 (C-1'), 123.6 (C-2'), 122.35 (d, J = 6.8 Hz, C-6'), 119.25 (d, J = 18.3 Hz, C-3'), 117.01 (d, J = 21.7 Hz, C-5') 116.9 (C-10), 109.0 (C-8), 108.8 (C-5), 56.8 (O-CH_3), 43.5 (N-CH_3*), 39.0 (N-CH_3*).

6.4.8 Synthesis of *S*-4-[(3-chloro-4-fluorophenyl)amino]-7-methoxyquinazolin-6-yldimethylcarbamothioate - 66

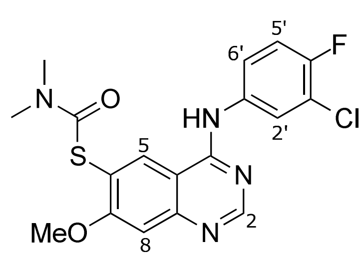

66

A mixture of *O*-4-[(3-chloro-4-fluorophenyl)amino]-7-methoxyquinazolin-6-yldimethylcarbamothioate **65** (0.2 g, 6 2x 10^{-4} moles) and diphenyl ether (2 mL) was stirred for 12 hours at 210 °C in a silicon bath. The reaction can be followed by TLC using 20:1 DCM: MeOH. And completion was confirmed using NMR. Hexane was added to the cooled reaction mixture, causing the product to precipitate out of the diphenyl ether. The reaction was the filtered and washed with cold hexane (10 mL).(0.2 g, 3.8 x 10^{-4} moles, 62%). When a ^{1}H NMR spectrum was obtained, it was predicted that the correct compound was synthesised. However, there were too many contaminants to fully characterise and confirm the structure. In trying to purify the compound using column chromatography, the material was not successfully isolated. Due to time constraints in the laboratory, a repetition of this experiment was not possible.

$\mathbf{R_f}$: 0.76 (20:1 DCM:MeOH); **LRMS** $(M+H)^+$= 433.4.

Bibliography

[1] World Health Organisation. Cancer - key facts. *http://www.who.int/mediacentre/factsheets/fs297/en/*, 2015.

[2] McGuire S. World Cancer Report 2014. Geneva, Switzerland: World Health Organization, International Agency for Research on Cancer, WHO Press, 2015. Technical Report 2161-8313, 2014.

[3] Cancer. *http://www.who.int/mediacentre/factsheets/fs297/en/*, 2015.

[4] Z. Song, Y. Ge, C. Wang, S. Huang, X. Shu, K. Liu, Y. Zhou, and X. Ma. Challenges and Perspectives on the Development of Small-Molecule Egfr Inhibitors against T790M-Mediated Resistance in Non-Small-Cell Lung Cancer. *Journal of Medicinal Chemistry*, 59(14):6580 – 6594, 2016.

[5] American Cancer Society. Lung cancer (non-small cell). *http://www.cancer.org/acs/groups/cid/documents/webcontent/003115-pdf.pdf*.

[6] J. L. Kuiper, D. A. M. Heideman, E. Thunnissen, M. A. Paul, A. W. Van Wijk, P. E. Postmus, and E. F. Smit. Incidence of T790M Mutation in (sequential) Rebiopsies in EGFR-mutated NSCLC-patients. *Lung Cancer*, 85(1):19 – 24, 2014.

[7] A. Matikas, D. Mistriotis, V. Georgoulias, and A. Kotsakis. Current and Future Approaches in the Management of Non-Small-Cell Lung Cancer Patients With Resistance to EGFR TKIs. *Clinical Lung Cancer*, 16(4):252 – 261, 2015.

[8] A. F. Abdel-Magid. Inhibitors of the Epidermal Growth Factor Receptor (EGFR) May Provide Effective Treatment for Lung Adenocarcinoma. *ACS Medicinal Chemistry Letters*, 6(7):732 – 733, 2015.

[9] C. Zappa and S. A. Mousa. Non-Small Cell Lung Cancer: Current Treatment and Future Advances. *Translational Lung Cancer Research*, 5(3):288 – 300, 2016.

[10] V. Nelson, J. Ziehr, M. Agulnik, and M. Johnson. Afatinib: Emerging Next-Generation Tyrosine Kinase Inhibitor for NSCLC. *OncoTargets and Therapy*, 6:135 – 143, 2013.

[11] C. Tan, D. Gilligan, and S. Pacey. Treatment Approaches for EGFR-Inhibitor-Resistant Patients with Non-Small-Cell Lung Cancer. *The Lancet Oncology*, 16(9):447 – 459, 2015.

[12] N. Normanno, M. R. Maiello, and A. De Luca. Epidermal Growth Factor Receptor Tyrosine Kinase Inhibitors (EGFR-TKIs): Simple Drugs with a Complex Mechanism of Action? *Journal of Cellular Physiology*, 194(1):13 – 19, 2003.

[13] J. Zhang, Yang P.L., and N. S. Gray. Targeting Cancer with Small Molecule Kinase Inhibitors. *Nature Reviews Cancer*, 9:28 – 39, 2009.

[14] Fabbro D., Ruetz S., Buchdunger E., Cowan-Jacob S. W., Fendrich G., Liebetanz J., J. Mestan, T. O'Reilly, P. Traxler, B. Chaudhuri, H. Fretz, J. Zimmermann, T. Meyer, G. Caravatti, P. Furet, and P. W. Manley. Protein Kinases as Targets for Anticancer Agents from Inhibitors to Useful Drugs. *Pharmacology & Therapeutics*, 93:79 – 98, 2002.

[15] H. Modjtahedi, B. Cho, M. C. Michel, and F. Solca. A Comprehensive Review of the Preclinical Efficacy Profile of the ErbB Family Blocker Afatinib in Cancer. *Naunyn-Schmiedeberg's Archives of Pharmacology*, 387(6):505 – 521, 2014.

[16] P. Traxler and P. Furet. Strategies Toward the Design of Novel and Selective Protein Tyrosine Kinase Inhibitors. *Pharmacology & Therapeutics*, 82(2 - 3):195 – 206, 1999.

[17] S. V. Sharma, D. W. Bell, J. Settleman, and D. A. Haber. Epidermal Growth Factor Receptor Mutations in Lung Cancer. *Nat Rev Cancer*, 7(3):169 – 181, 2007.

[18] R. S. Herbst. Review of Epidermal Growth Factor Receptor Biology. *International Journal of Radiation Oncology*, 59(2):S21 – S26, 2004.

[19] C. Yewale, D. Baradia, I. Vhora, S. Patil, and A. Misra. Epidermal Growth Factor Receptor Targeting in Cancer: A Review of Trends and Strategies. *Biomaterials*, 34(34):8690 – 8707, 2013.

[20] H. M. Berman, J. Westbrook, Z. Feng, G. Gilliland, T. N. Bhat, H. Weissig, I. N. Shindyalov, and P. E. Bourne. The Protein Data Bank, Nucleic Acids Research, 2000. 28: 235-242.

[21] D. W. Fry, Kraker A. J., A. McMichael, L. A. Ambroso, J. M. Nelson, W. R. Leopold, R. W. Connors, , and Bridges AJ. A Specific Inhibitor of the Epidermal Growth Factor Receptor Tyrosine Kinase. *Science*, (0036 - 8075), 1994.

[22] Y. Cai-Hong, K. E. Mengwasser, A. V. Toms, M. S. Woo, H. Greulich, K. Wong, M. Meyerson, and M. J. Eck. The T790M Mutation in EGFR Kinase Causes Drug Resistance by Increasing the Affinity for ATP. *Proceedings of the National Academy of Sciences*, 105(6):2070 – 2075, 2008.

[23] Y. Yosaatmadja, S. Silva, J. M. Dickson, A. V. Patterson, J. B. Smaill, J. U. Flanagan, M. J. McKeage, and C. J. Squire. Binding Mode of the Breakthrough Inhibitor AZD9291 to Epidermal Growth Factor Receptor Revealed. *Journal of Structural Biology*, 192(3):539 – 544, 2015.

[24] W. Li, S. Ren, J. Li, A. Li, L. Fan, X. Li, C. Zhao, Y. He, G. Gao, X. Chen, S. Li, J. Shi, C. Zhou, K. Fei, and G. Schmid-Bindert. T790M Mutation is Associated with Better Efficacy of Treatment Beyond Progression with EGFR-TKI in Advanced NSCLC Patients. *Lung Cancer*, 84(3):295 – 300, 2014.

[25] Non-Small Cell Lung Cancer Treatment (PDQ) Patient Version. *https://www.cancer.gov/types/lung/patient/non-small-cell-lung-treatment*, 2016.

[26] M. Juchum, M. Gunther, and S. A. Laufer. Fighting Cancer Drug Resistance: Opportunities and Challenges for Mutation-Specific EGFR Inhibitors. *Drug Resistance Updates*, 20:12 – 28, 2015.

[27] H. Cheng, S. K. Nair, and B. W. Murray. Recent Progress on Third Generation Covalent EGFR Inhibitors. *Bioorganic & Medicinal Chemistry Letters*, 26(8):1861 – 1868, 2016.

[28] C. Tan, B. Cho, and R.A. Soo. Next-Generation Epidermal Growth Factor Receptor Tyrosine Kinase Inhibitors in Epidermal Growth Factor Receptor - Mutant Non-Small Cell Lung Cancer. *Lung Cancer*, 93:59 – 68, 2016.

[29] M. G. Denis, A. Audrey Vallace, and S. Thacoleyre. EGFR T790M Resistance Mutation in Non Small-Cell Lung Carcinoma. *Clinica Chimica Acta*, 444:81 – 85, 2015.

[30] C. Ma, S. Wei, and Y. Song. T790M and Acquired Resistance of EGFR TKI: a Literature Review of Clinical Reports. *Journal of Thoracic Disease*, 3:10 – 18, 2011.

[31] M. Da Arcangelo and F. Cappuzzo. Focus on the Potential Role of Ficlatuzumab in the Treatment of Non-Small Cell Lung Cancer. *Biologics : Targets & Therapy*, 7:61 – 68, 2013.

[32] J. M. Bradshaw, J. M. McFarland, V. O. Paavilainen, A. Bisconte, D. Tam, V. T. Phan, S. Romanov, D. Finkle, J. Shu, V. Patel, T. Ton, X. Li, D. G. Loughhead, P. A. Nunn, D. E. Karr, M. E. Gerritsen, J. O. Funk, T. D. Owens, E. Verner, K. A. Brameld, R. J. Hill, D. M. Goldstein, and J. Taunton. Prolonged and Tunable Residence Time Using Reversible Covalent Kinase Inhibitors. *Nature Chemical Biology*, 11(7):525 – 531, 2015.

[33] S. Krishnan, R. M. Miller, B. Tian, R. D. Mullins, M. P. Jacobson, and J. Taunton. Design of Reversible, Cysteine-Targeted Michael Acceptors Guided by Kinetic and Computational Analysis. *Journal of the American Chemical Society*, 136(36):12624 – 12630, 2014.

[34] M. Asif. Chemical Characteristics, Synthetic Methods, and Biological Potentials of Quinazoline and Quinazoline Derivatives. *Internarional Journal of Medicinal Chemistry*, 2014.

[35] I. Khan, S. Zaib, S. Batool, N. Abbas, Z. Ashraf, J. Iqbal, and A. Saeed. Quinazolines and Quinazolinones as Ubiquitous Structural Fragments in Medicinal Chemistry: An Update on the Development of Synthetic Methods and Pharmacological Diversification. *Bioorganic & Medicinal Chemistry*, 24(11):2361 – 2381, 2016.

[36] I. Khan, A. Ibrar, N. Abbas, and A. Saeed. Recent Advances in the Structural Library of Functionalized Quinazoline and Quinazolinone Scaffolds: Synthetic Approaches and Multifarious Applications. *European Journal of Medicinal Chemistry*, 76:193 – 244, 2014.

[37] P. Knesl, D. Roseling, and U. Jordis. Improved Synthesis of Substituted 6,7-Dihydroxy-4-quinazolineamines: Tandutinib, Erlotinib and Gefitinib. *Molecules*, 11(1420-3049 (Linking)):286 – 297, 2006.

[38] Y. Chen, M. Feng, S. Li, J. Xu, H. Ning, Y. He, X. Wang, R. Ding, and C. Qi. Synthesis and Evaluation of Novel F-18 Labeled 4-Aminoquinazoline Derivatives: Potential PET Imaging Agents for Tumor Detection. *Bioorganic & Medicinal Chemistry Letters*, 22(14):4745 – 4749, 2012.

[39] V. Chandregowda, A.K. Kush, and G. C. Reddy. Synthesis and in Vitro Antitumor Activities of Novel 4-Anilinoquinazoline Derivatives. *European Journal of Medicinal Chemistry*, 44(7):3046 – 3055, 2009.

[40] A. M. Prior. Post Doctoral. *University of Witwatersrand*, 2014 - 2015.

[41] M. M. J. P. E. Sthijns, M. J. Randall, A. Bast, and G. R. M. M. Haenen. Adaptation to Acrolein Through Upregulating the Protection by Glutathione in Human Bronchial Epithelial Cells: The Materialization of the Hormesis Concept. *Biochemical and Biophysical Research Communications*, 446(4):1029 – 1034, 2014.

[42] H. Kwart and E. R. Evans. The Vapor Phase Rearrangement of Thioncarbonates and Thioncarbamates. *Journal of Organic Chemistry*, 31(2):410 – 413, 1966.

[43] M. S. Newman and H. A. Karnes. The Conversion of Phenols to Thiophenols via Dialkylthiocarbamates. *Journal of Organic Chemistry*, 31(12):3980 – 3984, 1966.

[44] K Miyazaki. *Journal Annual Meeting of the Chem Society of Japan*, (9505):175, 1965.

[45] C. Zonta, O. De Lucchi, R. Volpicelli, and L. Cotarca. Thion-Thiol Rearrangement: Miyazaki Newman Kwart Rearrangement and Others. In *Sulfur-Mediated Rearrangements II*. 2007.

[46] I. Hoffmann and J. Schatz. Microwave-mediated Newman-Kwart Rearrangement in Water. *RSC Advances*, 6(84):80692 – 80699, 2016.

[47] H. Jacobsen and J. P. Donahue. Expanding the Scope of the Newman Kwart Rearrangement: A computational assessment. *Canadian Journal of Chemistry*, 84(11):1567 – 1574, 2006.

[48] M. Burns, G. C. Lloyd-Jones, J. D. Moseley, and J. S. Renny. The Molecularity of the Newman- Kwart Rearrangement. *Journal of Organic Chemistry*, 75(19):6347 – 6353, 2010.

[49] A. Schönberg and L Vargha. Über die (thermische) Umlagerung von Thion-Kohlensäure-estern in Thiol-kohlensäure-ester. (16. Mitteil.) über organische Schwefelverbindugen. *European Journal of Inorganic Chemistry*, 63:178 – 180, 1930.

[50] A. Kaji, Y. Araki, , and K. Miyazaki. Studies of the Thiocarbonyl Compounds. III. The Mechanisms of the Thermal Rearrangement of Aryl Thionocarboxylates. *Bulletin of the Chemical Society of Japan*, 44:1393 – 1399, 1971.

[51] K. Miyazaki. The Thermal Rearrangement of Thionocarbamates to Thiolcarbamates. *Tetrahedron Letters*, 9(23):2793 – 2798, 1968.

[52] H. M. Relles. Steric Rate Enhancement in the Chapman Rearrangement. *Journal of Organic Chemistry*, 33(6):2245 – 2249, 1968.

[53] G. C. Lloyd-Jones, J. D. Moseley, and J. S. Renny. Mechanism and Application of the Newman-Kwart O-S Rearrangement of O-Aryl Thiocarbamates. *Synthesis*, 2008(5):661 – 689, 2008.

[54] J. P. Gilday, P. Lenden, J. D. Moseley, and B. G. Cox. The Newman-Kwart Rearrangement: A Microwave Kinetic Study. *Journal of Organic Chemistry*, 73(8):3130 – 3134, 2008.

[55] A. J. Perkowski, C. L. Cruz, and D. A. Nicewicz. Ambient-Temperature Newman-Kwart Rearrangement Mediated by Organic Photoredox Catalysis. *Journal of American Chemistry Society*, 137(50):15684 – 15687, 2015.

[56] V. M. Buha, Dharmaraj N. R., Mahesh T. C., Kishor H. C., Bhushan M. M., Pathik S. B., and Nisha K. S. Synthesis, Biological Evaluation and QSAR Study of a Series of Substituted Quinazolines as Antimicrobial Agents. volume 22, pages 4096 – 4109, 2012.

[57] K. C. Srivastava. Studies on the Ionization of Substituted Benzoic Acids. *Journal fur praktische Chemie*, 35(3-4):118 – 121, 1967.

[58] K. Ochiai, S. Takita, T. Eiraku, A. Kojima, K. Iwase, T. Kishi, K. Fukuchi, T. Yasue, D. R. Adams, R. W. Allcock, Z. Jiang, and Y. Kohno. Phosphodiesterase Inhibitors. Part 3: Design, Synthesis and Structure- Activity Relationships of Dual PDE3/4-Inhibitory Fused Bicyclic Heteroaromatic-

Dihydropyridazinones with Anti-Inflammatory and Bronchodilatory Activity. *Bioorganic & Medicinal Chemistry*, 20(5):1644 – 1658, 2012.

[59] K. P. Machumele. Phonour's project. *University of Witwatersrand*, 2016.

[60] L. Fu, C-J. Yao, N-J. Chang, J-R. Chen, and L-Q. Lu. Oxidative Cross-Esterfication of Dithiolanes with Alcohols through a Cross-Dehydrogenative Coupling (CDC)/ Deprotective Sequence. *Organic & Biomolecular Chemistry*, 42, 2011.

NMR spectra

RC-2-3.1.10.fid
Robyn: RC-2-3.1: DMSO: 26/01/2015

1H NMR (300 MHz, DMSO-d_6) δ 12.45 (s, 1H), 8.14 (s, 1H), 8.11 (d, J = 8.5 Hz, 1H), 7.73 (d, J = 2.0 Hz, 1H), 7.56 (dd, J = 8.5, 2.1 Hz, 1H).

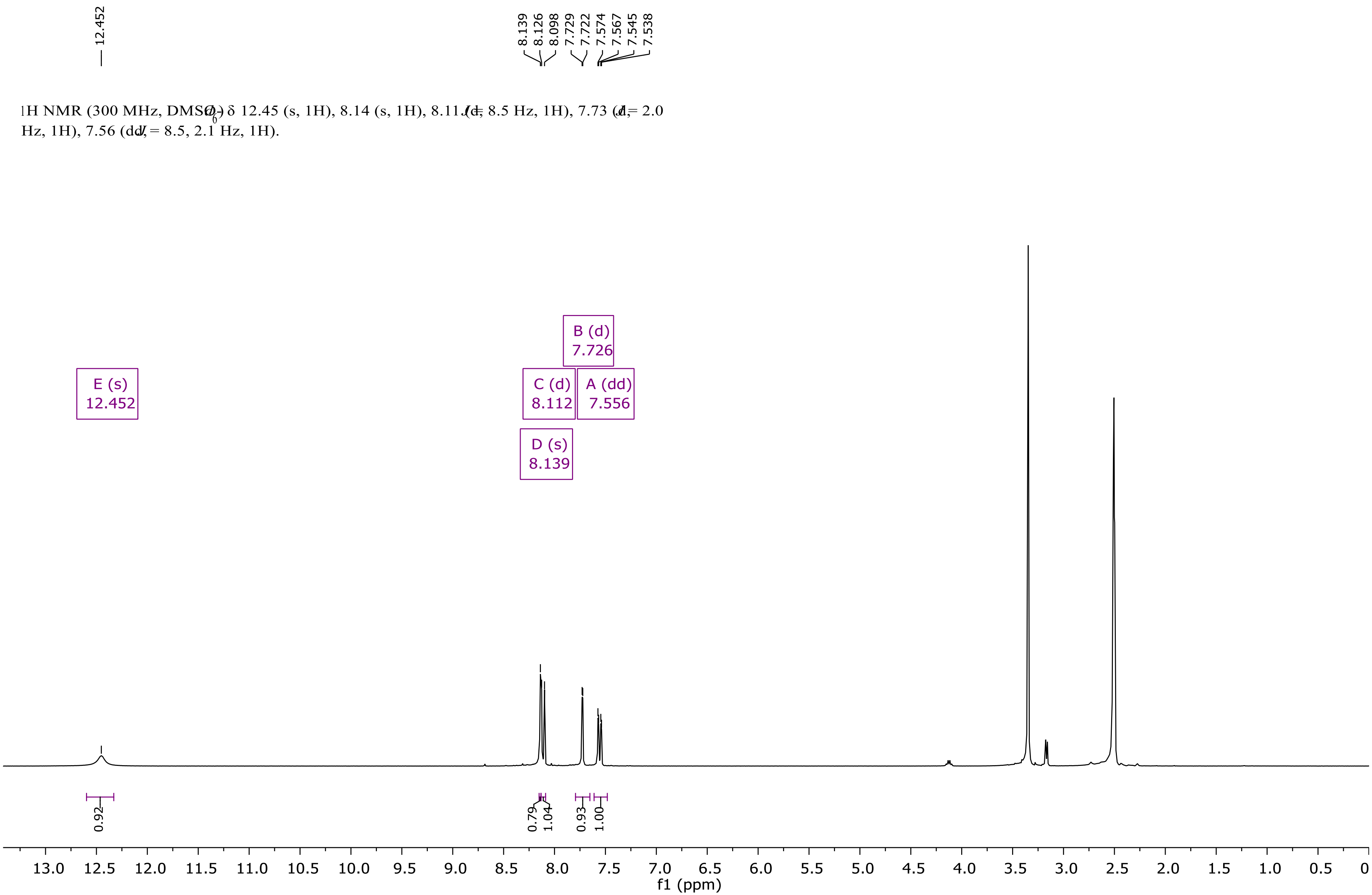

RC-202.2.fid
Robyn: RC-202: CDCL3: 13/01/2016: 300K: 1H: 500: AP

[1]H NMR (500 MHz, Chloroform-*d*) δ 7.68 (dd, *J* = 8.4, 2.0 Hz, 1H), 7.54 (d, *J* = 2.0 Hz, 1H), 6.87 (d, *J* = 8.4 Hz, 1H), 4.35 (q, *J* = 7.1 Hz, 2H), 3.93 (s, 6H), 1.38 (t, *J* = 7.2 Hz, 3H).

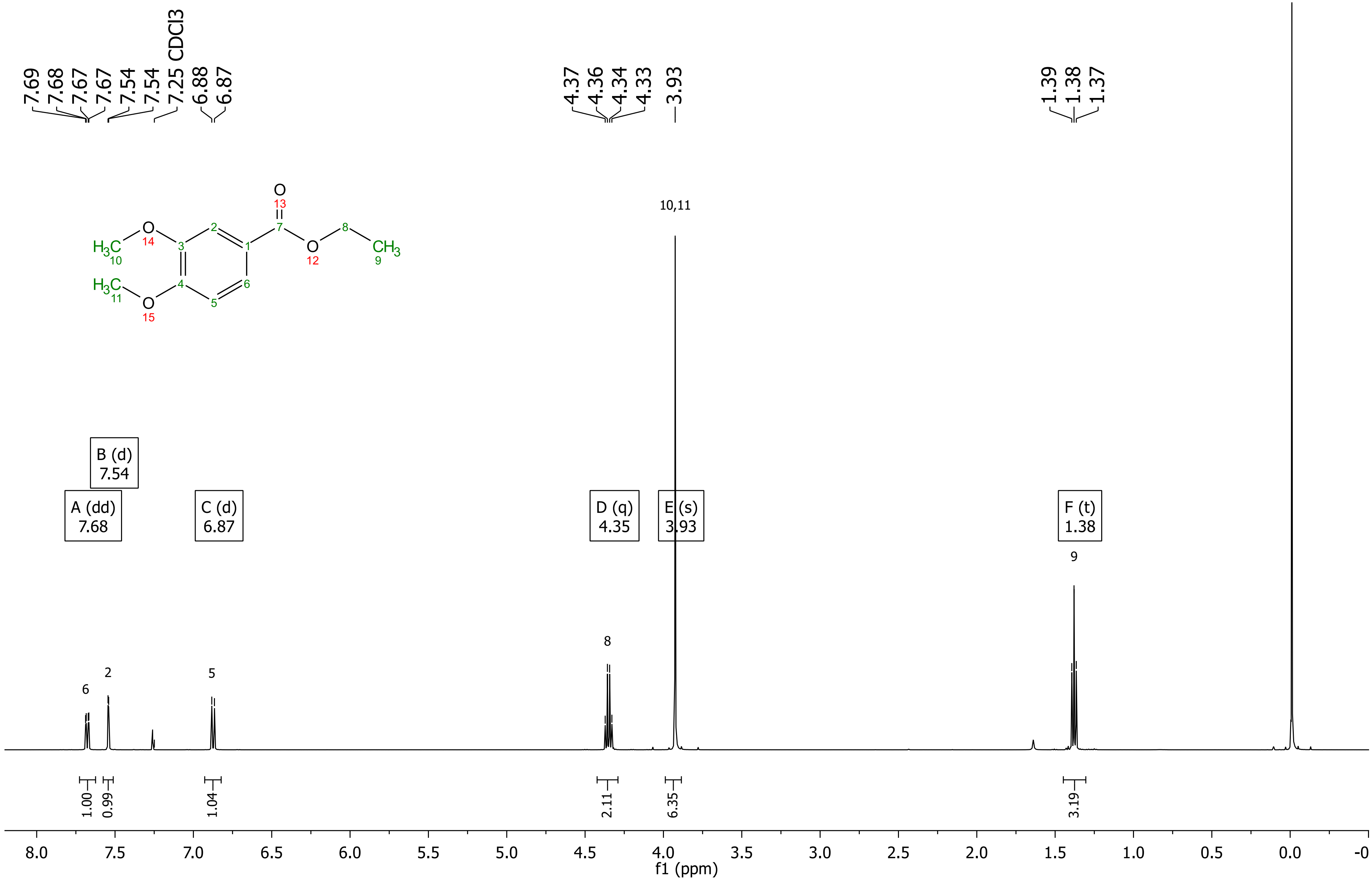

RC-202.3.fid
Robyn: RC-202: CDCL3: 13/01/2016: 300K: 1H,13C, COSY, NOESY, HSQC: 500: AP

[13]C NMR (126 MHz, $CDCl_3$) δ 166.3 (7), 152.8 (4), 148.5 (3), 123.4 (6), 122.9 (1), 111.9 (2), 110.1 (5), 77.0, 60.7 (8), 55.9 (10, 11), 14.3 (9).

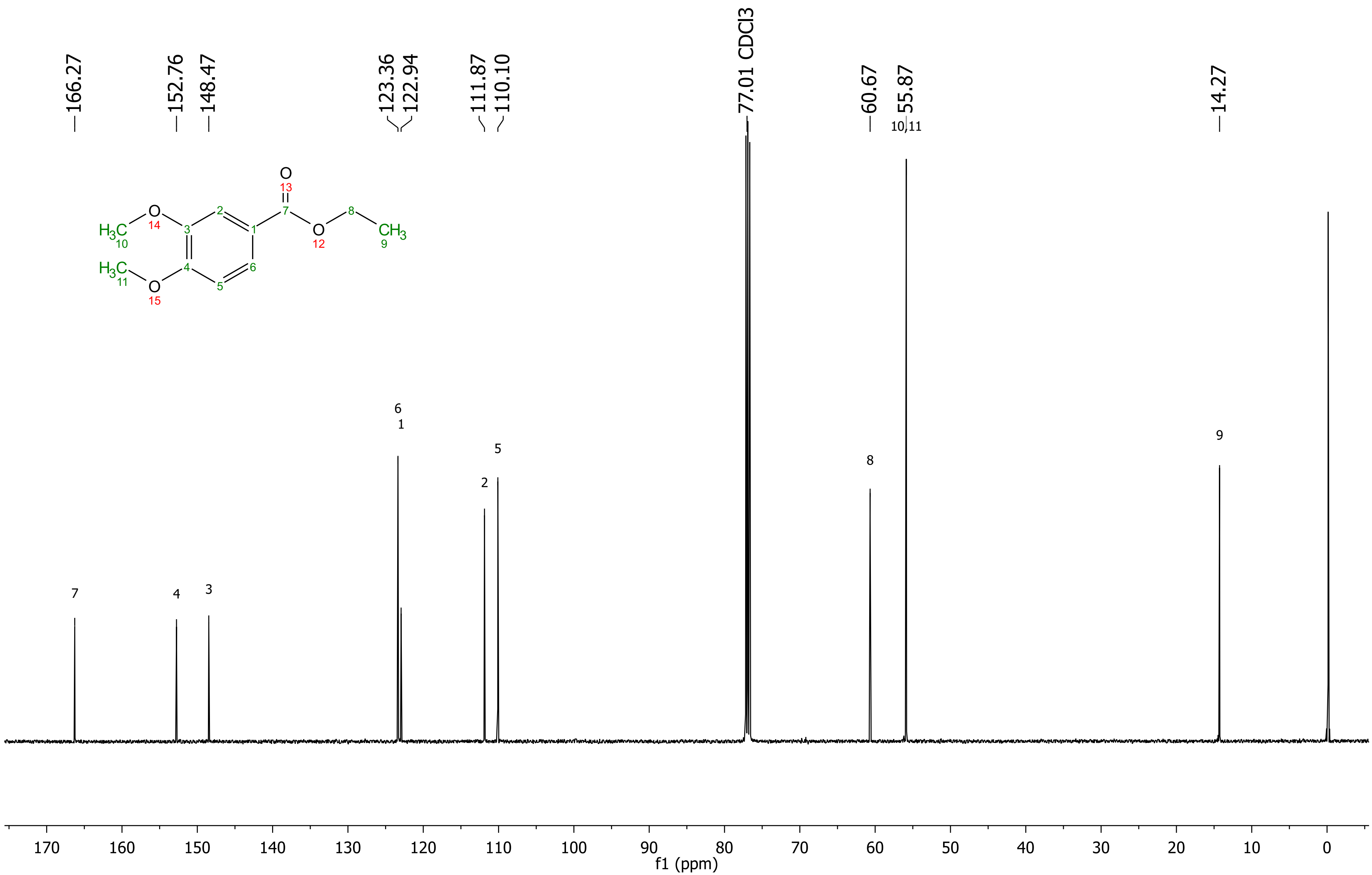

RC-203.30.fid
Robyn: RC-203: CDCL3: 08/06/2016: 1H, 13C, COSY, HSQC: AP

[1]H NMR (300 MHz, $CDCl_3$) δ 7.45 (s, 1H), 7.07 (s, 1H), 4.37 (q, *J* = 7.1, 7.1, 7.1 Hz, 2H), 3.97 (s, 3H), 3.96 (s, 3H), 1.34 (t, *J* = 7.1, 7.1 Hz, 3H).

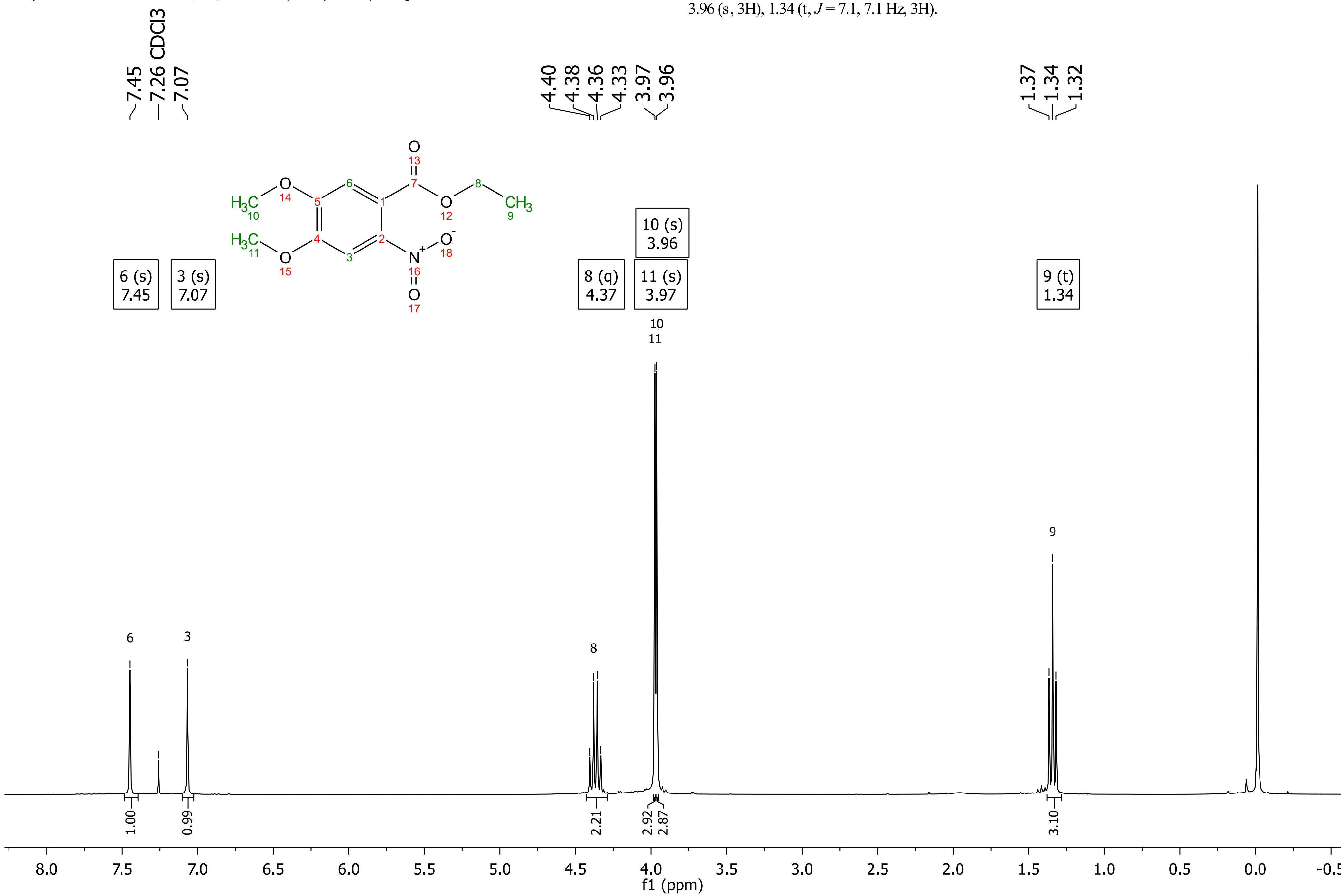

RC-203.31.fid
Robyn: RC-203: CDCL3: 08/06/2016: 1H, 13C, COSY, HSQC: AP

^{13}C NMR (75 MHz, $CDCl_3$) δ 165.96, 152.63, 150.44, 141.34, 122.18, 110.95, 107.10, 77.27, 62.59, 56.76, 56.72, 13.90.

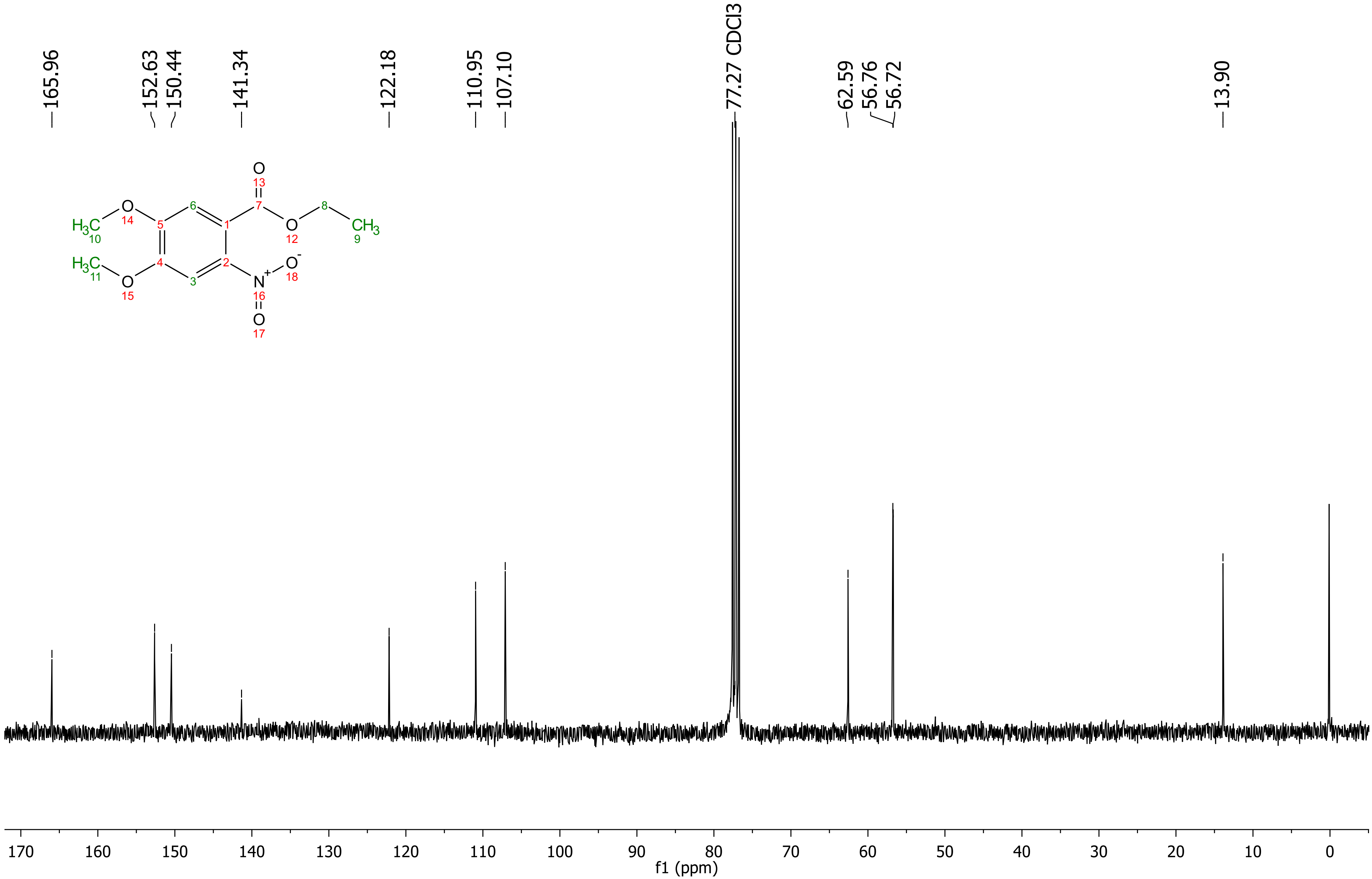

RC-204.10.fid
Robyn: RC-204: CDCL3: 08/06/2016: 1H, 13C, COSY, HSQC: AP

^{1}H NMR (300 MHz, $CDCl_3$) δ 7.30 (s, 1H), 6.13 (s, 1H), 5.22 (s, 3H), 4.30 (q, J = 7.1, 7.1, 7.1 Hz, 2H), 3.84 (s, 3H), 3.81 (s, 3H), 1.36 (t, J = 7.1, 7.1 Hz, 3H).

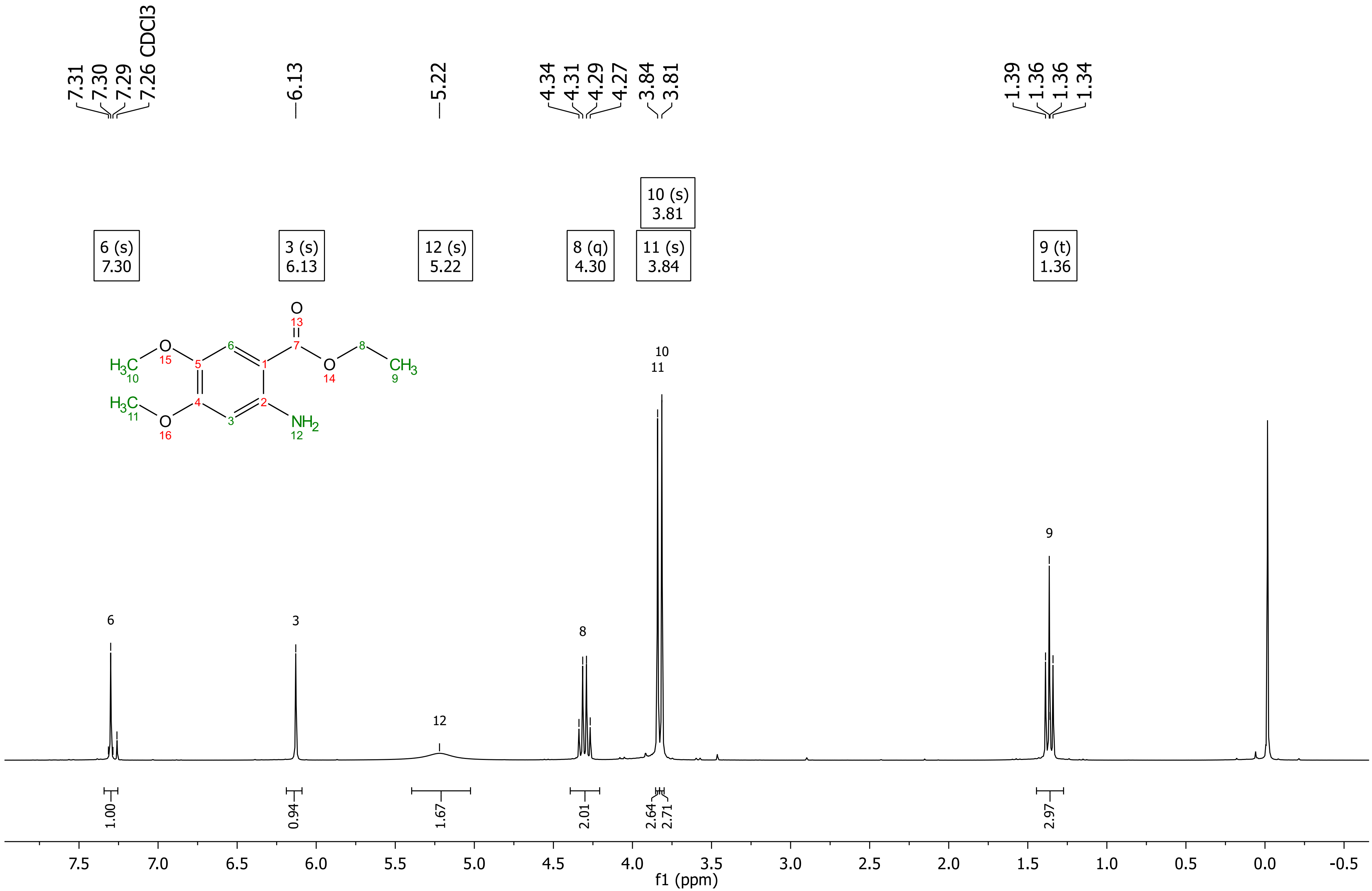

RC-204.11.fid
Robyn: RC-204: CDCL3: 08/06/2016: 1H, 13C, COSY, HSQC: AP

^{13}C NMR (75 MHz, $CDCl_3$) δ 167.88, 154.89, 147.20, 140.66, 113.05, 102.53, 99.48, 77.25, 60.17, 56.60, 55.85, 14.60.

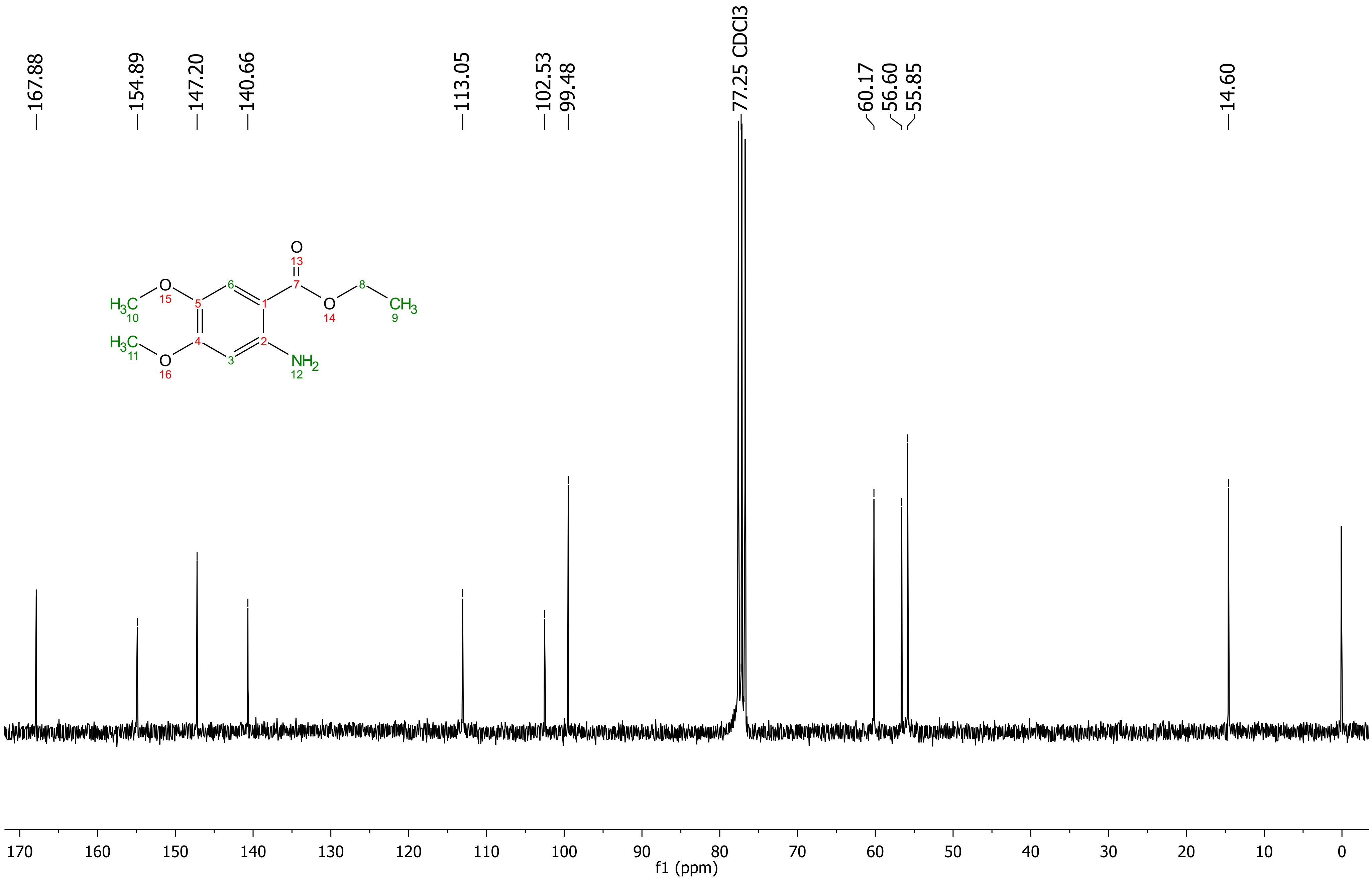

RC-205.1.fid
Robyn: RC-205: DMSO: 06/11/2016: 300K: 1H, 13C: 500NMR: AP

^{1}H NMR (500 MHz, DMSO) δ 12.05 (s, 1H), 7.98 (s, 1H), 7.44 (s, 1H), 7.12 (s, 1H), 3.90 (s, 3H), 3.86 (s, 3H).

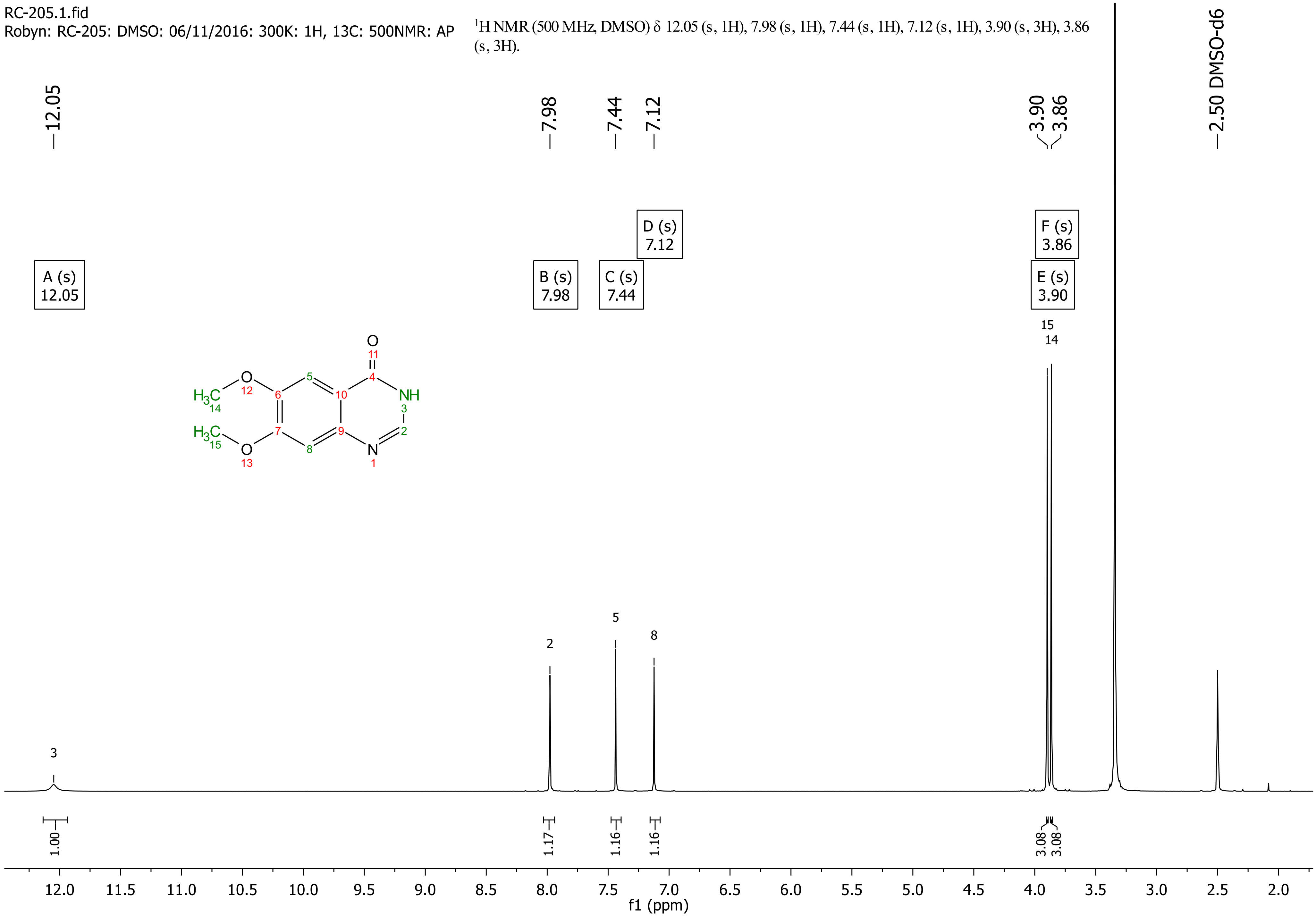

RC-205.2.fid
Robyn: RC-205: DMSO: 06/11/2016: 300K: 1H, 13C: 500NMR: AP

[13]C NMR (126 MHz, DMSO) δ 160.53, 154.93, 149.02, 145.34, 144.30, 116.07, 108.49, 105.40, 56.40, 56.17.

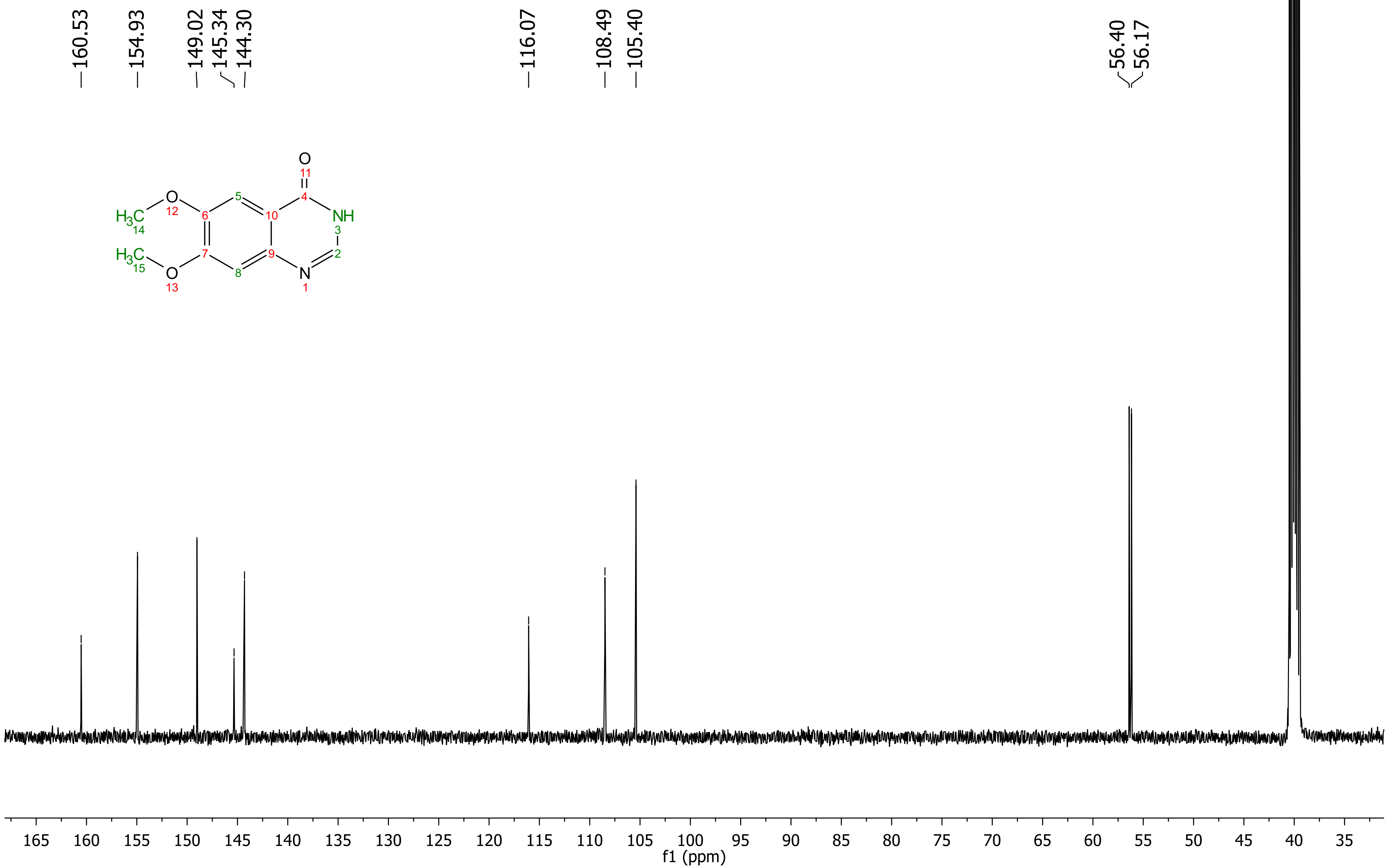

RC-2-55.10.fid
Robyn: RC-2-55: DMSO: 16/02/2016: 1H: AP

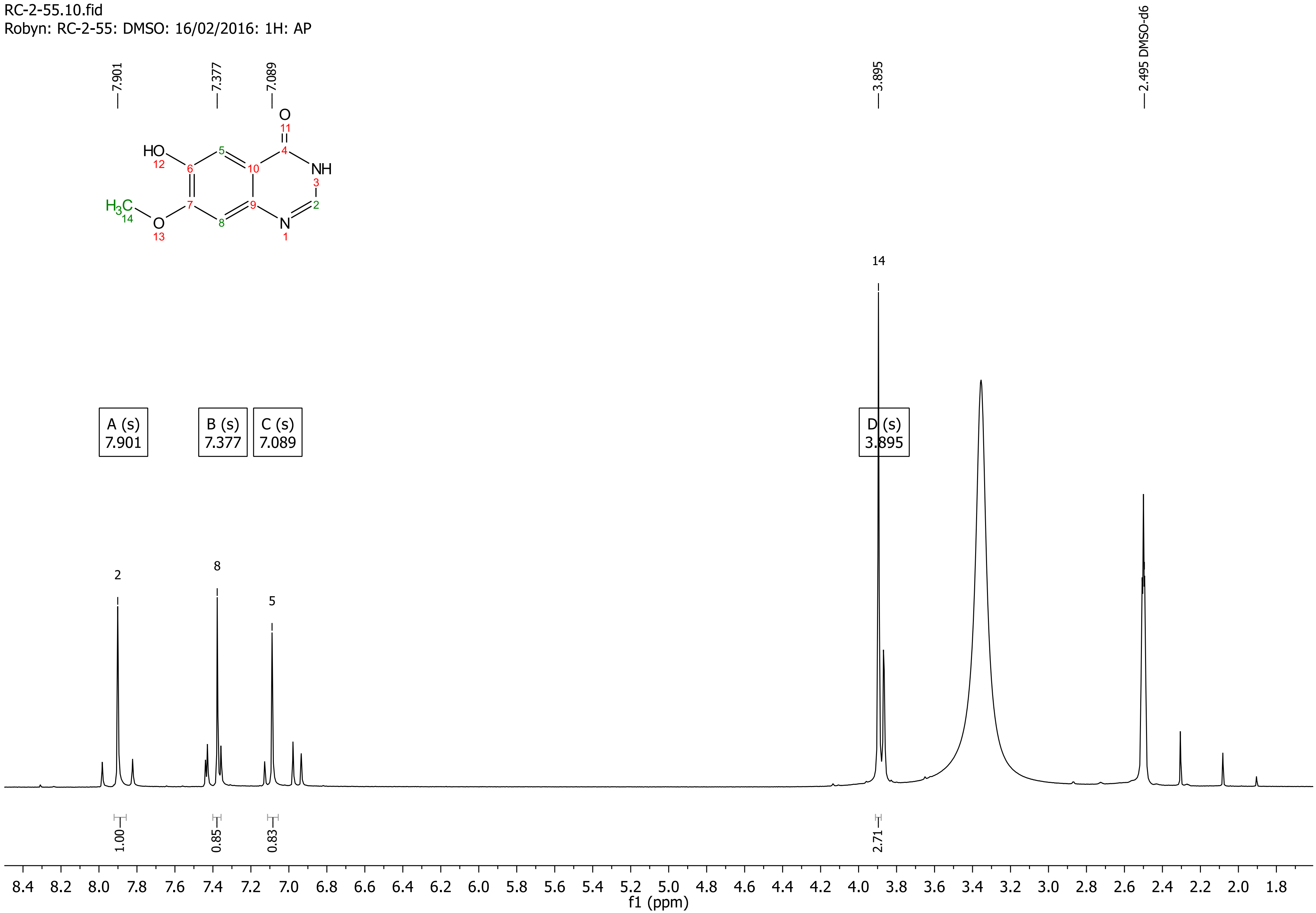

RC-207.3.fid
Robyn: RC-207: DMSO: 13/07/2016: 300K: 1H, 13C: 500NMR: AP

[1]H NMR (500 MHz, DMSO-d_6) δ 12.22 (s, 1H), 8.08 (s, 1H), 7.76 (s, 1H), 7.28 (s, 1H), 3.92 (s, 3H), 2.30 (s, 3H).

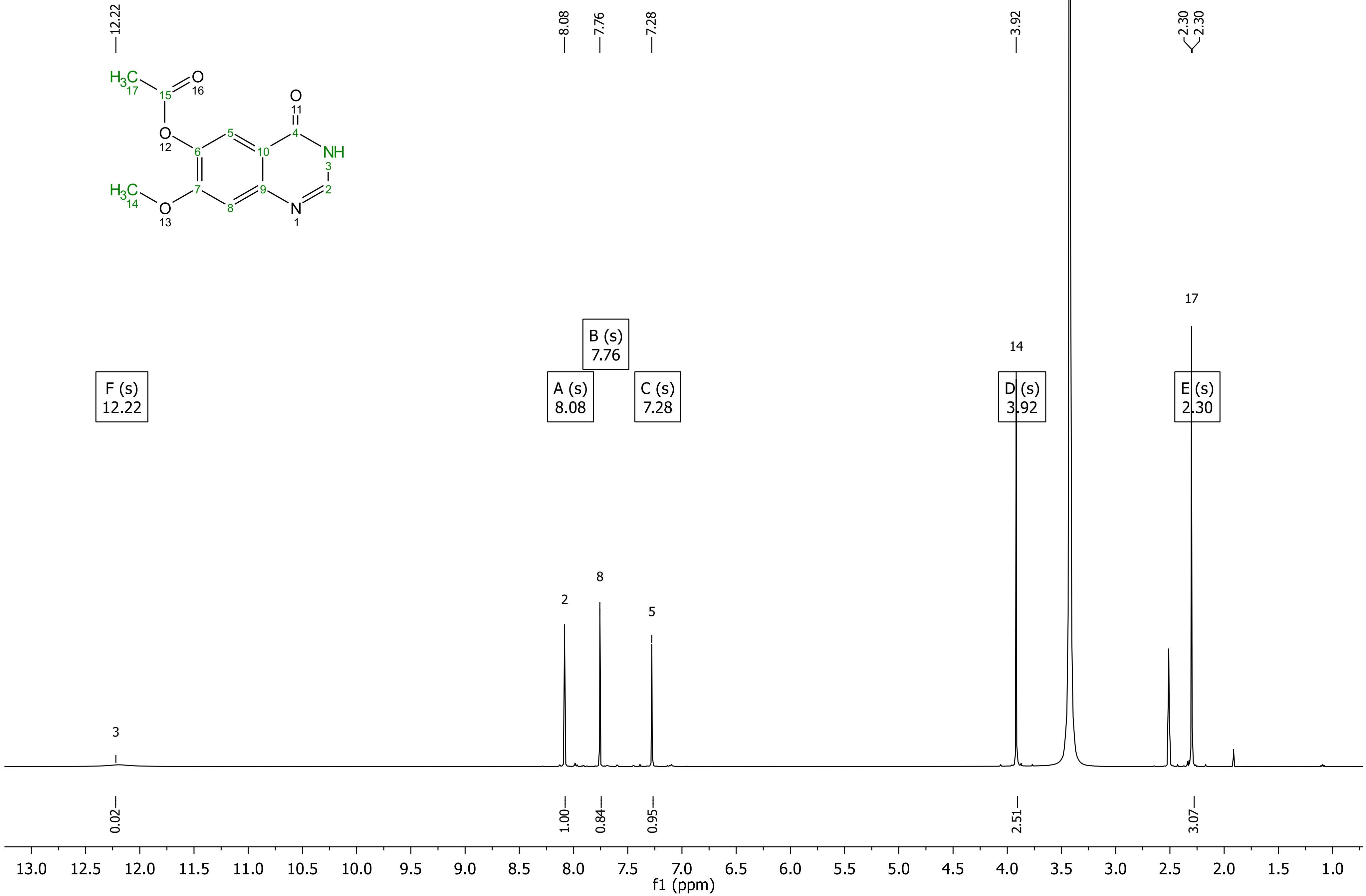

RC-207.4.fid
Robyn: RC-207: DMSO: 13/07/2016: 300K: 1H, 13C: 500NMR: AP

^{13}C NMR (126 MHz, DMSO) δ 169.1, 160.4, 156.6, 149.3, 146.3, 139.3 (6), 119.5 (8), 116.0 (10), 109.6 (5), 56.9, 20.8.

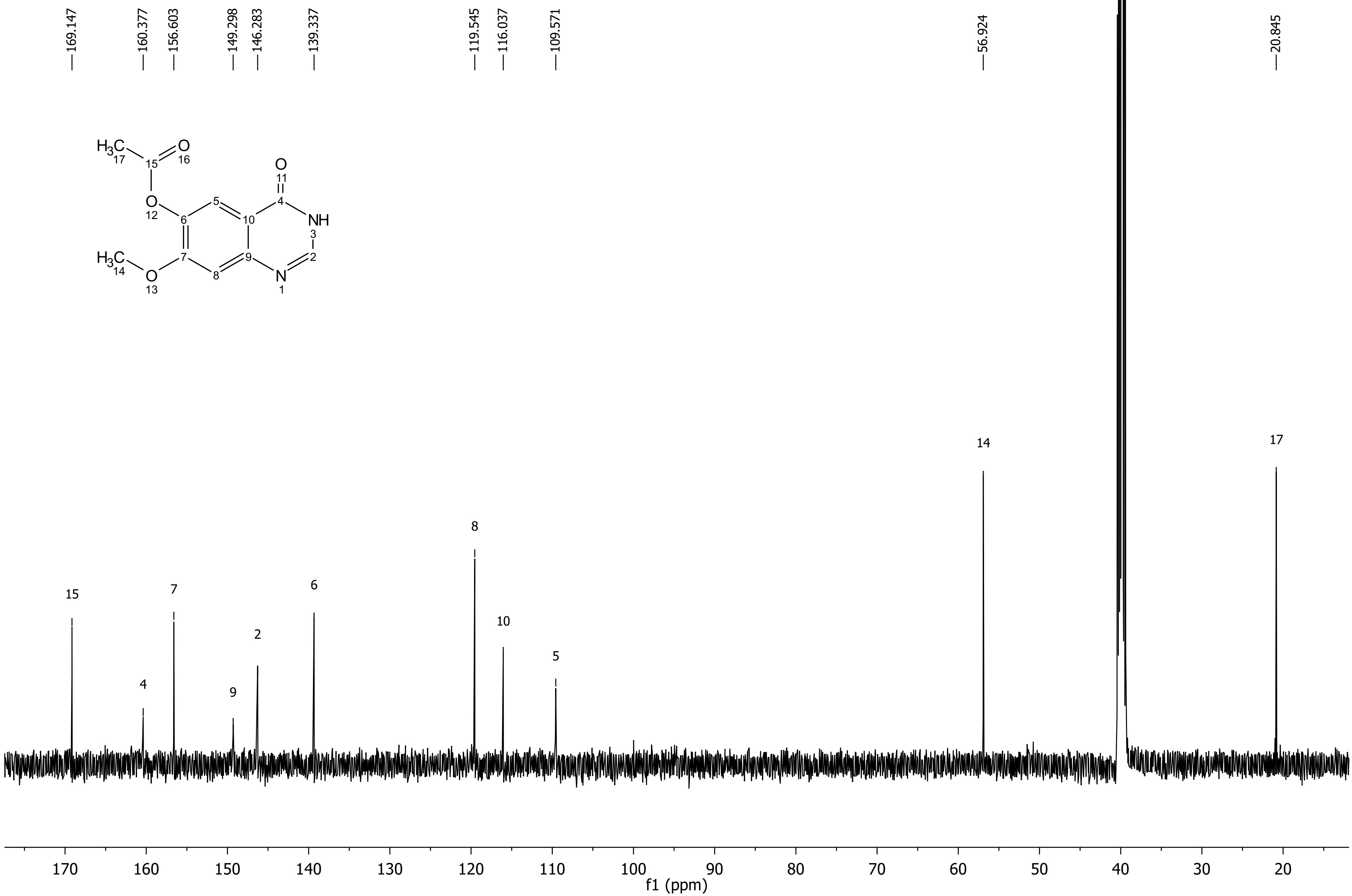

RC-208.6.fid
Robyn: RC-208: DMSO: 08/11/2016: 297K: 1H, 13C: 500NMR: AP

[1]H NMR (500 MHz, DMSO-d_6) δ 9.02 (s, 1H), 8.02 (s, 1H), 7.64 (s, 1H), 4.02 (s, 3H), 2.35 (s, 3H).

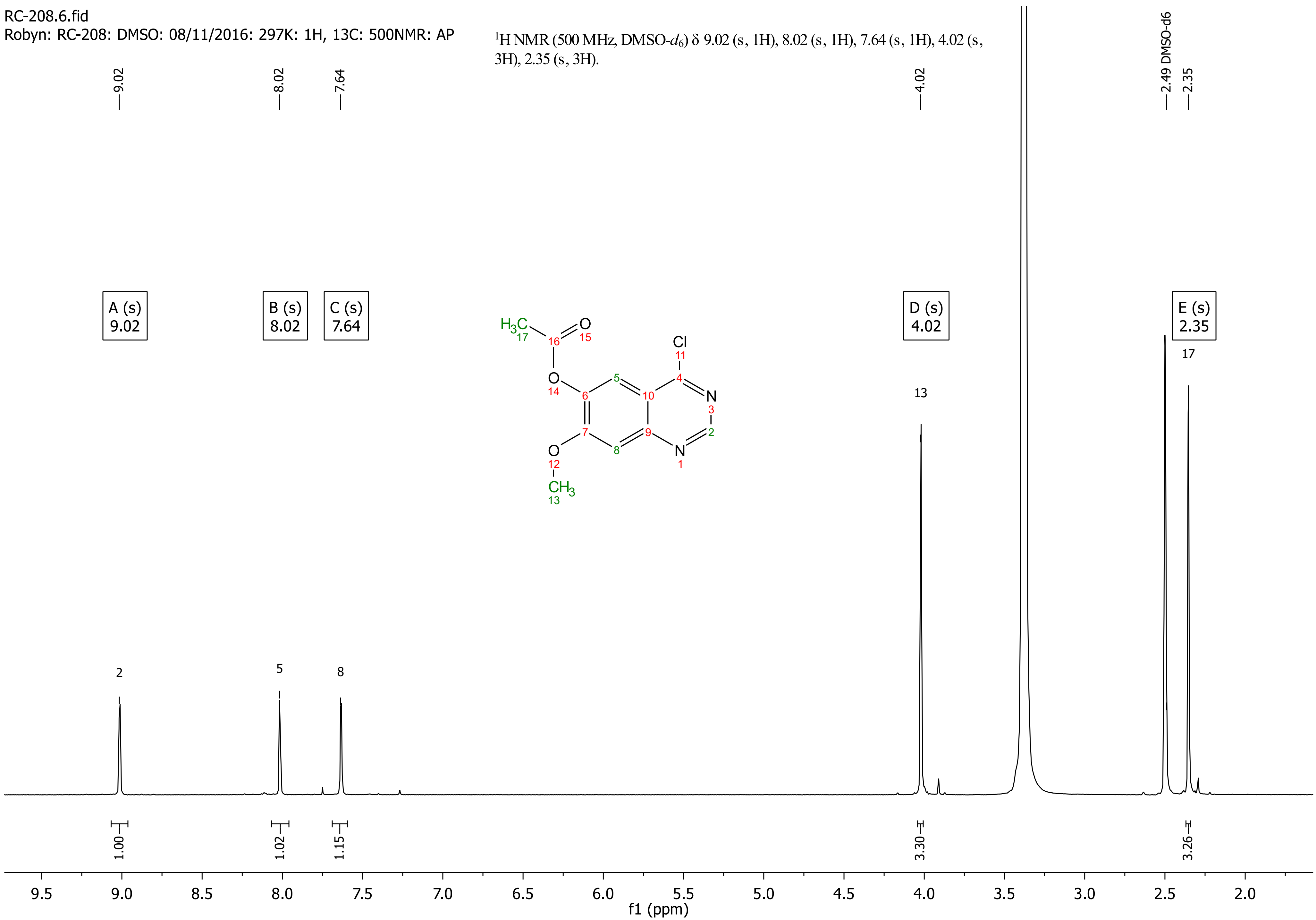

RC-208.22.fid
Robyn: RC-208: DMSO: 30/03/2016: 1H: AP

^{13}C NMR (75 MHz, DMSO) δ 168.5, 158.9, 156.6, 148.2, 147.4, 139.4, 119.7, 114.8, 106.0, 56.6, 20.3.

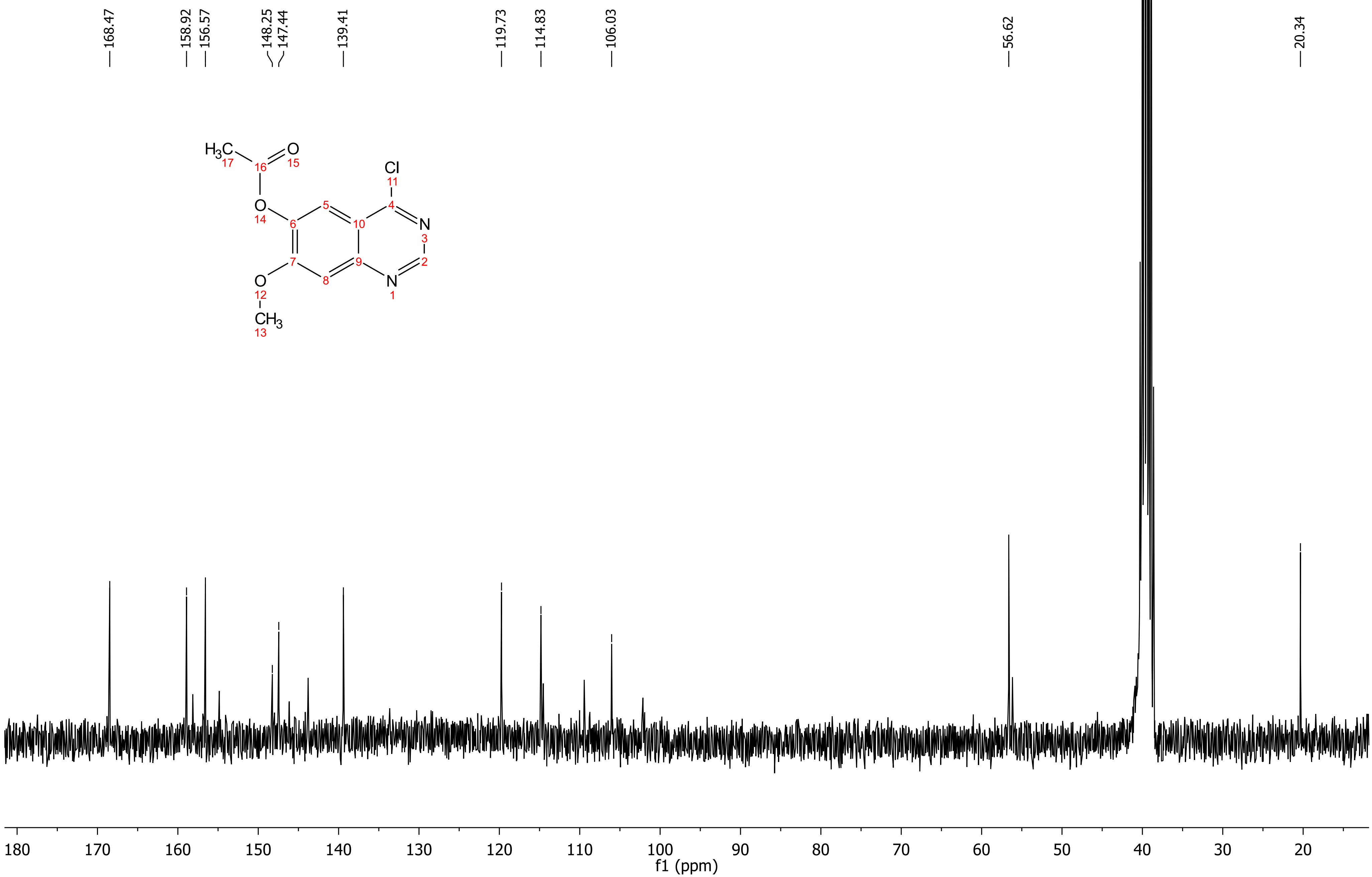

RC-209.10.fid
Robyn: RC-209: DMSO: 24/10/2016: 1H, 13C, COSY and HSQC : AP

[1]H NMR (300 MHz, DMSO-d_6) δ 11.59 (s, 1H), 8.96 (s, 1H), 8.86 (s, 1H), 8.06 (s, 0H), 7.78 (d, J = 7.9 Hz, 1H), 7.58 (s, 1H), 7.53 – 7.40 (m, 2H), 4.01 (s, 3H), 2.39 (s, 3H).

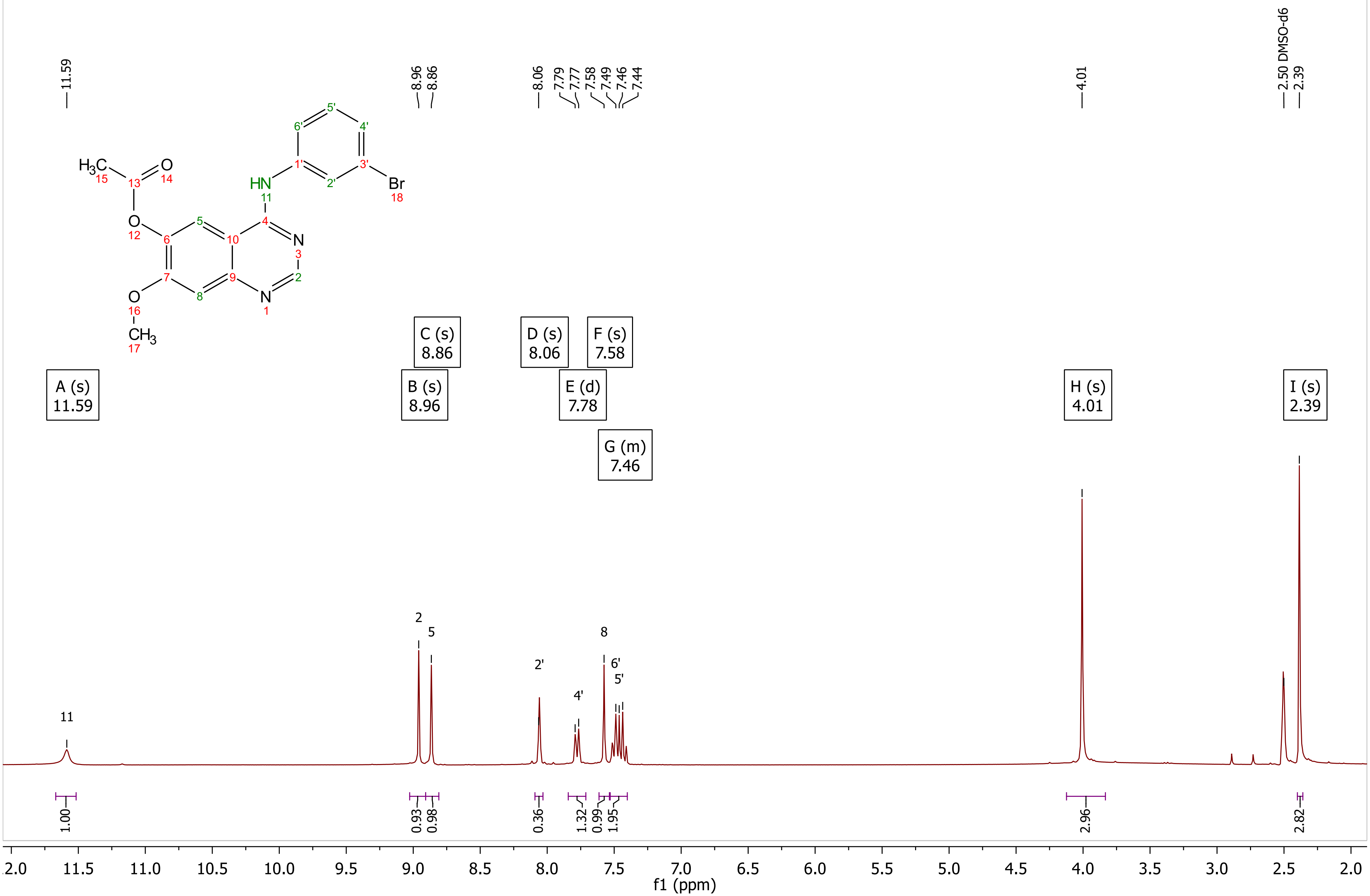

RC-220.10.fid
Robyn: RC-2-108: DMSO: 02/11/2016: 1H: AP

^{1}H NMR (300 MHz, DMSO-d_6) δ 11.63 (s, 1H), 8.95 (s, 1H), 8.83 (s, 1H), 8.05 (dd, J = 6.8, 2.6 Hz, 1H), 7.75 (ddd, J = 9.0, 4.3, 2.6 Hz, 2H), 7.59 – 7.49 (m, 2H), 4.00 (s, 3H), 2.38 (s, 3H).

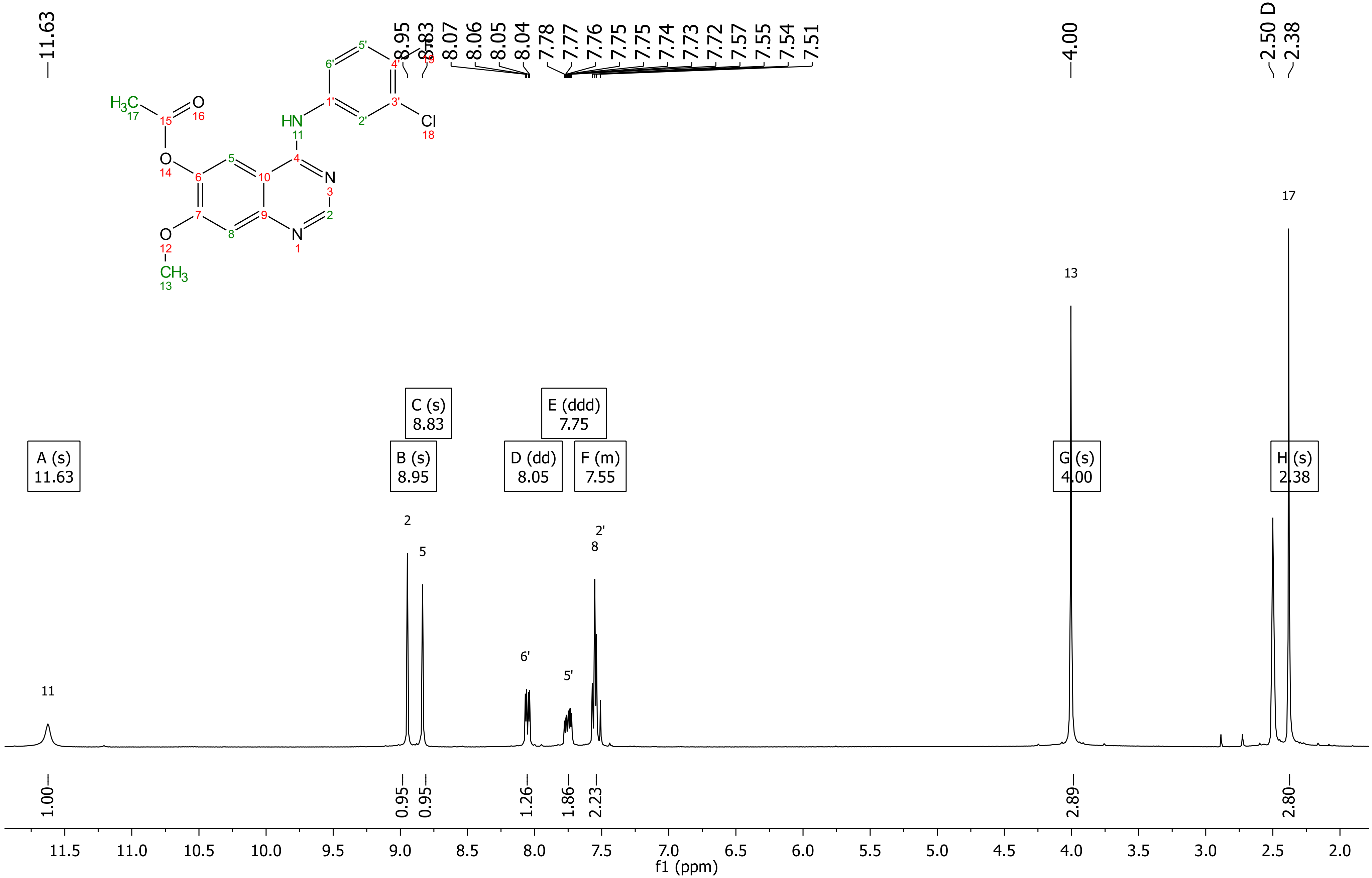

RC-210.10.fid
Robyn: RC-210: DMSO: 24/10/2016: 1H, 13C, COSY and HSQC : AP

^{1}H NMR (300 MHz, DMSO-d_6) δ 9.61 (s, 1H), 9.45 (s, 1H), 8.49 (s, 1H), 8.24 (t, J = 2.0 Hz, 1H), 7.90 (ddd, J = 8.1, 2.2, 1.1 Hz, 1H), 7.81 (s, 1H), 7.31 (t, J = 8.0 Hz, 1H), 7.24 (dd, J = 2.0, 1.1 Hz, 0H), 7.21 (s, 1H).

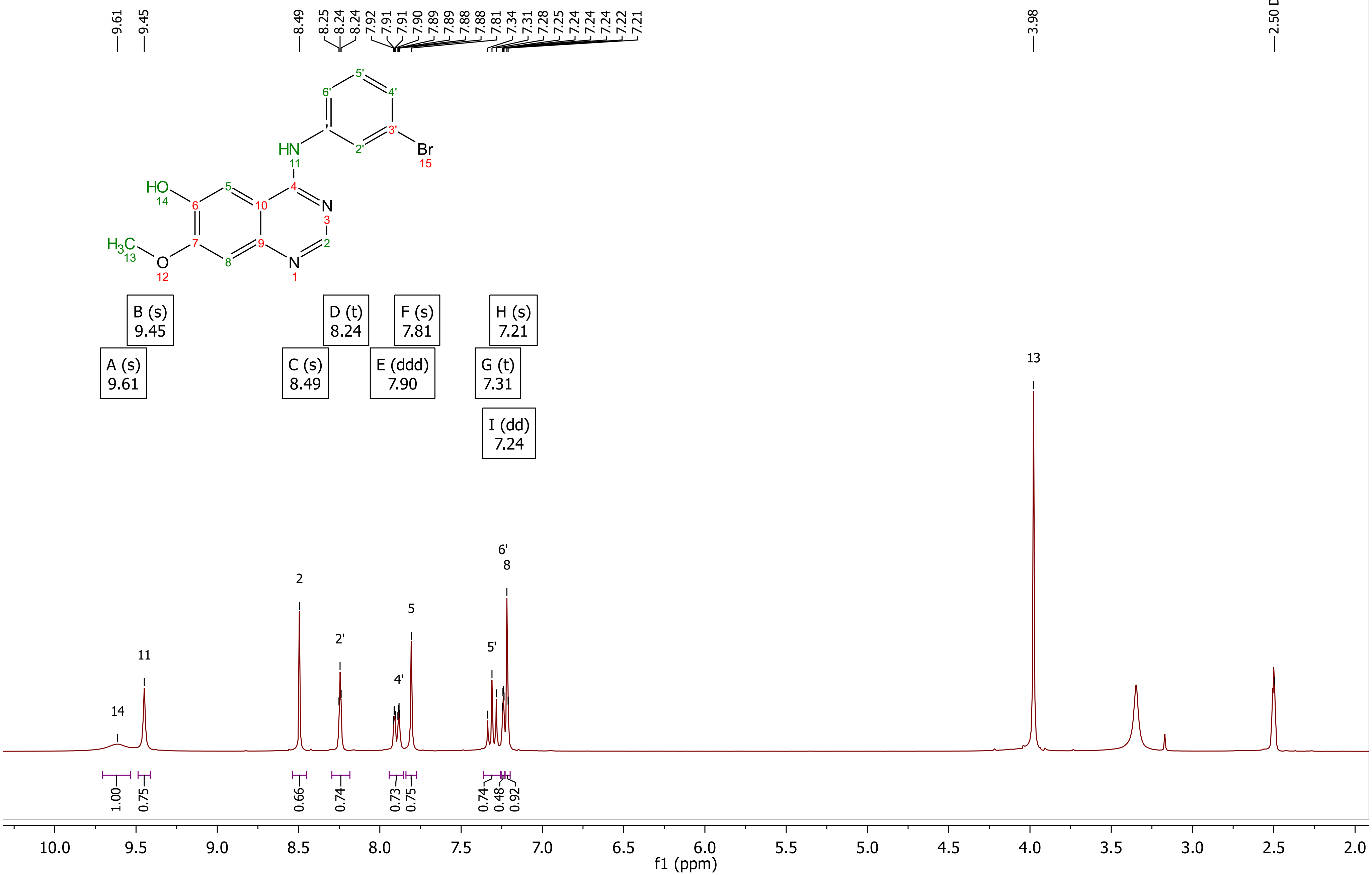

RC-210.11.fid
Robyn: RC-210: DMSO: 24/10/2016: 1H, 13C, COSY and HSQC : AP

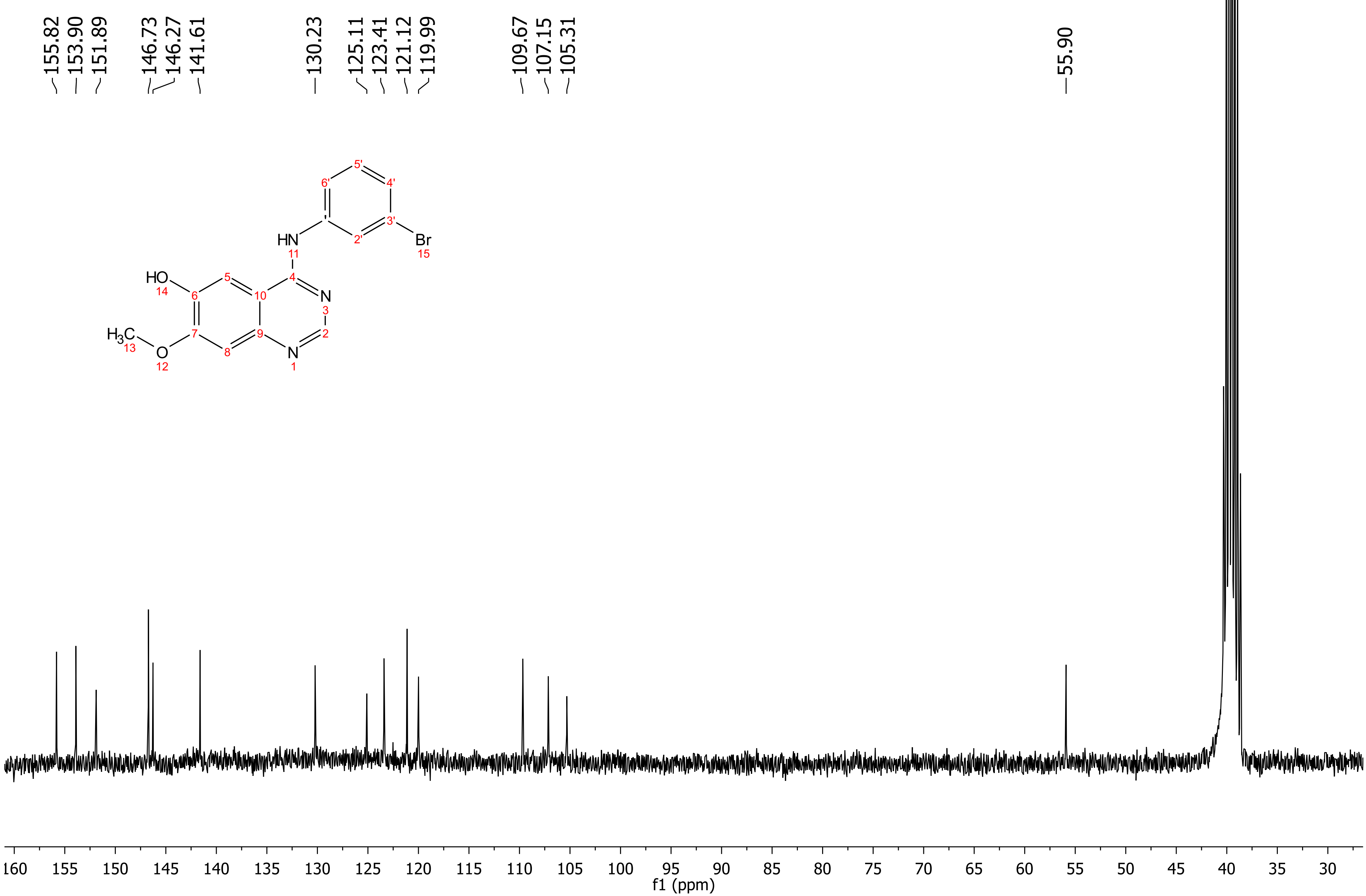

RC-232.20.fid
Robyn: RC-232: DMSO: 08/01/2017: 1H, 13C, HSQC, COSY: AP

[1]H NMR (300 MHz, DMSO-d_6) δ 9.70 (s, 1H), 9.47 (s, 1H), 8.47 (s, 1H), 8.22 (dd, 1H), 7.86 – 7.78 (m, 1H), 7.77 (s, 1H), 7.39 (t, 1H), 7.21 (s, 1H), 3.97 (s, 3H).

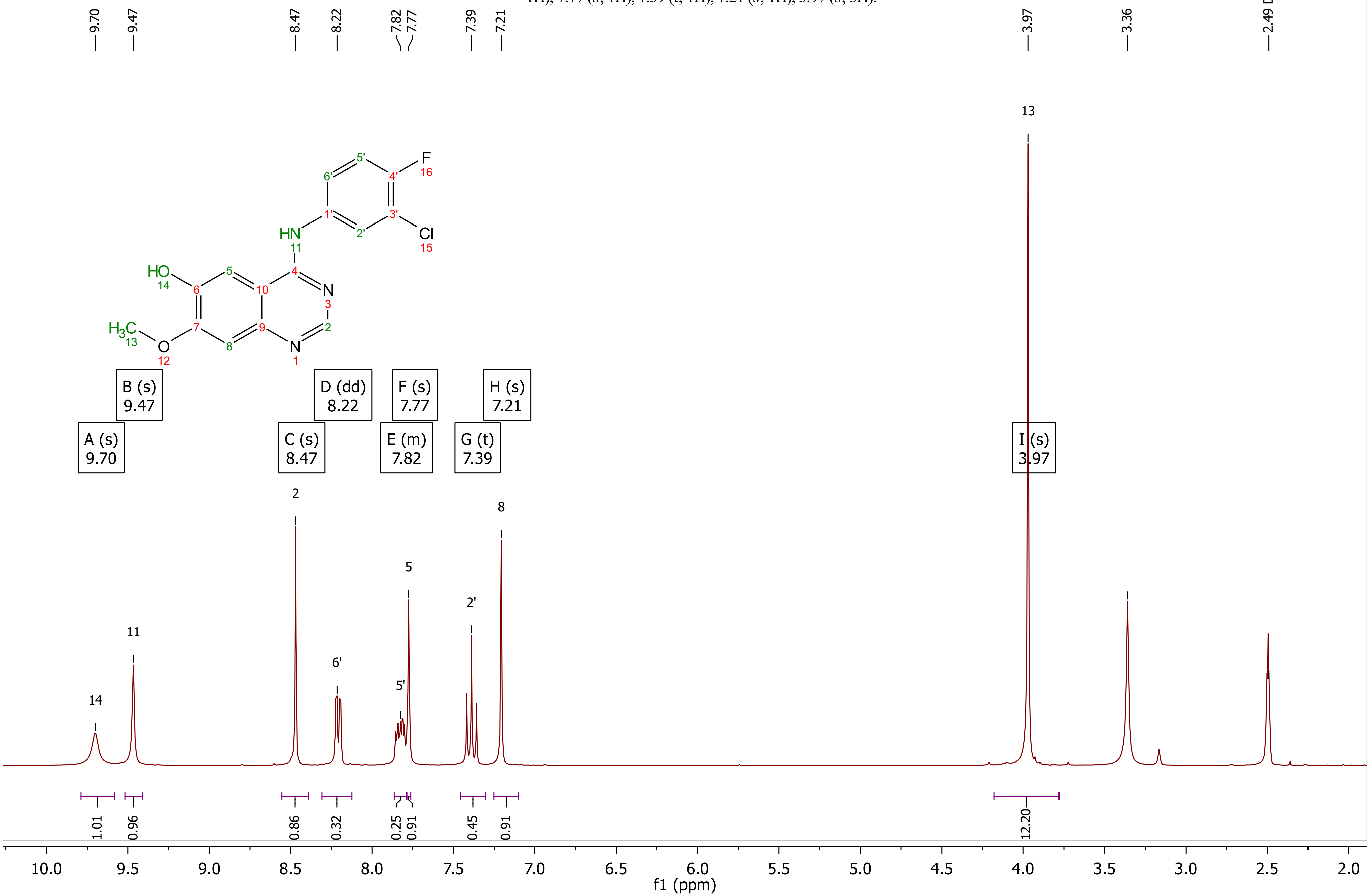

RC-232.21.fid
Robyn: RC-232: DMSO: 08/01/2017: 1H, 13C, HSQC, COSY: AP

^{13}C NMR (75 MHz, DMSO) δ 155.8, 153.9, 151.9, 151.2, 146.7, 146.2, 137.1, 122.7, 118.7, 118.5, 116.5, 116.2, 109.5, 107.1, 55.9.

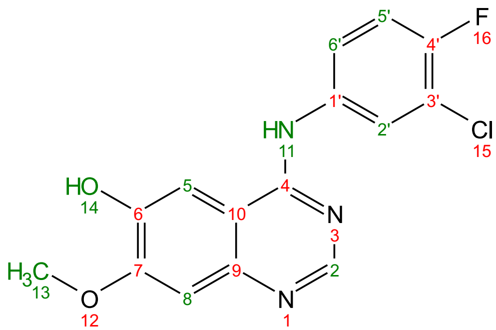

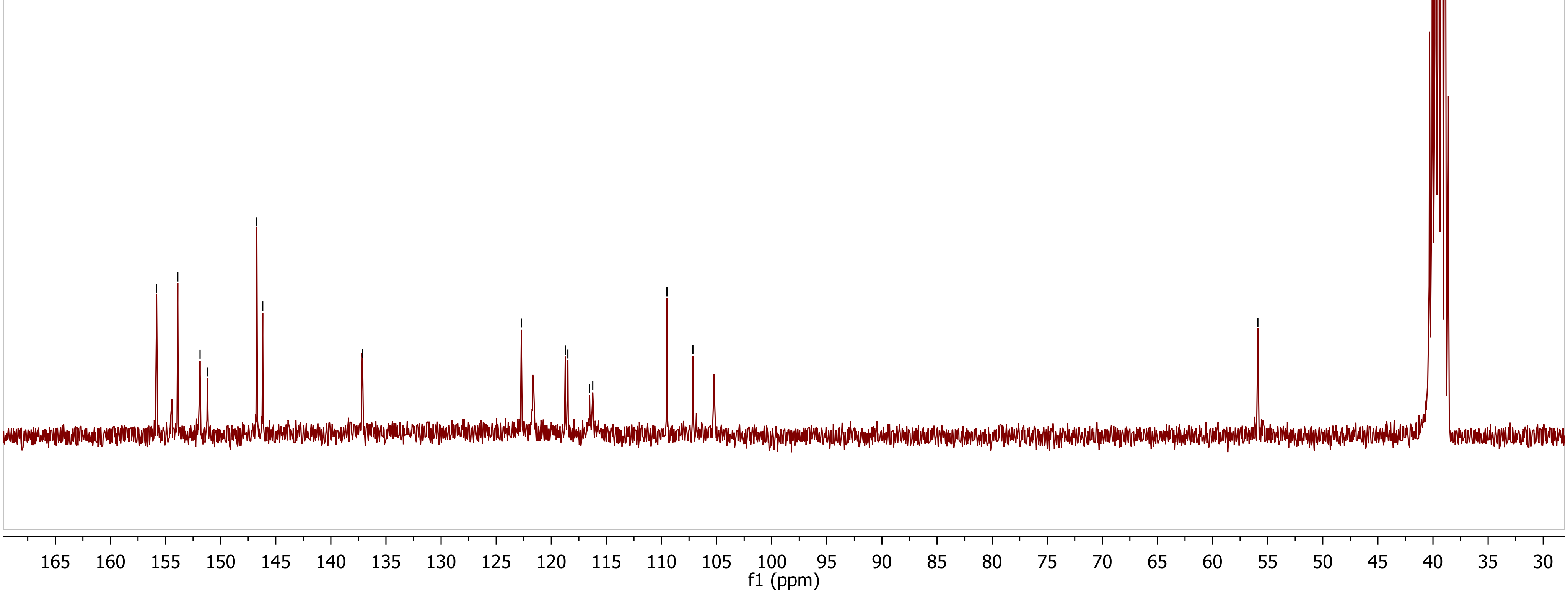

RC-2-32.1.2.fid
Robyn: RC-2-32.1: DMSO: 19/08/2015: 25ºC: 1H, 13C: 500NMR: AP: Solution

^{1}H NMR (500 MHz, DMSO-d_6) δ 7.20 (t, J = 7.8 Hz, 1H), 7.09 (d, J = 8.2 Hz, 1H), 7.00 (d, J = 7.8 Hz, 1H), 6.93 (t, J = 7.6 Hz, 1H), 3.74 (s, 3H), 3.34 (s, 3H), 3.29 (s, 3H).

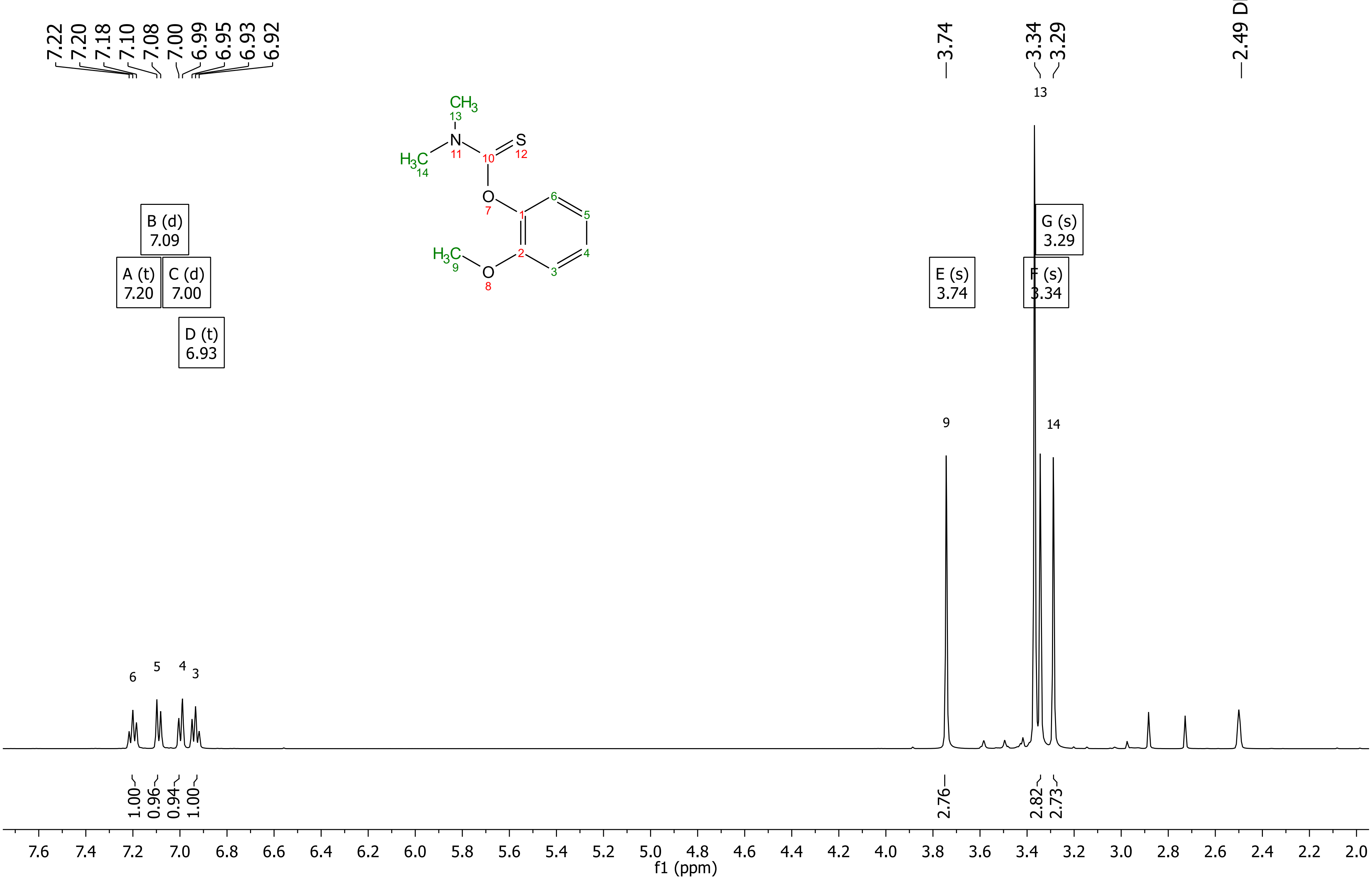

RC-2-32.1.3.fid
Robyn: RC-2-32.1: DMSO: 19/08/2015: 25ºC: 1H, 13C: 500NMR: AP: Solution

^{13}C NMR (126 MHz, DMSO) δ 186.8, 151.4, 142.6, 126.9, 124.2, 120.5, 113.1, 55.9, 43.0, 39.2, 38.5.

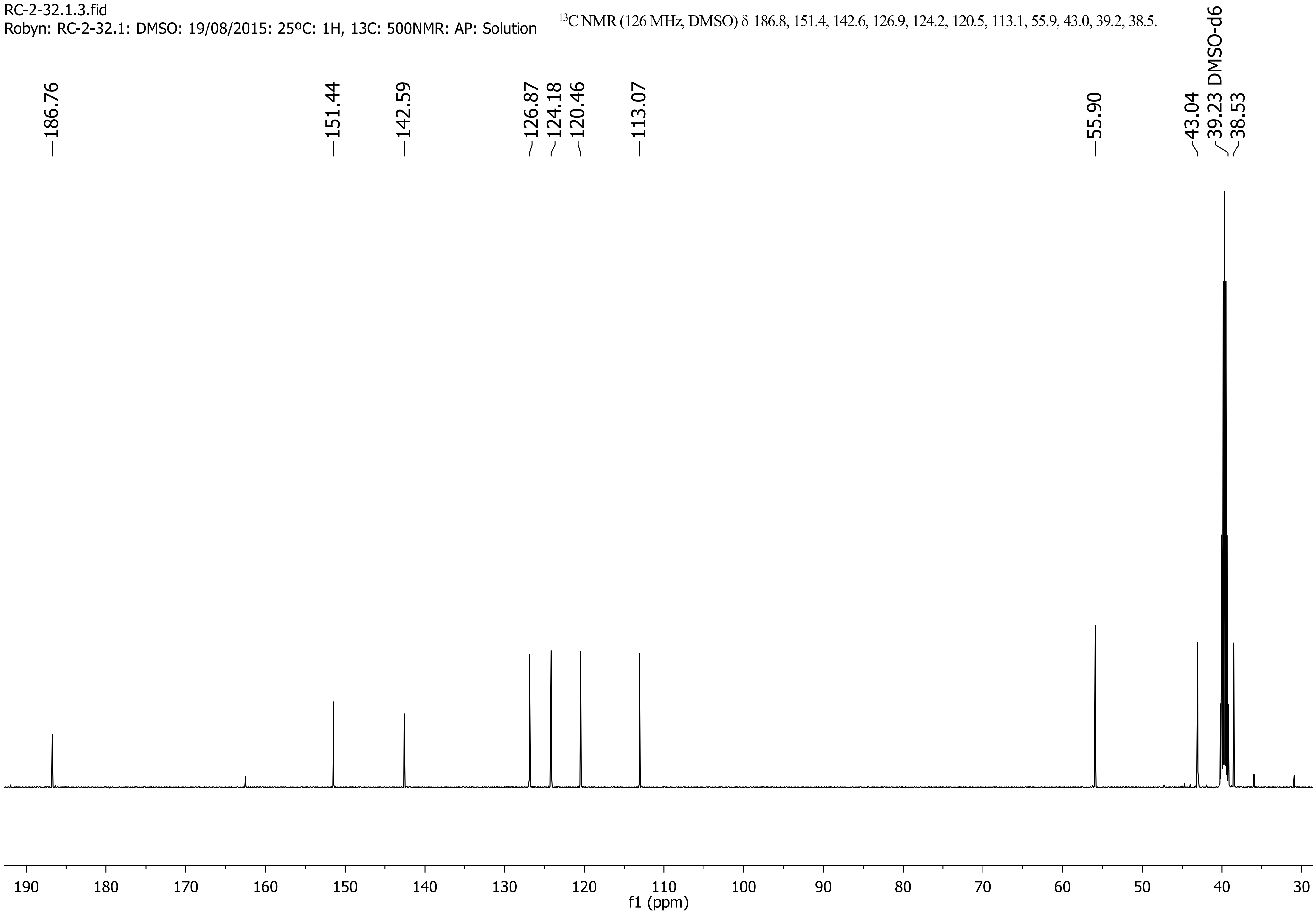

RC-2-34.1.2.fid
Robyn: RC-2-34.1: DMSO: 21/08/2015: 25ºC: 1H: 500NMR: AP: Solution

[1]H NMR (500 MHz, DMSO-d_6) δ 7.42 (t, 1H), 7.37 (d, J = 7.6 Hz, 1H), 7.08 (d, J = 8.3 Hz, 1H), 6.96 (t, J = 7.5 Hz, 1H), 3.77 (s, 4H), 3.01 (d, J = 34.1 Hz, 4H), 2.89 (s, 2H).

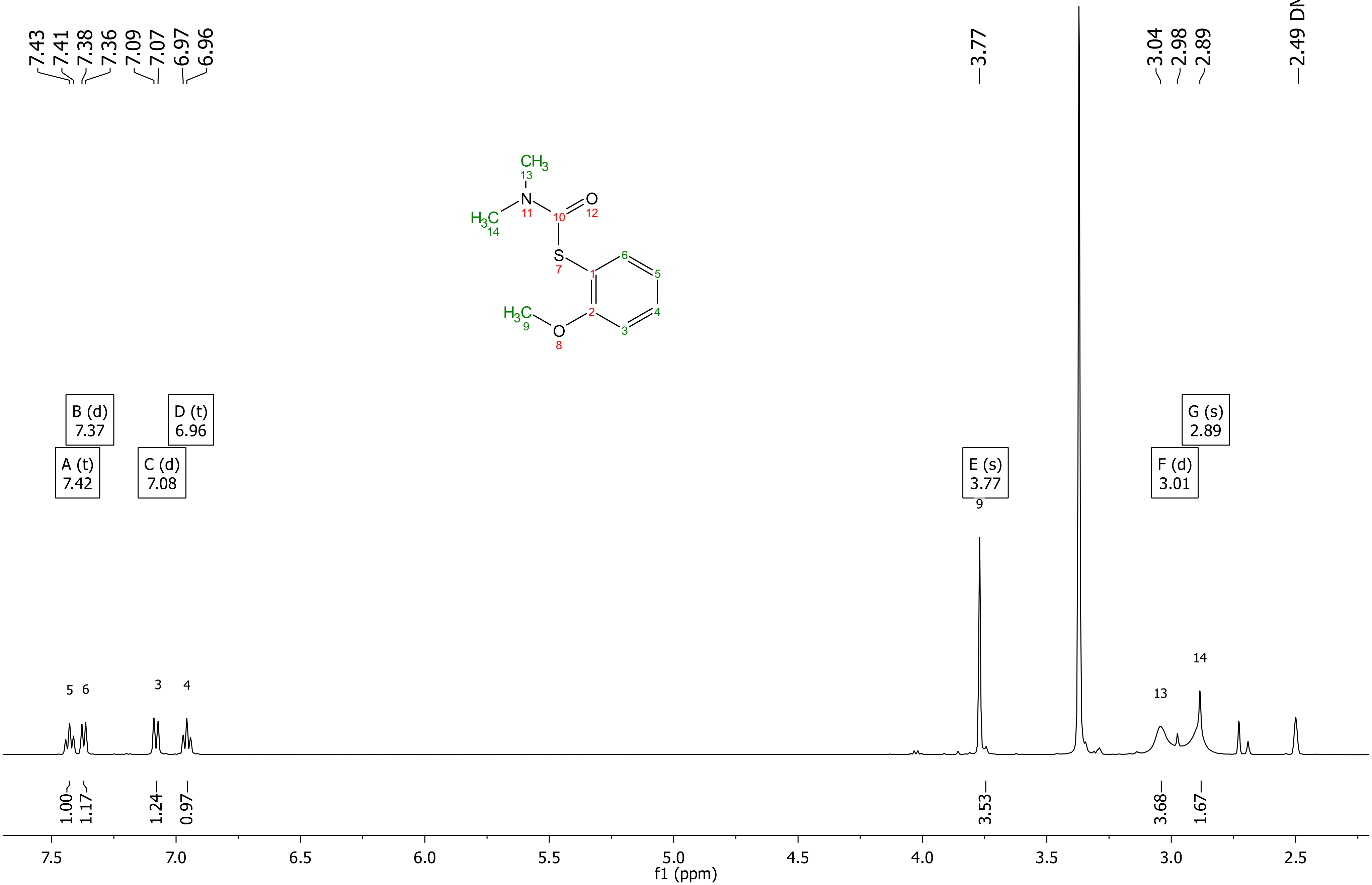

RC-2-34.1.3.fid
Robyn: RC-2-34.1: DMSO: 21/08/2015: 25ºC: 1H: 500NMR: AP: Solution

^{13}C NMR (126 MHz, DMSO) δ 164.6, 159.8, 137.8, 131.5, 120.6, 116.3, 111.8, 55.8, 39.1, 36.5.

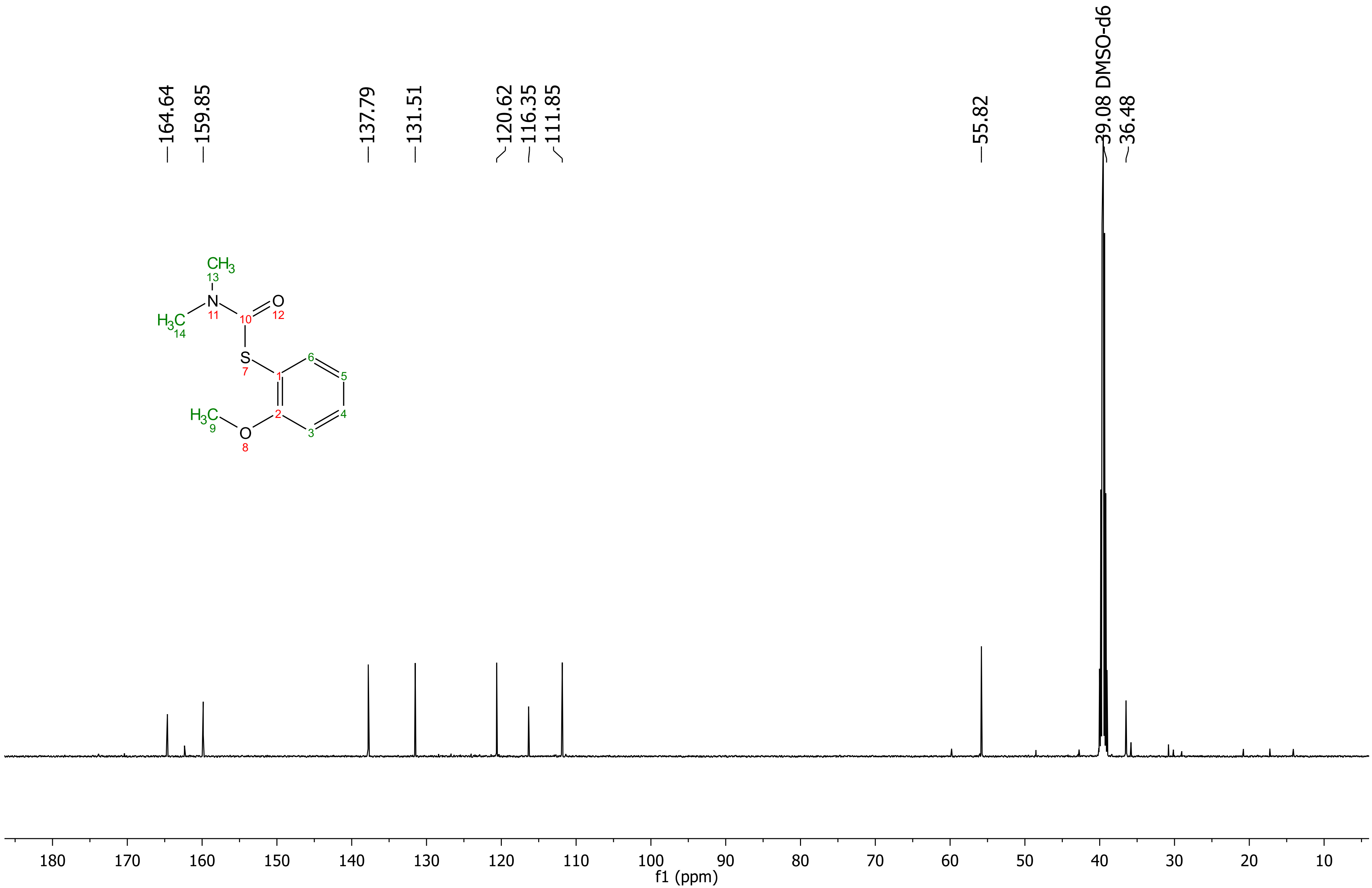

KPM-26-fr15-18(spot 1).10.fid
Khanani KPM-26-fr15-18(spot 1) CDCl3 20/04/2016 1H KP

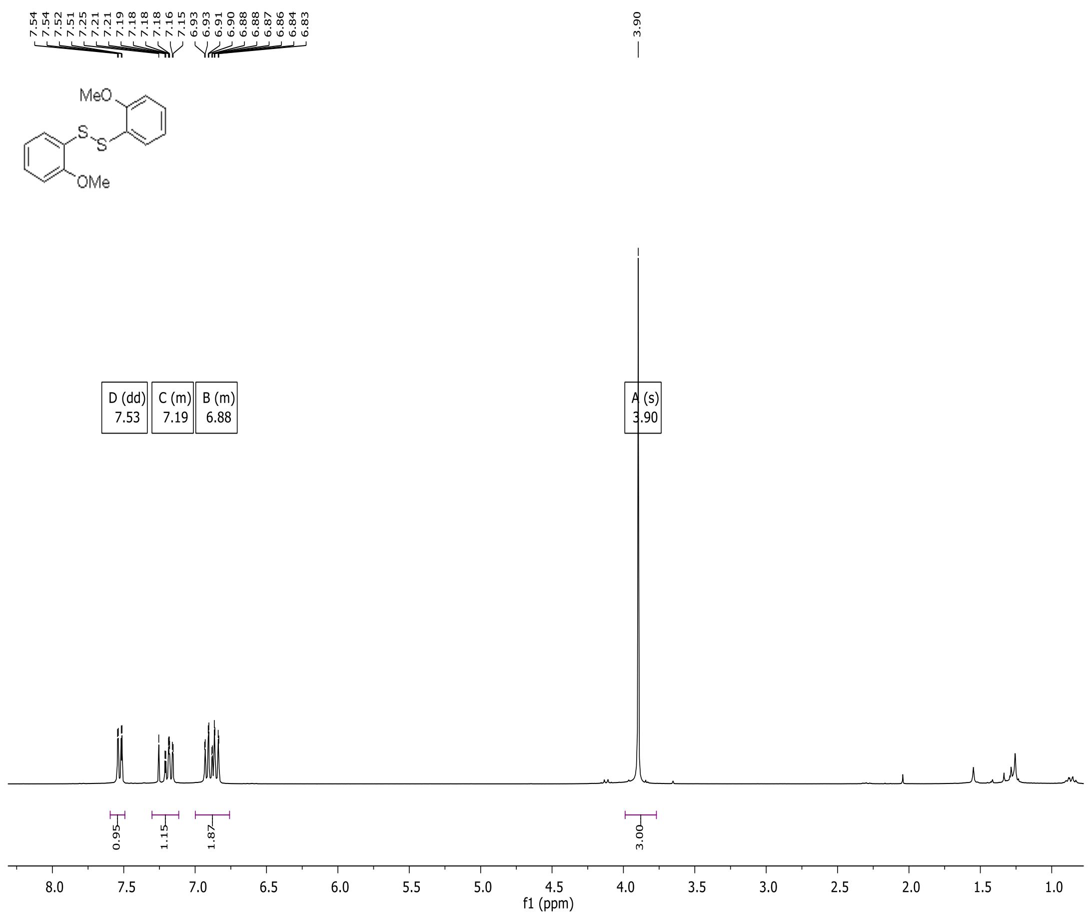

KPM-26-fr15-18(spot 1).11.fid
Khanani KPM-26-fr15-18(spot 1) CDCl3 20/04/2016 1H KP

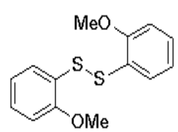

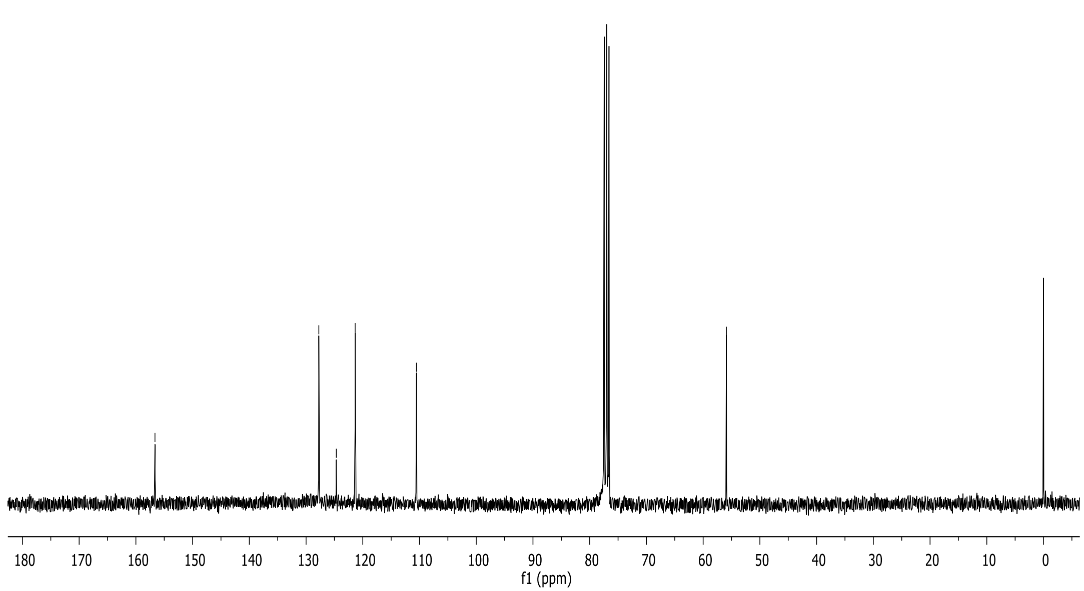

RC-2-68-NKR.60.fid
Robyn: RC-2-68-NKR: CDCL3: 20/06/2016: 1H, 13C: AP

^{1}H NMR (300 MHz, Chloroform-d) δ 8.90 (dd, J = 4.2, 1.7 Hz, 1H), 8.23 – 7.99 (m, 2H), 7.50 – 7.45 (m, 2H), 7.40 (dd, J = 8.3, 4.2 Hz, 1H), 3.48 (s, 2H), 3.40 (s, 2H).

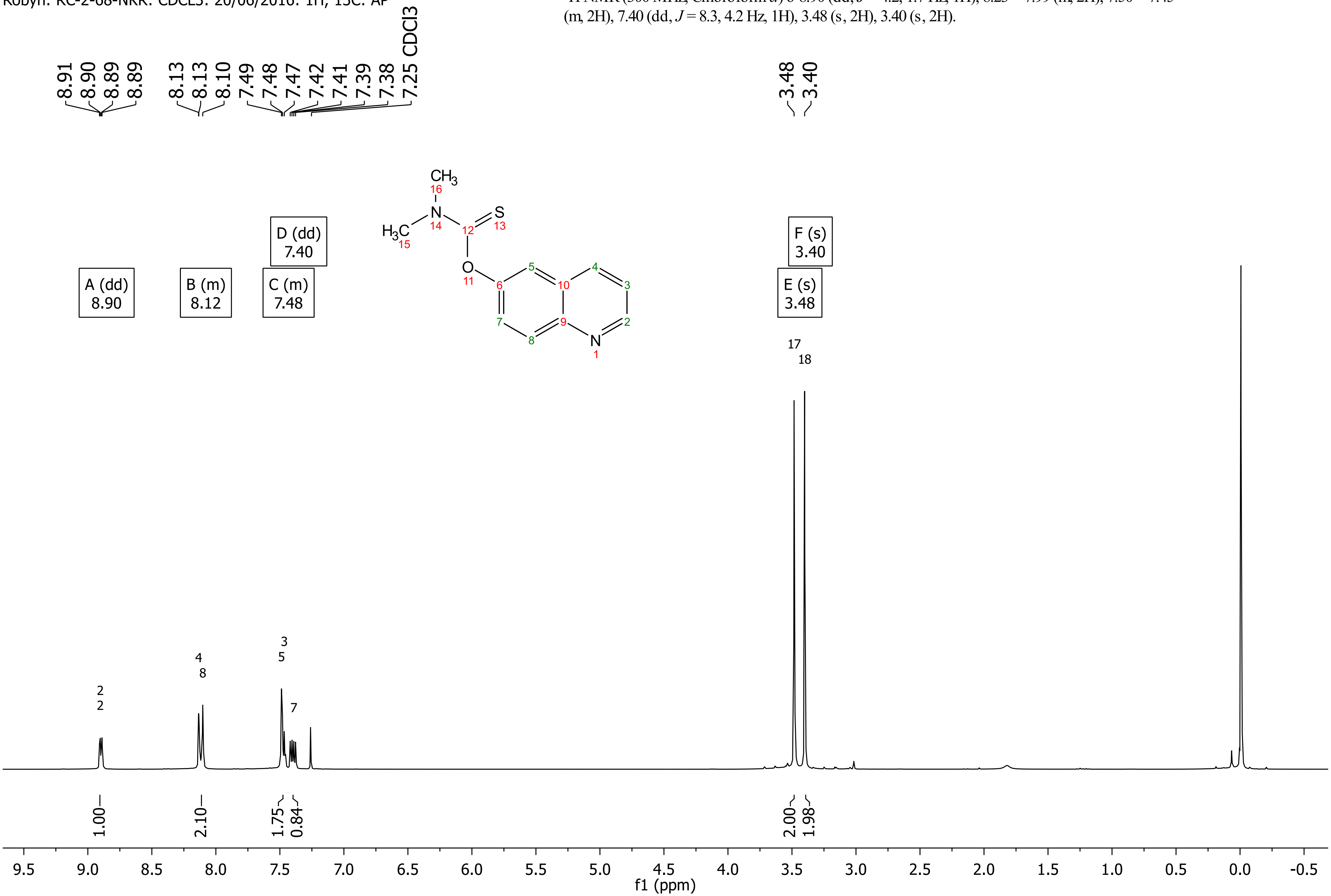

RC-2-68-NKR.71.fid
Robyn:RC-2-68-NKR:CDCL3:20/06/2016:1H, 13C, COSY, HSQC:AP

^{13}C NMR (75 MHz, $CDCl_3$) δ 187.2, 151.4, 149.9, 146.1, 135.5, 130.3, 128.1, 125.9, 121.2, 119.1, 76.9, 43.1, 38.6.

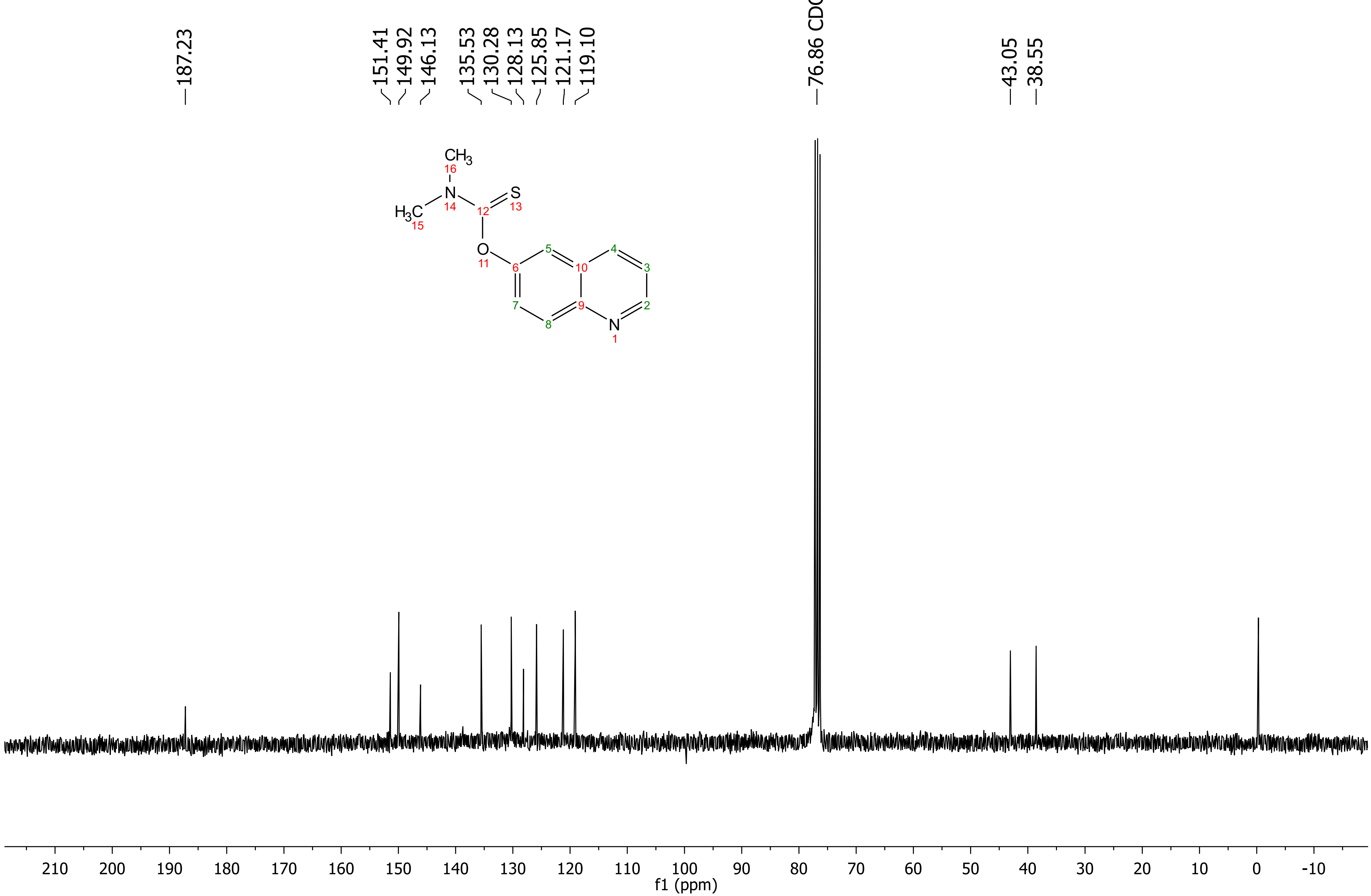

RC-2-72-NKR.30.fid
Robyn: RC-2-72-NKR: CDCL3: 27/06/2016: 1H: AP After Full work up

[1]H NMR (300 MHz, Chloroform-*d*) δ 8.93 (dd, *J* = 4.3, 1.7 Hz, 1H), 8.15 – 8.07 (m, 2H), 8.01 (d, *J* = 1.8 Hz, 1H), 7.77 (dd, *J* = 8.8, 1.9 Hz, 1H), 7.41 (dd, *J* = 8.3, 4.2 Hz, 1H), 3.09 (d, *J* = 20.2 Hz, 6H).

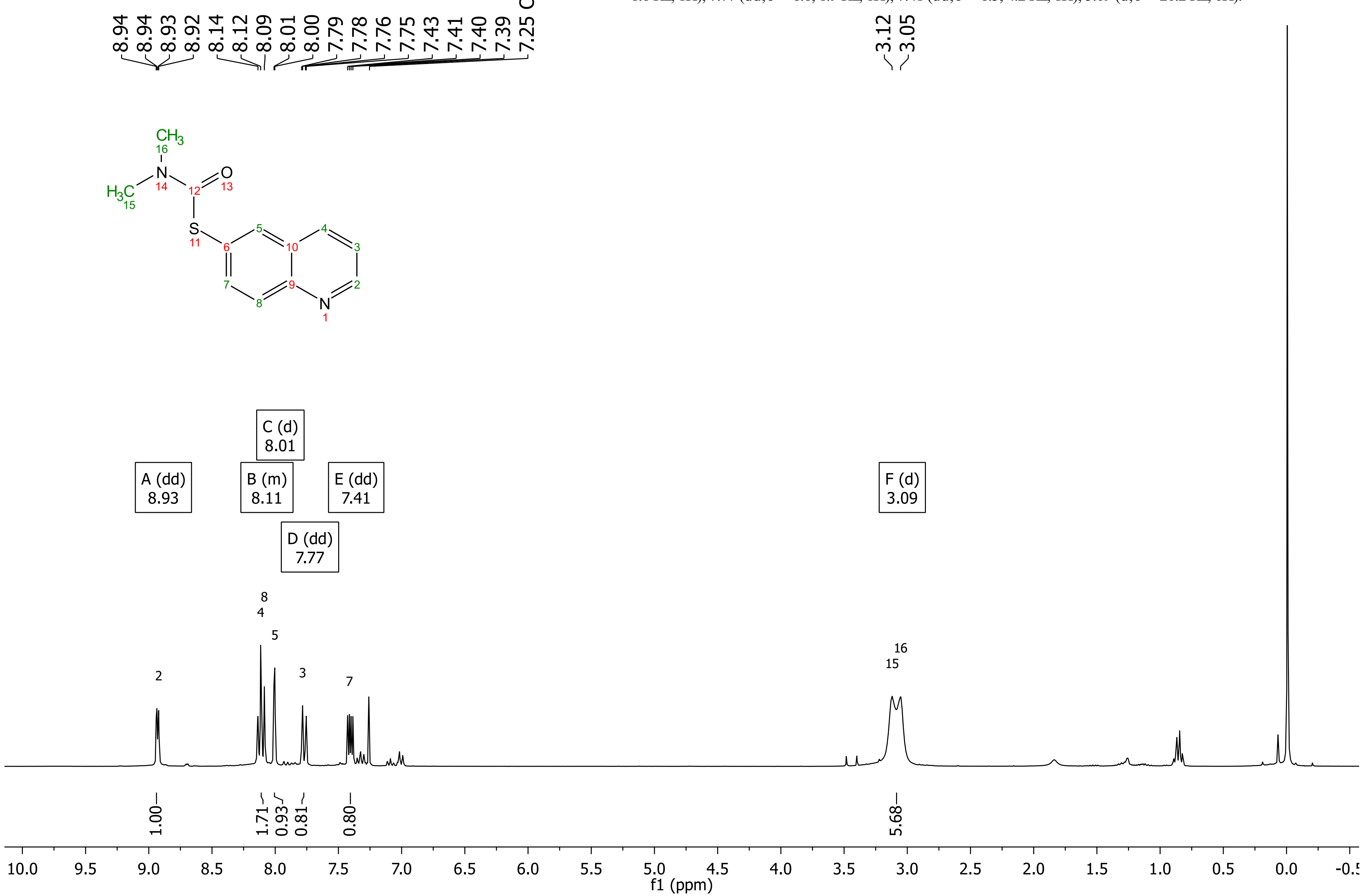

ɔ 210.1.fid
ɔbyn: RC-210: DMSO: 29/01/2016: 300K: 1H, 13C, HSQC, COSY, HMBC: 500: AP

[1]H NMR (500 MHz, DMSO-d_6) δ 9.64 (s, 1H), 8.62 (s, 1H), 8.28 (s, 1H), 8.24 (s, 0H), 7.90 (d, J = 8.2 Hz, 1H), 7.35 – 7.31 (m, 2H), 7.27 (d, J = 8.0 Hz, 1H), 3.92 (s, 3H), 3.40 (s, 3H), 3.38 (s, 3H).

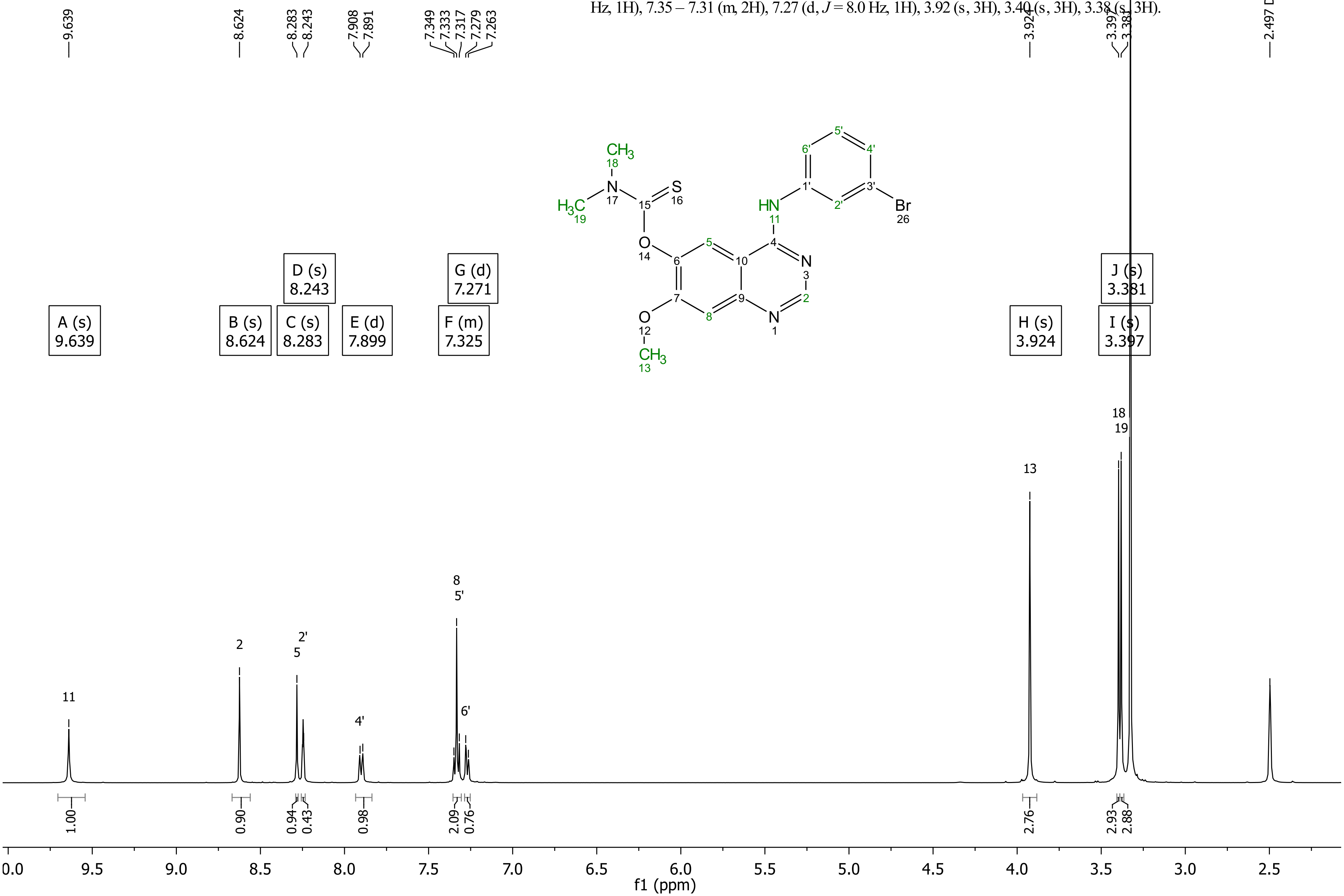

RC-210.2.fid
Robyn: RC-210: DMSO: 29/01/2016: 300K: 1H, 13C, HSQC, COSY, HMBC: 500: AP

^{13}C NMR (126 MHz, DMSO) δ 186.7, 157.3, 156.5, 155.0, 150.6, 142.7, 141.6, 130.9, 126.2, 124.2, 121.7, 120.7, 117.6, 109.2, 108.8, 56.8, 43.5.

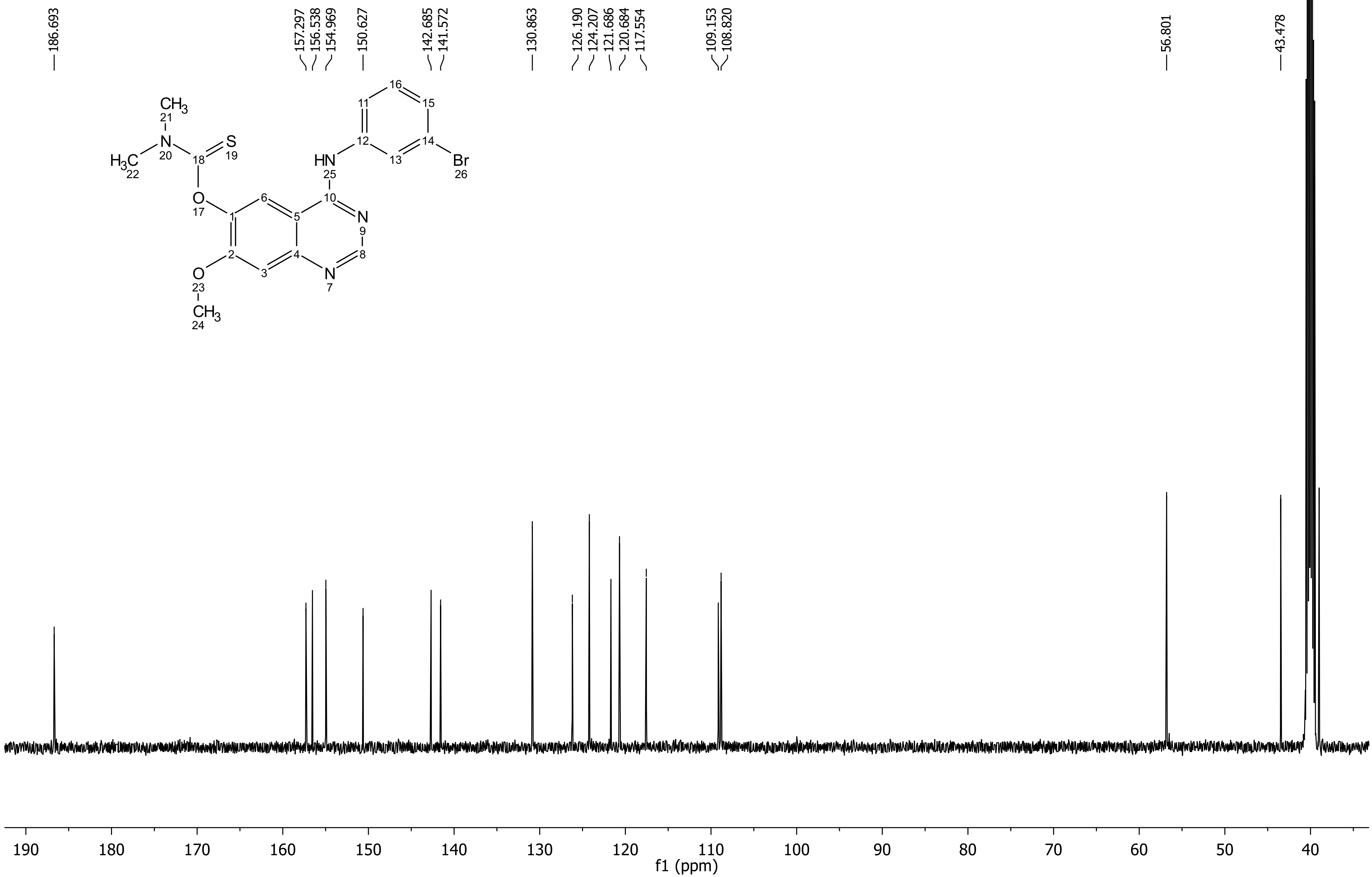

RC-241.1.fid
Robyn: RC-241: DMSO: 21/01/2017: 300K: 1H,13C,COSY, HSQC: 500NMR: AP

^{1}H NMR (500 MHz, DMSO-d_6) δ 9.66 (s, 1H), 8.60 (s, 1H), 8.24 (s, 1H), 8.22 (dd, J = 6.8, 2.7 Hz, 1H), 7.86 – 7.80 (m, 1H), 7.42 (t, J = 9.1 Hz, 1H), 7.33 (s, 1H), 3.92 (s, 3H), 3.40 (s, 3H), 3.38 (s, 3H).

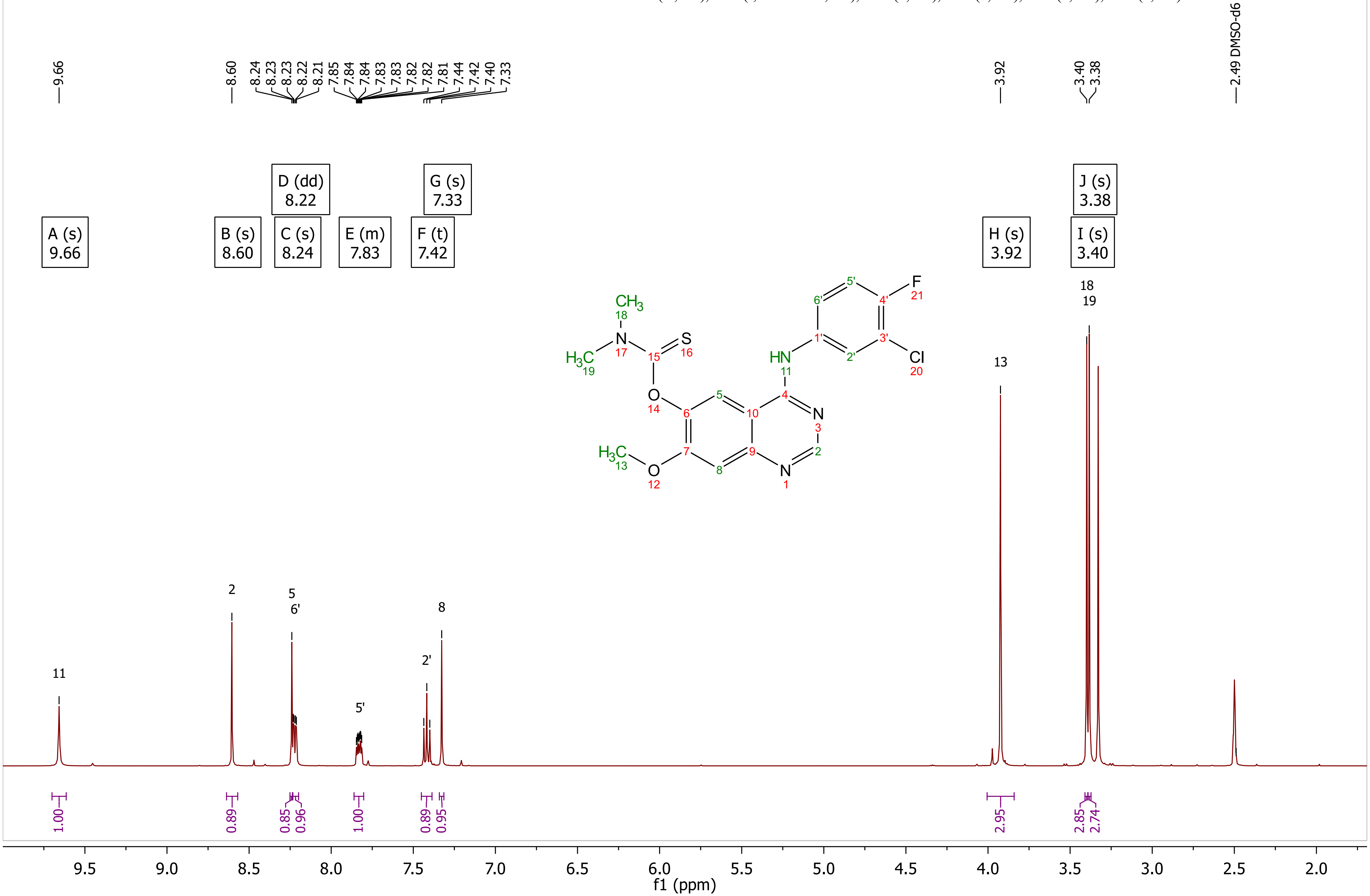

RC-241.2.fid

Robyn: RC-241: DMSO: 21/01/2017: 300K: 1H,13C,COSY, HSQC: 500NMR: AP

^{13}C NMR (126 MHz, DMSO) δ 186.7, 157.3, 156.5, 154.9, 154.4, 150.6, 142.7, 137.1, 123.6, 122.4, 122.3, 119.3, 119.2, 117.5, 117.1, 116.9, 109.0, 108.8, 56.8, 43.5, 39.0.

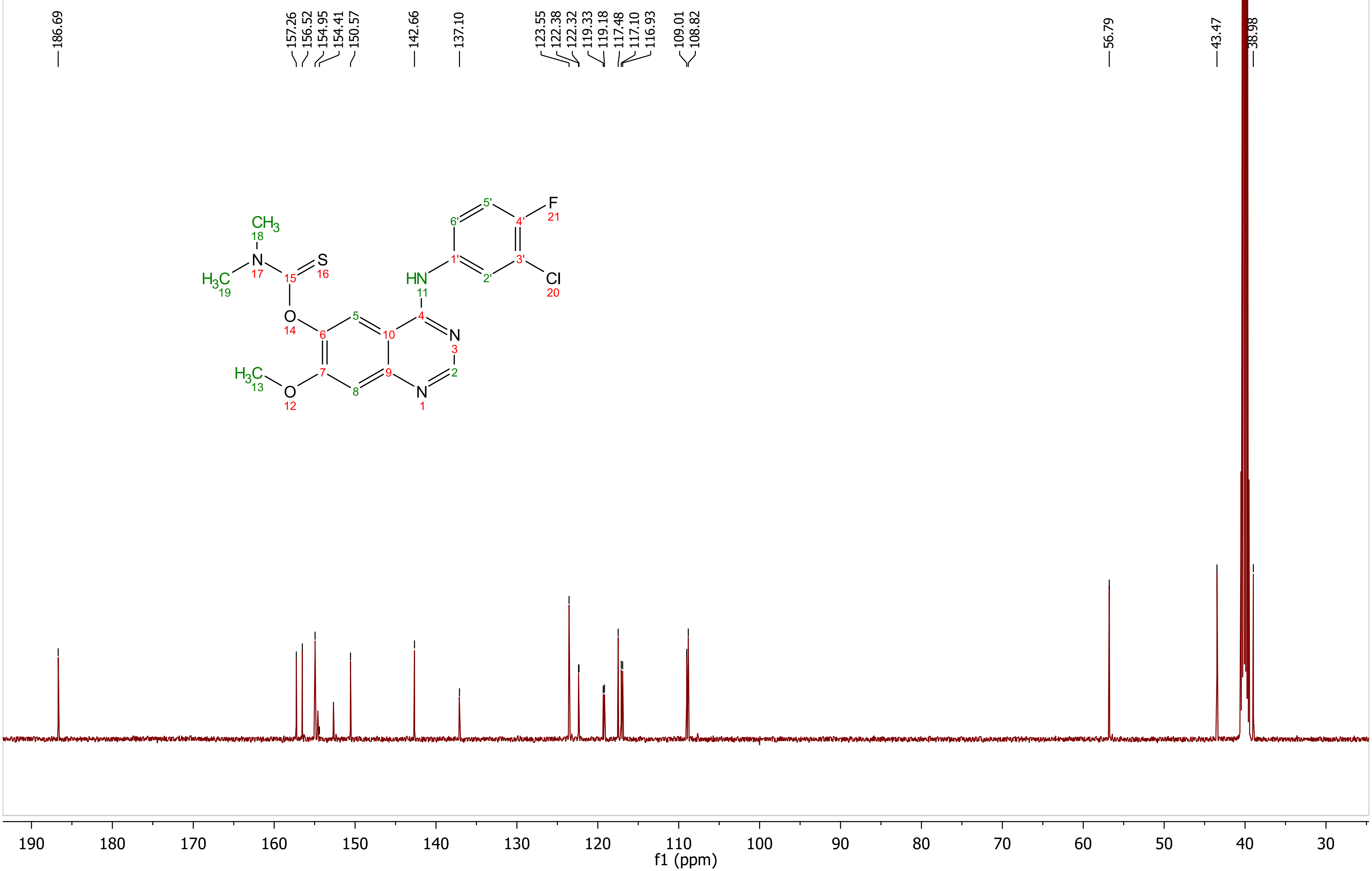

RC-2-52.2.fid
Robyn: RC-2-52.2: DMSO: 02/02/2016: 300K: 1H: 500: AP

[1]H NMR (500 MHz, DMSO-d_6) δ 9.85 (s, 1H), 8.74 (s, 1H), 8.64 (s, 1H), 8.23 (t, J = 1.9 Hz, 2H), 7.94 – 7.88 (m, 2H), 7.35 (d, J = 8.0 Hz, 1H), 7.32 – 7.27 (m, 3H), 3.95 (s, 3H), 3.13 (s, 3H), 2.94 (s, 3H).